Environmental and Molecular Control of the Uropathogenic *Escherichia coli* Extracellular Matrix

by

David Andrew-Essman Hufnagel

A dissertation submitted in partial fulfillment
of the requirements for the degree of
Doctor of Philosophy
(Molecular, Cellular and Developmental Biology)
in the University of Michigan
2016

Doctoral Committee:

Associate Professor Matthew R. Chapman, Chair
Emeritus Professor Robert A. Bender
Professor Steven E. Clark
Assistant Professor Alexander H. Rickard

To my loving family

Acknowledgements

I have too many people to thank for their help, but I have to start with Matt. Matt has been the best possible mentor I can imagine. I came to Michigan with very little laboratory experience, and he has instilled enthusiasm and all the tools necessary to become a successful scientist and adult. These past few years have developed me more as a person than as a researcher, which is saying a lot if you had a scientific conversation with me 5 years ago vs. today. He has been an incredible mentor and friend that has pushed me in multiple areas of my life from travel, to dating (he encouraged me to ask my now fiancé out), and definitely in science. I have gotten this far and I haven't even mentioned how fun he has made graduate school. These 5 and a half years have been a transformative ride that have defined me. I cannot think of another mentor who would vouch for me, care for me, or develop me as deeply as Matt.

I want to thank my lab mates in the Chapman Empire that have shared so many experiences with me. I want to thank Maggie Evans and Will DePas for being incredible friends in graduate school. Our relationship goes well beyond peers pushing each other scientifically, as we would hang out often during long days or weeks in the lab. I was always blown away by Maggie's ability to focus on specific problems, problem solving, and her incredible proficiency in writing gorgeous papers. Will trained me and was a perfect example of how to approach graduate school. I have tried to emulate his hard work, humility, and humble attitude. Adnan

Syed has been an unbelievable laboratory partner, ranging from his time in the Boles lab, to his time in the Chapman lab the last year. Our friendship has been incredibly tight and meaningful throughout graduate school. I want to thank Yizhou Zhou who was one of the happiest folks in the Chapman lab and could turn my day around with her cheerful nature. I was always blown away with the productivity she could squeeze out. I want to thank Neha Jain and her ever joyful attitude (except in winter). Her unparalleled knowledge of protein folding and amyloids has really made a splash in the Chapman lab. Janet Price has recently joined the lab, and I had the great pleasure of training her during her rotation in the lab. Kim Seed and her lab have been great new residents of 2095, I could not have asked for a nicer group of people to occupy the space the last 2 years. I also want to thank my undergraduates and high school students I have worked with: Matt Benoit, Mike Sesi, Jesse Kelly, and Isabella Comai. Jesse did a great job taking control of his own project and showing great dedication to lab. Isabella Comai is one of the most talented high school students I have ever met. She came into the lab over a summer and not only understood the concepts and details of the projects but also contributed valuable data to my thesis project. I want to thank Blaise Boles and his lab. Blaise was one of the primary reasons why I wanted to pursue my PhD at Michigan. His knowledge of biofilms and microbes was truly inspiring to me and really shaped the approaches that I took in graduate school. Boles lab members Kelly Schwartz and David Payne were great friends that were always available for laboratory venting and hangouts.

I want to thank my committee for all the scientific advice and pushing me down new avenues during my pursuit of this degree. Bob Bender always had a new metabolic pathway that I needed to investigate if there was any relation to my project. He was also a great friend who often would come into lab and tell me of old scientific stories and explanations that cannot be

found in text. Teaching with him was also a pleasure, as he has an incredible gift for group communication that I have tried to replicate. I also taught under Steve Clark, and his ability to communicate science meshed perfectly with the way that I learn. This made him an invaluable member to my committee as he would have the ability to ask important questions or suggest un-thought of experiments that could provide important answers to questions. Whenever asked by younger PhD students about people to include on their committees, I whole-heartedly recommend Steve Clark. I want to thank Alex Rickard for his great enthusiasm for biofilms and the field of microbiology in general. This enthusiasm really comes through with his suggested topics for study and novel approaches for experimental design.

I want to thank the Department of MCDB for all the help they have given me. Mary Carr has been an invaluable resource and friend. She took the worry out of meeting deadlines and remaining afloat during the pursuit of my degree. I want to thank Gregg Sobocinski for all the help he provided with imaging. I want to thank Jim Bardwell for helpful discussions on my projects. I want to thank Ann Miller for the use of her laboratory's microscope, software, and graduate students.

I want to thank my funding sources: MCubed, Bernard Maas Dean's Fellowship, and Rackham Dissertation Fellowship.

Finally, I want to thank my family: my parents, siblings, and Rachel. For always believing in me.

Table of Contents

List of Figures

List of Tables

Chapter 1

The Biology of *Escherichia coli* Extracellular Matrix and Microbial Amyloids

Chapter Summary

Escherichia coli (*E. coli*) is one of the world's best-characterized organisms, as it has been extensively studied for over a century. However, most of this work has focused on *E. coli* grown under laboratory conditions that do not faithfully simulate its natural environments. Therefore, the historical perspectives on *E. coli* physiology and life cycle are somewhat skewed toward experimental systems that feature *E. coli* growing logarithmically in a test tube. Typically a commensal bacterium, *E. coli* resides in the lower intestines of a slew of animals. Outside of the lower intestine, *E. coli* can adapt and survive in a very different set of environmental conditions. Biofilm formation allows *E. coli* to survive, and even thrive, in environments that do not support the growth of planktonic populations. *E. coli* can form biofilms virtually everywhere; in the bladder during a urinary tract infection, on indwelling medical devices, and outside of the host on plants and in the soil. The *E. coli* extracellular matrix, composed primarily of the protein polymer named curli and the polysaccharide cellulose, promotes adherence to organic and inorganic surfaces, as well as resistance to desiccation, the host immune system and other antimicrobials. The pathways that govern *E. coli* biofilm formation, cellulose production, and curli biogenesis will be discussed in this chapter, which concludes with suggestions for the future of *E. coli* biofilm research and potential therapies.

Basic History, Phylogeny, and Habitats of *Escherichia coli*

The bacterial family Enterobacteriaceae includes a variety of intestinal symbionts as well as notable pathogens such as *Salmonella enterica, Serratia marcescens, Klebsiella pneumoniae,* and *Yersinia pestis* (1). Also included among the family Enterobacteriaceae is the most well-documented bacterial species on Earth, *Escherichia coli*. *E. coli* is a fascinatingly diverse bug, featuring a cadre of strains that have adapted to diverse environmental conditions and lifestyles. Although the typical *E. coli* genome contains roughly 4800 genes, only approximately 1700 are shared by every *E. coli* strain (2). In total, there are over 15,000 genes that make up the *E. coli* pangenome (2, 3). The genomic plasticity of various *E. coli* isolates provides *E. coli* the ability to proliferate and survive in an array of environments (4, 5).

A major niche of *E. coli* is the lower intestinal tract of mammals, birds, and reptiles (6). Indeed, *E. coli* was first isolated by Theodor Escherich from a human stool sample in 1886 (7). Among the first bacteria to colonize the intestinal tract of human infants, *E. coli* establishes a stable population of roughly 10^8 CFU/g of feces by adulthood (5, 8, 9). The intestinal tract is an oxygen limiting environment, and *E. coli* is a facultative anaerobe that can reduce several alternate terminal electron acceptors such as nitrate, fumarate, dimethyl sulfoxide (DMSO), and trimethylamine N-oxide (TMAO) (10). Mouse colonization studies have revealed that in the intestine fumarate reductase, nitrate reductase, and *bd* oxidase (high affinity oxygen cytochrome) are particularly important for *E. coli* fitness (11, 12). The physiological flexibility of *E. coli* renders it well-suited for the diverse environments encountered in the intestinal tract.

While the lower digestive tract is the primary habitat of *E. coli,* fecal dissemination leads to the passage of *E. coli* to its secondary environment outside of the host. The host and non-host environments can be dynamic and differ in nutrient availability, temperature, and the number and nature of competitors, among other things. Once *E. coli* is excreted in stool, there is generally a net-negative fitness cost compared to growth in most host environments (9, 13). *E. coli* doubles about every two days in a human host, but outside of the host, instead of dividing, *E. coli* perishes after an average of four days depending on the environment into which it is passaged (9). However, as *E. coli* is constantly being excreted, it has been estimated that half of the *E. coli* cells on Earth exist outside the host (9). Interestingly, studies have found that *E. coli* can grow in soil not only in tropical conditions, but also in colder temperatures (14).

Many studies have investigated how enterohemorrhagic *E. coli* (EHEC) strains, particularly EHEC O157:H7, make their way from environmental reservoirs to humans (15). *E. coli* is transmitted from host to host by the fecal-oral route. The ability to survive outside of the host therefore facilitates the host-to-host transmission of all *E. coli* variants, including pathogenic strains. EHEC strains cause diarrhea, abdominal cramps, and in certain cases the life threatening hemolytic-uremic syndrome (16). The intestinal tract of domesticated cattle serves as the primary reservoir for EHEC in the United States and EHEC can contaminate meat during the slaughter process (17, 18). Additionally, EHEC is shed in feces and can survive in manure for months (17, 19-21), making contact with animal feces a risk factor for EHEC infections. Even using untreated manure as fertilizer can result in contaminated produce products (15, 22-24). While contaminated manure or water can foul the surface of plants, there is also evidence that EHEC can invade plant tissue (23-25). *E. coli*'s ability to survive outside of the intestinal tract is integral to EHEC's ability to cause outbreaks.

Extraintestinal pathogenic *E. coli* (ExPEC) are strains that cause disease outside of the intestinal tract of animals, including uropathogenic or 'UPEC' strains. Urinary tract infections (11) are one of the most common bacterial infections, costing over 3 billion dollars to health care in the United States alone (26). UPEC can live in the intestine without causing disease, and recent work has shown that UPEC has no fitness defects in the gut environment when compared with commensal *E. coli* strains (27). How ExPEC strains like UPEC transmit from the intestine to the site of disease is not completely understood, but at least some strains can spread via the fecal-oral route (28). In fact, the primary source of UPEC that colonizes the urethra is a patient's own intestinal tract (29). ExPEC, including UPEC strains, can also be found on food products, and clonal UPEC outbreaks have been reported (30-32). Taken together these data suggest that UPEC are at least partly dependent on survival outside of the host before they can recolonize a second host and cause disease.

UPEC have specifically adapted to cause disease in the urinary tract (26). UPEC ascend the urinary tract to the bladder and cause infection (26). UPEC invasion of bladder epithelia cells is type 1 pili-dependent, where they form tight knit and aggregated intracellular bacterial communities called IBCs (33, 34). IBCs are drug resistant and can evade the host immune responses allowing for cells within the IBC to proliferate and to further infect additional bladder epithelial cells (35, 36).

Introduction to Biofilms and the Extracellular Matrix

Biofilm formation can increase bacterial fitness in both host and non-host environments (37, 38). In this chapter we will use the general definition of a biofilm as a group of surface-

associated bacteria enveloped in a self-produced extracellular matrix (39). The *E. coli* extracellular matrix contains a major protein polymer called curli and the carbohydrate polymer, cellulose (40-42). Although curli and cellulose are typically the most abundant biofilm constituents, the extracellular matrix of *E. coli* can also include type 1 pili, flagella, antigen 43, DNA, β-1,6-N-acetylglucosamine (β-1,6-GlcNAc), capsule sugars, and colonic acid (43). Most pathogenic strains of *E. coli* form robust biofilms, however, some laboratory strains of *E. coli* are attenuated in their ability to produce biofilms. The K12 strain of *E. coli* was first isolated from a patient at Stanford in 1922, and was subsequently passaged for more than 50 years (44). This passaging led to evolutionary adaptation to the laboratory growth conditions, and to the loss of certain traits that influence biofilms (45). K12 *E. coli* therefore requires extended periods of time to adhere to surfaces and form biofilms (40). On the other hand, a host of pathogenic, environmental, and commensal *E. coli* isolates readily form biofilms in the laboratory and therefore make excellent model organisms for biofilm formation studies (46-50).

Biofilm formation correlates with resistance to a variety of environmental stresses, including antibiotics, the immune system, and predation (38). Resistance is conferred through at least two distinct mechanisms. First, the extracellular matrix forms a physical barrier that can resist shear stress as well as recognition and phagocytosis by immune cells (38). Second, bacteria within biofilms often assemble into subpopulations that have distinct physiological characteristics (46, 51, 52). Subpopulation development can be triggered by mutations, stochastic gene expression, or chemical gradients that develop during biofilm formation (37, 52-54). For instance, bacteria at the biofilm surface are exposed to more oxygen, stimulating a higher rate of aerobic respiration (37, 55, 56). Metabolic changes often coincide with resistance to different stresses (54, 57). A biofilm community with multiple subpopulations, each resistant to different

stresses, therefore demonstrates resistance to a broader range of environmental pressures to the biofilm community as a whole (37, 54, 57).

Laboratory biofilm models

Laboratory biofilm models have been used to determine most of the spatiotemporal and molecular characteristics of biofilms (Figure 1.1). *E. coli* forms at least two distinct types of biofilm in static liquid cultures—both form at the air liquid interface and both require production of extracellular polymers (41, 43, 47, 58, 59) (Figure 1.1A, Figure 1.1B, and Figure 1.1C). The accumulation of biomass at the air-exposed edges of polyvinyl chloride wells or glass culture tubes with cultures grown in lysogeny broth (LB) media is reliant on type-1-pili, poly-β-1,6-GlcNAc, and flagella (47, 58, 60) (Figure 1.1A top image). The crystal violet stained biofilm rings can be visualized in the top image in Figure 1.1A, whereas the flagella mutant (*fliC::*kan) grown in the tube shown in the bottom image did not form rings on the glass culture tube (Figure 1A).

E. coli can also form a pellicle biofilm that floats at the air liquid interface. Pellicles are films of curli/cellulose-encased cells that span the entire air-liquid interface of a single well (47, 59, 61). Pellicle formation can be quantified by crystal violet staining of the biofilm biomass (62, 63) (Figure 1.1B). The culture in the top well in Figure 1.1B formed a robust pellicle at the air-liquid interface of the culture, whereas the culture in the bottom well did not.

Pellicle biofilm formation relies on the biofilm master regulator, CsgD. CsgD regulates expression of the matrix components, curli and cellulose (41, 64). CsgD-mediated biofilms can be inhibited by the presence of glucose, temperatures greater than 30°C, or high osmolarity,

because all of these conditions repress CsgD activity (47, 65-67). When *E. coli* is grown in conditions that are conducive for *csgD* expression, curli- and cellulose-dependent biofilms can manifest in a variety of ways. The culture grown in the bottom image of Figure 1.1B is a *csgD* mutant that is unable to produce curli or cellulose (Figure 1.1B). The pellicle architecture at the air-biofilm interface can be highlighted by growing the static culture in media amended with the diazo dye Congo red (61, 68) (Figure 1.1C). Congo red stains both curli and cellulose, allowing for visualization of the pellicle biofilms and the ornate wrinkled morphology at the surface of the culture (Top image Figure 1.1C).

Confocal laser scanning microscopy (CLSM) and electron microscopy (EM) analysis revealed that two separate populations exist at the pellicle biofilm air-liquid interface (59, 61, 69). At the air-biofilm interface cells are encased in a thick fibrous extracellular matrix, whereas cells at the liquid interface are more evenly spaced and often not surrounded by a fibrous extracellular matrix (59). Additionally, pili are involved in pellicle development and maturation, as deletion of type-1-pili leads to a less-robust pellicle (59). Flagella are also required for pellicle development, since motile cells are necessary for colonization at the top of the static culture (47, 59).

The CsgD-induced matrix components curli and cellulose are also required for colony biofilm formation in *E. coli* and *Salmonella* spp. A variety of bacterial species, including *E. coli*, produce wrinkled colony biofilms on agar plates (Figure 1.1D). The nomenclature for the wrinkled colony phenotype varies between species, but some common names are rugose biofilms, wrinkled colony biofilms, and red dry and rough (rdar) biofilms. Here, we will use the term rugose biofilms to describe all wrinkled colony biofilms on agar plates. The mechanics of rugose biofilm formation have been studied extensively in multiple species including *E. coli*,

Vibrio cholera, *Pseudomonas aeruginosa*, *Bacillus subtilis*, and *S. enterica* serovar Typhimurium (41, 70-78).

When grown under CsgD-inducing conditions on agar plates, *E. coli* will form rugose colony biofilms (41, 79) (Left image Figure 1.1D). Curli and cellulose are required for rugose development, and are the major extracellular structures in the rugose biofilm matrix (41, 46, 80). Rugose biofilms of UPEC have two distinct cell populations, a top layer at the colony-air interface containing curliated cells, and a non-curliated interior population. The development of these two populations is triggered by exposure to reactive oxygen stress, either through superoxide accumulation or through the addition of iron in *E. coli, Salmonella* spp., and *Citrobacter* spp. (46). Rugose biofilms provide resistance to desiccation, as WT *S. enterica* rugose colonies incubated at room temperature for 3 and 9 months had greatly increased survival compared to curli and cellulose mutants (81). Curli and cellulose mutant strains form non-spreading and unwrinkled colonies that do not bind Congo red (Right image Figure 1.1D). While flagella are not required for the rugose colony morphotype, including colony spreading, the interior cells in a rugose colony are heavily flagellated (51). Since *E. coli* K12 strains have acquired a mutation that prevents cellulose production, they do not form rugose biofilms unless the cellulose synthesis defect is repaired (82). Indeed, repeated culturing tends to select for genetic suppressors of biofilm formation in a variety of bacteria (45). However, more recently isolated commensal *E. coli*, ExPEC, and IPEC are able to form rugose biofilms (62, 83, 84) (Figure 1.1D). Curli, cellulose, and rugose biofilms are not only produced in *E. coli* and *Salmonella* spp., but also in other Enterobacteriaceae, such as *Citrobacter* spp. (46, 85). As curli and cellulose are required for rugose biofilm development, the environmental signals leading to rugose development coincide with those affecting CsgD expression (78, 86).

CsgD-Mediated Control of the Extracellular Matrix

CsgD is a FixJ/LuxR/UhpA type response regulator that contains a typical C-terminal helix-turn-helix DNA-binding domain (64, 87). The N-terminus of CsgD is thought to respond to environmental signals that affect the protein's ability to bind DNA and regulate transcription (87-89). The N-termini of FixJ type response regulators are typically modified by phosphorylation on highly conserved aspartic acid residues (90, 91). However, CsgD is missing the conserved phosphorylation sites, which has confused the role that phosphorylation plays in regulating CsgD (89, 92). However, acetyl phosphate can phosphorylate CsgD *in vitro* (90), which reduces the ability of CsgD to bind particular promoters, suggesting that post-translational phosphorylation regulation occurs (90).

The expression of *csgD* is controlled by a large number of transcriptional regulators and small RNAs (93, 94). In general, low salt, low temperature, and low glucose conditions trigger *csgD* expression (64, 66, 93, 95, 96). Additionally, *csgD* expression requires the stationary-phase sigma factor RpoS (67, 77), and CsgD activity is regulated by the small molecule, cyclic-di-GMP (97). Diguanylate cyclases contain a GGDEF domain that promotes cyclic-di-GMP production and phosphodiesterases contain an EAL domain that promotes the breakdown of c-di-GMP (97). *E. coli* and *S. enterica* encode a number of diguanylate cyclases and phosphodiesterases to regulate cytoplasmic levels of cyclic-di-GMP (98-100). The GGDEF and EAL containing proteins, STM2123 (YegE) and STM3388, are both required for WT CsgD protein levels in *Salmonella enterica* serovar Typhimurium (100). Alternatively, the diguanylate cyclases, YdaM and YfiN, are required for WT CsgD protein levels in *E. coli* (68, 99). The

mechanism by which these diguanylate cyclases control CsgD protein levels is unknown. C-di-GMP can be bound by RNA (riboswitches) and by multiple binding motifs in proteins (101). In addition the diguanylate cyclases themselves can have secondary function outside of c-di-GMP production, leading to suppression of CsgD protein levels by a variety of potential causes (101).

CsgD controls a modest regulon of roughly 13 genes/operons (64, 102-104). Included in the regulon that CsgD upregulates is *iraP*, which leads to a relay system where the IraP protein stabilizes RpoS, which results in more CsgD expression (103). CsgD directly represses *fliE* and *fliF* which are involved in flagella biosynthesis (104), and induces expression of curli by binding directly to the *csgBAC* promoter (Figure 1.2) (64). CsgD induces cellulose production indirectly by positively regulating the diguanylate cyclase AdrA (41) (Figure 1.2). Cyclic-di-GMP produced by AdrA activates the cellulose synthase and promotes cellulose production (41) (Figure 1.2). The complex regulation of CsgD and the promotion of curli and cellulose go hand-in-hand (Figure 1.2), suggesting that only specific conditions promote the cell to decrease motility and produce an extracellular matrix.

History and Diversity of Bacterial Amyloids

Curli were first described in 1989 when Stafan Normark and colleagues were investigating Bovine mastitis isolates for the ability to bind to host cell matrix components (95). The authors noticed that half of the isolates bound fibronectin when grown under conditions that we now know to favor curli production (95). Electron microscopy revealed that the fibronectin binding isolates produced fibrous coiled surface structures that they called ‘curli’ (95). The presence of curli fibers in *S. enterica* was discovered a few years later by Collinson *et al.* (105).

Originally termed thin aggregative fimbriae or Tafi, the authors did not initially think that these fibers were related to curli (105) because *S. enterica* produced Tafi fibers when grown at both 30°C and 37°C (105). However, Arnqvist *et al.* found that both *S. enterica* tafi and *E. coli* curli are the same fiber and that they were both primarily composed of the protein monomer, CsgA (106). In 2002 curli fibers were biochemically shown to be amyloid fibers (107).

Amyloid fibers are β-sheet-rich protein polymers that are highly resistant to denaturation. The distinguishing amyloid fold can be adopted by a variety of proteins, without a shared primary structure, and is found in nearly all cell types. Despite the fact that amyloids have a richly informed scientific history, the diverse biology contributed by amyloids is only beginning to be appreciated. Initial amyloid studies focused on the intimate association of amyloid formation with cytotoxicity and neurodegenerative diseases like Alzheimer's, Huntington's and the prion encephalopathies. Despite amyloid's somewhat sinister past, recent work on "functional" amyloids has revealed numerous ways that amyloids contribute to normal cellular biology (108). Included among the activities in which amyloids participate are melanin production, the ability to act as non-Mendelian inheritable genetic elements, and as extracellular molecular scaffolds that hold bacterial communities together. The amyloid fold is tailor-made for the extracellular space, as amyloid polymers can self-assemble without requiring exogenous energy and the polymers are resistant to a slew of harsh denaturants that would devastate most protein folds.

Many bacterial species produce amyloid fibers extracellularly, where they typically function as part of a complex protein and polysaccharide matrix that protects communities of cells. *E. coli, S. enterica*, *Bacillus subtilis, Staphylococcus aureus, and Mycobacterium tuberculosis*, among many others, produce extracellular amyloid fibers (107, 109-111). Between

5-40% of species isolated from natural biofilms (seawater, sludge, and drinking water) produce amyloids, demonstrating the widespread occurrence of this extracellular structure (112). Amyloid production in biofilms provides structure for floating biofilms in *B. subtilis* and *E. coli* and for shear and degratory enzyme resistant biofilms in *S. aureus* (61, 109, 110). The functions and presence of bacterial amyloids were first unraveled in the study of curli fibers made by *E. coli* (107).

A variety of enteric bacteria utilize the functional bacterial amyloid curli as a community resource in biofilms. The curli biogenesis machinery is encoded within two *csg* (curli specific gene) operons that include a master transcriptional regulator of biofilm extracellular matrix (ECM) components called CsgD. The curli assembly machinery is widespread, as *csg* homologs are found within four phyla, Bacteroidetes, Proteobacter, Firmicutes, and Thermodesulfobacteria, and 9 different classes of sequenced bacteria (113). CsgA's imperfect glutamine and asparagine-rich repeating units, which are necessary for amyloid polymerization, are conserved in these differing versions of CsgA. Additionally, there is striking continuity among *csg* ORFs in disparate bacterial species, implying that the identified *csg* homologs are not pseudogenes. The *csgDEFG/csgBAC* intergenic region is highly conserved in different *E. coli* isolates, with a 98.6% average pair-wise identity in 284 different *E. coli* strains (114). Along with *asnS/ompF* and *uspC/flhDC* , the *csgDEFG/csgBAC* intergenic sequence can be used to construct a phylogenetic tree with a more accurate prediction of *E. coli* phylogeny with fewer base pairs than the traditional MLST method (114). The broad distribution of *csg* genes and bacterial amyloids discovered in a myriad of species points to amyloids being a common and important part of the communal bacterial lifestyle.

The Curli Biogenesis Pathway

Curli fibers were the first case of extracellular fibers to polymerize by the nucleation-precipitation mechanism, also known as the type VII secretion system (107, 115-118). Curli fiber subunits and their assembly machinery are encoded in two divergently transcribed operons, *csgDEFG* and *csgBAC* (Figure 1.2) (64). The *csgBAC* operon encodes the major and minor curli subunits, CsgA and CsgB, respectively. Both CsgA and CsgB are secreted across the outer membrane. On the cell surface, CsgB associates with the outer membrane and provides a template that induces CsgA to adopt an amyloid fold and form cell-associated curli fibers (119) (Figure 1.2). Electron microscopic analysis has led to the estimate that 30% of *E. coli* cells produce curli under curli inducing conditions (120). A *csgB* mutant secretes unfolded CsgA that can polymerize on the surface of a *csgA* mutant cell (which presents a surface-associated CsgB), in a process called 'interbacterial complementation' (107, 115). Interspecies curli production restores agar adherence to the mixed species bacterial communities (121), supporting the idea that curli subunits may be a 'community resource' that can be utilized indiscriminately by all cells in a localized community.

The *csgDEFG* operon encodes the CsgD regulator and three curli assembly proteins that are each required for WT levels of curli production (Figure 1.2) (64) CsgG forms a nonomeric pore in the outer membrane that facilitates curlin secretion (Figure 1.2) (120, 122-124). CsgG has an approximately 2 nm central pore that spans the outer membrane (120, 124). During curli assembly CsgG forms discrete puncta that associate with two other curli accessory proteins, CsgE and CsgF (Figure 1.2) (122). Electron microscopic analysis revealed that CsgG, CsgE, and

CsgF cluster together around curli fibers (120). CsgE is a periplasmic protein that provides substrate specificity to CsgG-mediated secretion and also has chaperone-like activity as it can prevent CsgA from assembling amyloid fibers *in vitro* (107, 125). CsgE caps the secretion vestibule on the periplasmic side of CsgG, which facilitates unidirectional migration of substrates to the cell surface (124). CsgE anti-amyloid activity can arrest CsgA fiber formation at different stages of CsgA polymerization, although it cannot disassemble preformed fibers (126). When CsgE is added exogenously to the growth medium, pellicle biofilm formation is interrupted (126). CsgC is a periplasmic protein that inhibits CsgA amyloid polymerization at very low substoichiometric ratios (127). When CsgA is not properly secreted to the cell surface, CsgC is required to hold CsgA in a non-aggregated state that allows for proteolytic degradation of CsgA (127). Interestingly, CsgC can also function to inhibit polymerization of other disease-associated amyloids like α-synuclein (127). Finally, CsgF is necessary for both cell surface association of curli and CsgA polymerization into fibers *in vivo* (107, 119) (Figure 1.2).

Chemical and Protein Modulation of CsgA Amyloid Formation

Curli are part of a growing class of β-rich, ordered, protein fibers called amyloid. Amyloids have a villainous history, as the amyloid fold is associated with type-2 diabetes, Alzheimer's disease, and Parkinson's disease, among many others (108). The signature and well-studied role of amyloid formation in human diseases has led to the search for drugs that can prevent amyloid formation. However, progress in the amyloid formation field has been somewhat hampered by lack of robust, reproducible and tractable cellular model systems. The curli biogenesis system in *E. coli* is ideally situated as a platform for screening drugs that might

interrogate the amyloid formation process. The curli system in *E. coli* provides sophisticated genetics and a suite of different assays to measure *in vivo* amyloid formation, including curli-dependent biofilm formation and Congo red binding. We have used the curli system to begin screening and characterizing a library of designer peptidomimetic compounds called 2-pyridones (61, 126, 128). Pyridone compounds were initially recognized as anti-amyloid compounds in a screen of small organic molecules testing for binding strength to the amyloid associated with Alzheimer's disease, $A\beta^{1-42}$ (129). The 2-pyridone compounds have a rigid bicyclic structure, which maintains the compounds in a straight conformation that mimics a β-strand (126). Altered 2-pyridone compounds were constructed that had increased solubility and were used to inhibit the type 1 pilus assembly in UTI89 via interruption of the chaperone-usher interaction (130, 131).

The CF_3-phenyl substituted 2-pyridone, FN075, is a potent amyloid inhibitor (61, 128, 131). FN075 inhibits CsgA amyloid polymerization *in vitro*, and it also blocks biofilm formation by preventing curli formation and inhibiting type 1 pilus assembly (61). FN075 inhibits CsgA amyloid fiber formation by directing CsgA into soluble oligomers that are not on pathway to the amyloid fiber (128). Interestingly, the CF_3-phenyl substitution does not abrogate 2-pyridone activity against the type 1 pilus. Thus, FN075 functions as a dual-function pilus-inhibitor (pilicide) and curli-inhibitor (curlicide). FN075 co-inoculation with UPEC in a mouse UTI-model caused decreases in initial titers of bacteria and IBC formation (61). Recently, FN075 was used as a scaffold for the production of new, chemically distinct compounds (126). Compounds from this library are being screened for their ability to inhibit CsgA amyloid formation and several interesting leads have been identified (126). Two of these compounds were found to accelerate CsgA amyloid formation (126). Interestingly, acceleration of amyloid formation may

be one route to prevent amyloid-related cellular toxicity, as conformationally-dynamic amyloid intermediates are hypothesized to be the root of amyloid toxicity (132). Therefore, small molecule 'accelerators' should facilitate the conversion of dynamic oligomers into the more stable and less cytotoxic amyloid state, and thus have promising therapeutic value.

Cellulose production

The other major polymer present in the *E. coli* extracellular matrix is cellulose, a linear chain of β-(1,4)-linked glucose monomers (41, 80). Bacterial cellulose production was first described in 1887, and in recent years *Gluconacetobacter xylinus* has been the model organism for studies of bacterial cellulose synthesis (133-135). Cellulose production by the family Enterobacteriaceae was first described in 2001 (41), which initiated the discovery of cellulose production in many *E. coli* strains (41, 46, 62, 85, 136). Most non-K12 *E. coli* strains can produce cellulose as a component of the biofilm matrix, while K12 laboratory strains do not (41, 136). In the case of K12 strains W3110 and MG1655, the cellulose defect is due to a single nucleotide polymorphism (SNP) in *bcsQ* that results in a pre-mature stop codon (82). Repairing this SNP in *bcsQ* restores cellulose synthesis in *E. coli* W3110 and induces rugose colony formation (82).

Expression of the cellulose synthesis genes is usually dependent on the master biofilm regulator, CsgD (41, 46). CsgD modulates cellulose synthesis by activating transcription of *adrA* (41, 46, 86, 136) (Figure 1.2). AdrA contains a GGDEF domain typical of diguanylate cyclases (86, 98), and AdrA-produced cyclic-di-GMP binds to the PilZ domain of the cellulose synthase, BcsA, which stimulates cellulose synthesis (137, 138) (Figure 1.2). BcsA covalently links UDP-

D-glucose monomers into a growing glucan chain (135, 139) (Figure 1.2). AdrA is not the only diguanylate cyclase that can produce cyclic-di-GMP to drive BcsA activation. *E. coli* 1094 can produce cellulose independently of CsgD, and does so via the diguanylate cyclase YedQ that works in place of AdrA (136). Furthermore, mutants in the disulfide bonding system (DSB) produce cellulose independently of CsgD in the uropathogenic strain UTI89 (68). The YfiN negative regulator protein, YfiR, is unstable and degraded in DSB mutants and can no longer repress activation of the diguanylate cyclase, YfiN (Chapter 2) (68, 140). Constitutive activation of YfiN leads to accumulation of cyclic-di-GMP and activation of the cellulose synthase in the presence of high salt, high temperature and glucose, conditions where CsgD is normally repressed (68). Additionally, YfiN and cellulose production are activated by reducing conditions, suggesting that under these conditions cellulose can be produced independently of curli (68).

The biophysics of BcsA activation and cellulose production has been recently elucidated (139, 141, 142). The BcsA glycosyl transferase domain is on the cytoplasmic C-terminus located next to the PilZ domain (141). In *Rhodobacter sphaeroides,* a salt bride between an arginine of the PilZ domain and a glutamine in the gating loop is broken once ci-di-GMP is bound, which allows the glycosyl transferase domain to engage UDP-glucose (141, 142). Mutation of the glutamine in the gating loop results in constitutive cellulose expression, as the inhibitory salt bride is not formed (142). The UDP-binding site allows space for a single addition to the nascent glucan chain (141). A glucan chain of approximately 10 glucose monomers aligns on the periplasmic side of BcsA, perpendicular to the axis of the BcsA β-barrel (141). Additionally, a by-product of cellulose formation, UDP, acts as a competitive feedback inhibitor of the glycosyl transferase (139, 142). Both *E. coli* and *Rhodobacter sphaeroides* BcsA and BcsB are sufficient for production of cellulose *in vitro,* but the reaction requires c-di-GMP, UDP-glucose, and both

BcsA and BcsB to be co-localized in the same liposome to function (139).

Enterobacteriaceae Extracellular Matrix in the Host and Disease

Despite the fact that many *E. coli* strains express curli and cellulose maximally at 26°C, as might be the case outside of the host, both components are expressed in the host environment and play a role in commensal and disease interactions. Both *E. coli* and *S. enterica* clinical isolates express CsgD, curli, and cellulose at 37°C (62, 77). *Salmonella* produces cellulose inside macrophages, which causes a decrease in virulence (143). Cellulose null strains and cellulose inhibition through the MgtC protein were found to increase virulence during infection, and it is hypothesized that cellulose can act as a mediator between pathogenicity and long-term survival to increase *Salmonella* transmission (143).

Curliated UPEC have greater survival during co-incubation with bladder epithelial cells compared to non-curliated variants, and this interaction appears to be due to curli interacting with the human antimicrobial peptide LL-37 (144). LL-37 normally perturbs membranes causing lysis, but the presence of polymerized curli fibers leads to inhibition of the antimicrobial activity. LL-37 can also inhibit amyloid polymerization of CsgA *in vitro*. LL-37 may be caught in binding to the curli fibers during the curli polymerization process vs. LL-37 being able to access the bacterial cell-membrane to cause lysis in a curli-null strain. UPEC curli production is part of early stage bladder colonization in a mouse model, as curli mutants have decreased bladder titers (61).

Untreated UPEC infections can lead to dissemination and infections of the bloodstream, also known as bacteremia (145). Interestingly, UPEC strains isolated from bacteremic patients

produce more curli at 37°C than UPEC strains isolated from non-bacteremic patients (146). Additionally, over 50% of *E. coli* isolates from patients with sepsis produce curli at 37°C (147). Serum samples from patients with sepsis had antibodies against the major curli subunit, CsgA, whereas control patients did not (147). Because curli and cellulose are expressed by clinical isolates under host-colonization conditions, it is imperative to understand how these matrix components shape the host-pathogen interaction and the molecular pathways that induce their production in these non-laboratory conditions.

In addition to curli and cellulose, the extracellular matrix components type-1-pili, K 1 capsule, and antigen 43 also have roles in promoting UPEC bladder colonization and biofilm formation. Antigen 43 is an outer-membrane protein required for biofilm formation in glucose minimal medium, but not LB medium (148). Antigen 43 drives aggregation and cell-surface and cell-cell interactions of *E. coli* biofilms via antigen 43-antigen 43 interaction (148, 149). Antigen 43 production increases interspecies biofilm formation between *E. coli* and *Pseudomonas fluorescens* (149). IBCs that form in the superficial facet cells that line the bladder epithelium are composed of densely compact and coccoid shaped cells. Mutant lacking type-1-pili have cells that are dispersed and retain their rod shape (34). The polysaccharide K 1 capsule is produced in IBCs and helps UPEC evasion of neutrophils in the host (150). Mutants lacking K 1 capsule form dispersed and disordered intracellular bacterial populations that have neutrophils within the confines of their communities (150).

The immune system and host cells interact with the extracellular matrix components produced by *E. coli* and *S. enterica*. Beyond causing disease in the urinary tract, most *E. coli* in the human body persists and associates within the lower intestinal tract by interacting with gut and colon epithelia (9, 13). Curli and cellulose are required for proper attaching and effacing of

E. coli to host colon cancer cells and to bovine cow colon explants (151). Curli also increase the colon cell internalization of *E. coli* commensal isolates (152). Colon cells have increased Il-8 production in the presence of both flagellated and curliated *E. coli*, and macrophages have increased nitrous oxide and IL-6 production in the presence of purified *S. enterica* curli fibers (152, 153). Host cells recognize amyloids and also *S. enterica* curli fibers through TLR1/2 heterodimer (154). CD14 on the host cell surface complexes with TLR1/2 and increases the colon cell response to curli fibers (153). Intestinal epithelial cells directly respond to curli fibers on *S. enterica* leading to an increase in PI3K expression and a subsequent decrease in epithelial cell barrier permeability. The permeability of host gut epithelial cells was visualized via the migration of labelled beads through a polarized cell epithelial monolayer in the presence and absence of curli (155). Conversely, infection with non-curliated bacteria results in an epithelial barrier with increased permeability. The more permeable epithelial barrier allows higher bacterial titers in the cecal tissue and mesenteric lymph nodes (Figure 1.3) (154, 155). However, it is also important to note that although the barrier is reinforced, the curliated pathogens can overcome the protective immune response and cause inflammation. Interestingly, when curliated cells cross the epithelial barrier, multiple immune cells such as macrophages, dendritic cells and T cells respond by upregulating various proinflammatory cytokines including IL-6, IL-23, IL-17A, and IL-22 (156). Collectively, this work suggests that commensal curliated bacteria may exert protective effects on the epithelial barrier via TLR2 activation, but additional work is needed to elucidate the complex interplay of: curli, enteric bacteria, gut epithelial cells, and immune cells.

It is unknown whether curli interact with other pathogenic amyloids in the host environment. Intravenous injection of curli (along with other amyloids) into mice increases the

occurrence of amyloid protein A amyloidosis in spleens isolated from mice (157). Some interesting studies have looked at curli interaction with other amyloids *in vitro*. For example, islet amyloid polypeptide cannot decrease the lag time of CsgA amyloid formation, but CsgA or CsgB addition to $PAP_{248-286}$ decreased lag time and increased elongation rate of amyloid formation (119, 158). Clearly, more work needs to be done to fully understand the relationship between functional amyloids like curli and those produced by humans that are associated with protein misfolding and disease.

Enterobacteriaceae Extracellular Matrix Outside of the Host

E. coli and *S. enterica* also utilize biofilms in their lifecycle outside of the host. The strategy of gut microbes outside of the host shifts from growth and nutrient acquisition to a lifestyle of attachment, aerobiosis, and prolonged survival (13). Conditions associated with life outside of the host such as low temperature, low glucose and nutrients, and oxidative stress induce extracellular matrix production (46, 159-161). Curli and cellulose are generally co-expressed due to their mutual dependence on the transcriptional regulator CsgD (41, 64, 96). The extracellular matrix components cellulose and curli contribute to the survival of *S.enterica* serovar Typhimurium in both desiccation and bleach stress environmental conditions (81). Expression of both curli fibers and cellulose in the extracellular matrix fraction of rugose biofilms correlates with H_2O_2 resistance (46, 81). CsgD orchestrates the matrix fraction of rugose biofilms, and Δ*csgD* colonies are unable to spread and wrinkle (Figure 1.4A) (41, 46, 64). Conditions outside of the host induce curli and cellulose, which protect Enterobacteriaceae from these harsh conditions.

Colanic acid is an extracellular polysaccharide that has several uses in different *E. coli* strain and biofilms. Colanic acid is upregulated in conditions that occur outside of the host (162). In K12, colanic acid does not contribute to surface adherence, but is necessary for development of three dimensional architecture in biofilms on glass slides and for robust LB biofilm development in static culture (163, 164). In contrast to other surfaces, colonic acid does increase adherence of *E. coli* to alfalfa sprouts and to certain plastic surfaces (165).

The extracellular matrix helps bacteria remain in close proximity with one another and also facilitates attachment to the surfaces colonized in the extra-host environment (40, 166). Polymicrobial communities can be readily found in the soil or associated directly with plant roots. Amyloids play important roles in bacterial association with plant roots and leaves (Figure 1.4B). Curli increase the adherence of the pathogen *E. coli* O157:H7 to spinach leaves (167). Curli are important for *E. coli* attachment to alfalfa sprouts and seed coats (168). *E. coli* O157:H7 expressing curli strains are more hydrophobic and have increased binding to surfaces on produce (169). Interaction with the lettuce rhizosphere upregulates a curli regulator, Crl, and attachment to the rhizosphere is decreased in a curli mutant (170). Hou *et al.* found that *E. coli csgA* mutants have decreased attachment to lettuce roots compared to WT *E. coli* in a hydroponic assay system used to replicate the interactions between bacteria and the rhizosphere (the area of soil directly surrounding plant roots that is rich in interspecies signaling and plant exudate) (170). Microbial amyloids appear to have broad interaction with the rhizosphere: *B. subtilis* pellicle biofilm formation and the *tapA* gene (which encodes a protein important for bacterial amyloid formation) are upregulated by tomato plant root exudate (171).

Because polymicrobial interactions are commonplace, it is rare for natural bacterial communities to be composed of a single bacterial species. Polymicrobial community

development can be driven by interactions between extracellular fibers like curli. *S. enterica, Citrobacter koseri, Shewanella oneidensis,* and *E. coli* CsgA fibers can interact *in vitro* (172). These species also have interactions between the curli templator, CsgB, and the main structural subunit of curli, CsgA. *S. enterica csgA* and *E. coli csgB* mutants, along with *S. enterica csgB* and *E. coli csgA* mutants can complement each other leading to curli fiber formation, pellicle biofilm formation, and increased surface attachment (173). Interactions with plant leaves, roots, and other bacterial species lend support to the notion that curli are a community resource that can be deployed for multiple functions in the environment. Bacterial amyloids influence the interaction between host and microbe in many different ways including augmentation of resistance to host defense and increasing the attachment of microbes to each other and to common food sources of humans.

Conclusions and thoughts for future studies

Microbial amyloids are a ubiquitous community resource utilized by bacteria both inside and outside of the host. Amyloid fibers have functions ranging from tightening gut epithelial cell junctions to increasing community and surface adherence. The role of curli in increasing adherence to various surfaces and resisting various stresses in the environment may shed light on how curli impact the development of communities within the host. Curli may increase *E. coli*'s ability to associate with one another or host tissues in the gastrointestinal tract or during pathogenesis. The complex interplay between microbial amyloids and the host is just beginning to be unraveled. Continued elucidation of bacterial amyloid biology will further our knowledge of the role of functional amyloids: in disease, commensal-host interaction, and microbial

community development. This knowledge could lead to potential therapies or pro-biotics to exploit amyloid formation in the host and environment.

The fantastic understanding we have of *E. coli* physiology, combined with the wealth of genetic tools afforded by *E. coli*, provides an exciting platform for understanding biofilm biology. We must better define the role that curli and cellulose play in the life cycle of enteric bacteria like *E. coli*. To date, only a few studies have attempted to assess the prevalence of curli and cellulose in environmental soil and water samples. Understanding fully the range of curli in natural environments will allow a greater appreciation of the importance of the ECM to Earth's microbiota. We must also better understand the role that the ECM plays in mediating interactions with plants and animals. Advancing the biochemical knowledge of the curli-plant interaction could foster various treatments for preventing and removing contaminating bacteria on fresh produce.

How the ECM shapes the infectious cycle of important human pathogens has yet to be defined. Antibodies are produced against curli in patients suffering from sepsis, so the host is clearly exposed to curli during an infection (147, 155). Curli have been shown to augment epithelial cell barriers, and to decrease titers in extraintestinal tissue of mice, suggesting that curliated bacteria in the intestinal tract might lead to a commensal relationship between resident flora and mammalian gut cells (155). An important part of this equation will be to determine how certain isolates of *E. coli* and *S. enterica* produce cellulose and curli at human body temperature, while other strains only produce curli in temperatures less than 30°C. Study of various ECM activation pathways of *E. coli* at human body temperatures could lead to potential powerful therapeutic molecular targets for ECM related *E. coli* infections.

This thesis aims to look at novel pathways that activate ECM production in UPEC at 26°C and 37°C. Reducing conditions induce cellulose production in UPEC in the presence of curli-inhibitory conditions including 37°C through the misfolding of the disulfide bound periplasmic protein YfiR (Chapter 2). I have found the reduced thiols in cysteine auxotrophs inhibited cellulose production at 26 and 37°C and promoted curli production at 37°C (Chapter 3). Patient isolates that are cysteine auxotrophs likewise show a greater propensity to produce curli at 37°C (Chapter 3). Finally I show glucose inhibits UPEC ECM production. In the absence of glucose CRP-cAMP directly regulates the promoter of *csgD* (Chapter 4). The following work contributes to the burgeoning field of ECM activation and inhibition pathways of UPEC and reveals novel questions about temperature-independent and redox-mediated ECM production.

Figures:

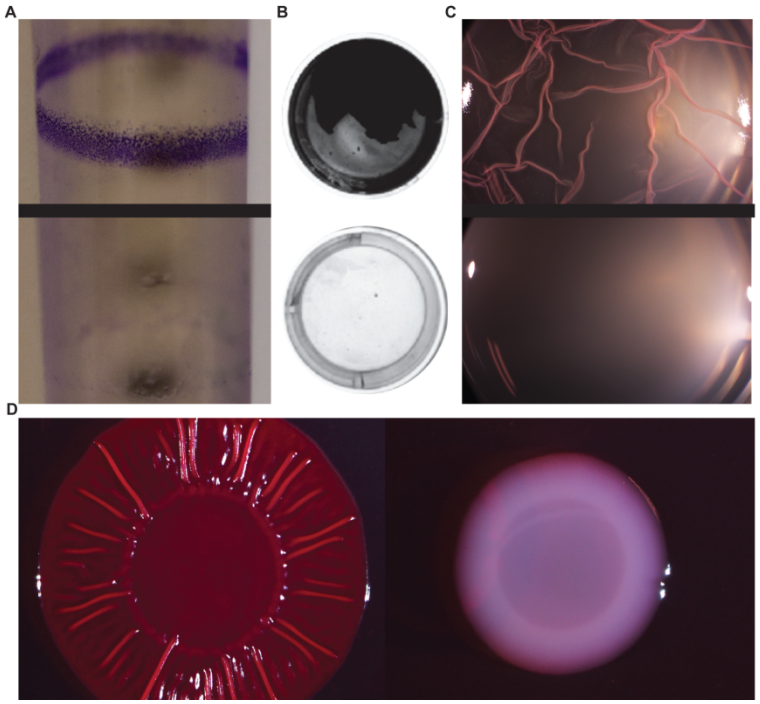

Figure 1.1- Laboratory *E. coli* biofilm models. A) Ring biofilm stained by crystal violet. Cultures were grown in LB media in glass tubes at 26°C for 48 hours. Liquid culture was removed and tube was stained with .1% (w/v) crystal violet (CV) for 5minutes. Tubes were subsequently washed with water. The top image is a WT strain and the lower image is a flagella mutant (*fliC*::kan) **B)** Pellicle biofilms grown in 24 well plate for 48 hours at 26°C. Liquid media was removed followed by 5 minutes of staining with .1% CV. Stained pellicles were washed 3x with water prior to imaging. The top image is a CV stained WT UTI89 pellicle, whereas the lower picture was a culture of a Δ*csgD* mutant that did not produce a pellicle. **C)** Pellicle biofilms grown in 1:7500 (Congo red:YESCA) media in a 24 well dish for 48 hours at 26°C. The top image shows a WT UTI89 culture that produced a pellicle, whereas the lower image is a culture of a Δ*csgD* mutant that did not form a pellicle. **D)** 4µL spots of 1-OD_{600} *E. coli* were grown at 26°C for 48 hours on YESCA CR plates. The colony on the left is UTI89 WT on the right is a *csgD* mutant colony.

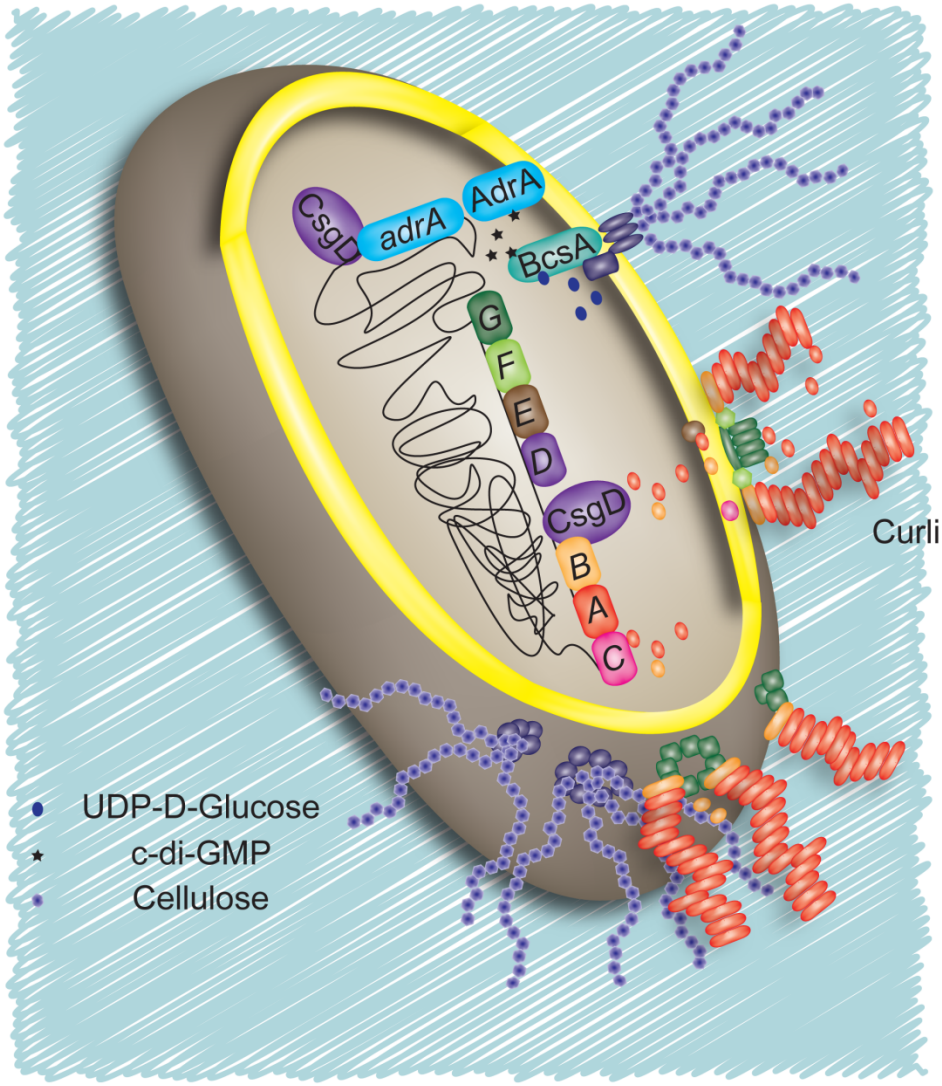

Figure 1.2- ECM production model. CsgD is the master regulator of the biofilm extracellular matrix. CsgD transcriptionally upregulates the *csgB* and *csgA* genes, which encode the minor and major curli fiber subunits, respectively. CsgA and CsgB are secreted through an outermembrane pore formed by CsgG. CsgE is thought to facilitate translocation of curli subunits across the outer membrane by capping the periplasmic side of the secretion vestibule so that movement in the channel is unidirectional. CsgB associates with the cell surface and templates amyloid polymerization of CsgA. CsgD also transcriptionally upregulates *adrA*. AdrA is an inner membrane diguanylate cyclase, which produces the secondary messenger, c-di-GMP. c-di-GMP binds and activates BcsA, which then produces cellulose fibers via the building block UDP-glucose. C-di-GMP that activates BcsA can also be produced via YedQ and YfiN.

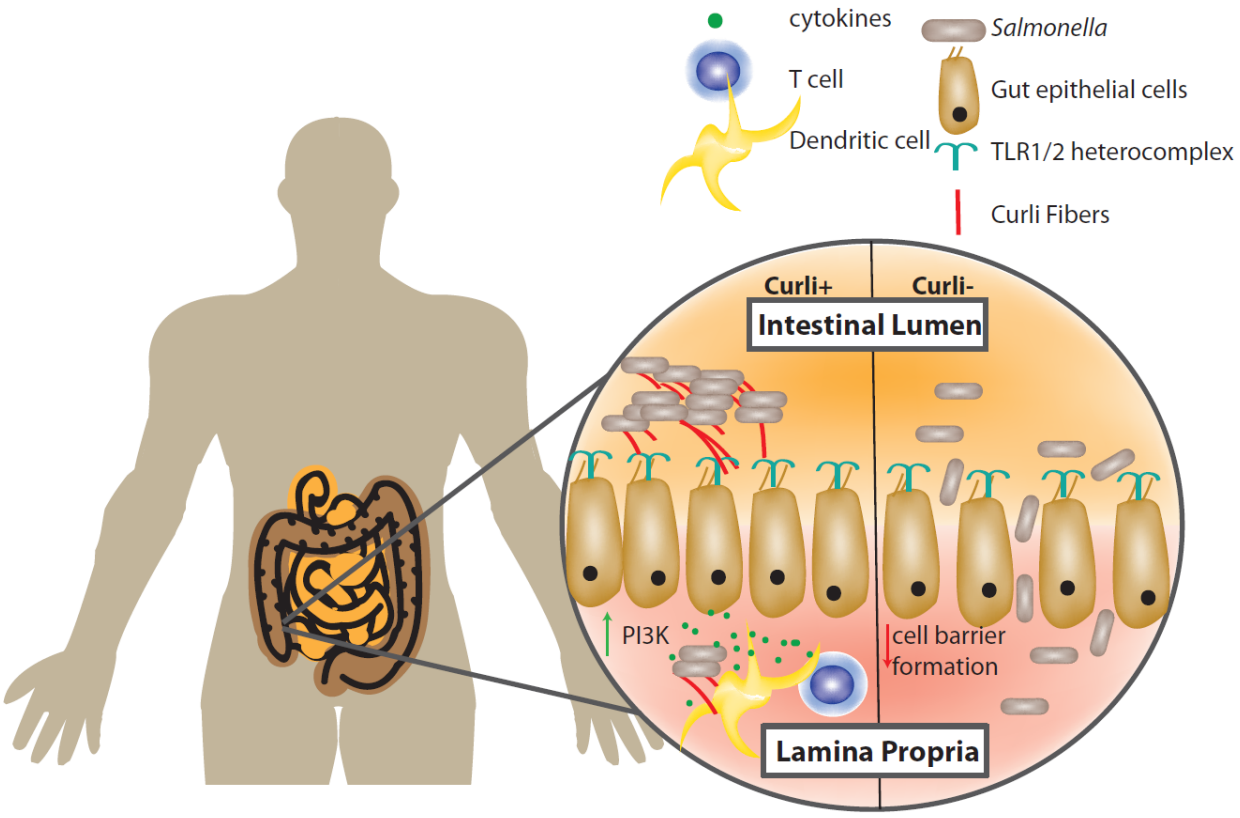

Figure 1.3- Gut epithelial cells and the host immune system recognize curli fibers. *S. enterica* and *E. coli* are intestinal dwelling bacteria, whose curli fibers are recognized by host epithelial cells. TLR1/2 heterocomplex recognizes the mature curli fiber and causes a signaling cascade in host cells. Recognition of curli results in an increase in PI3K in gut epithelial cells and increases gut epithelial cell barrier formation. Curliated *S. enterica* elicit an increase in cytokine production by T cells and dendritic cells. *S. enterica* curli mutants cause decreased epithelial cell barrier formation and lead to increased extraintestinal titers of *S. enterica*.

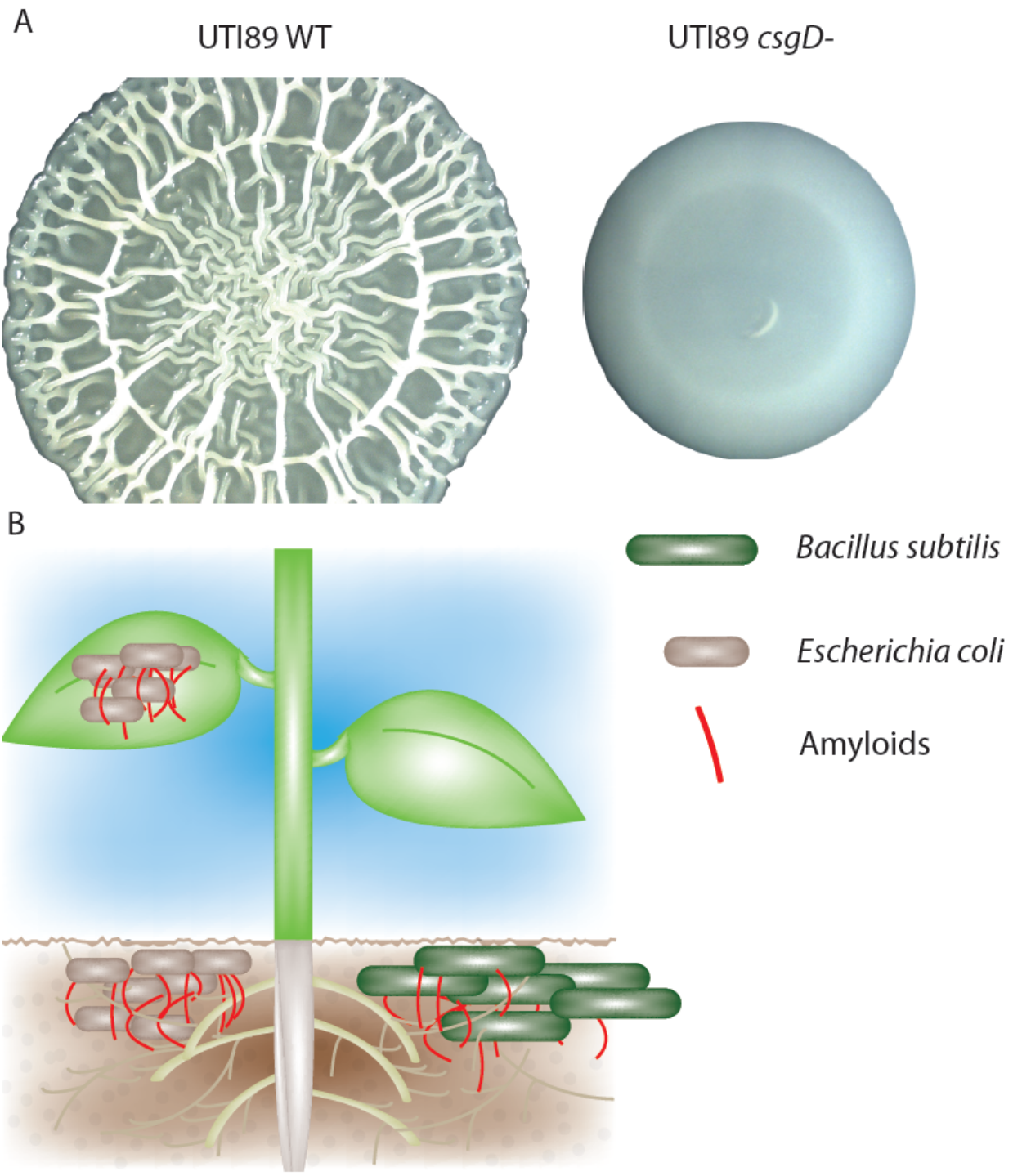

Figure 1.4- Bacterial amyloids are utilized in multiple environments. A) *E. coli* UPEC (UTI89) rugose biofilms form a complex spreading and wrinkling pattern that is dependent on the biofilm regulator CsgD. *csgD* mutant colonies do not spread or wrinkle. B) Curli are utilized by *E. coli* for increased adherence to lettuce roots and spinach leaves. *Bacillus subtilis* amyloid fiber proteins and biofilm formation are induced in the presence of tomato plant root exudate.

Notes and Acknowledgements

Portions of this Introduction and the Figures were published in *Plos Pathogens* (Hufnagel *et al.* 2013), *Microbial Spectrum (*Hufnagel *et al. 2015),* and *ASM Biofilms* (Hufnagel *et al.* 2015). Will DePas helped with the work that was published in *Microbial Spectrum* and *ASM Biofilms,* and Çagla Tükel (Temple University) helped with the work that is published in *Plos Pathogens.*

1. **Farmer JJ, Davis BR, Hickmanbrenner FW, Mcwhorter A, Huntleycarter GP, Asbury MA, Riddle C, Wathengrady HG, Elias C, Fanning GR, Steigerwalt AG, Ohara CM, Morris GK, Smith PB, Brenner DJ.** 1985. Biochemical-Identification of New Species and Biogroups of Enterobacteriaceae Isolated from Clinical Specimens. J Clin Microbiol **21:**46-76.
2. **Kaas RS, Friis C, Ussery DW, Aarestrup FM.** 2012. Estimating variation within the genes and inferring the phylogeny of 186 sequenced diverse *Escherichia coli* genomes. Bmc Genomics **13**.
3. **Touchon M, Hoede C, Tenaillon O, Barbe V, Baeriswyl S, Bidet P, Bingen E, Bonacorsi S, Bouchier C, Bouvet O, Calteau A, Chiapello H, Clermont O, Cruveiller S, Danchin A, Diard M, Dossat C, El Karoui M, Frapy E, Garry L, Ghigo JM, Gilles AM, Johnson J, Le Bouguenec C, Lescat M, Mangenot S, Martinez-Jehanne V, Matic I, Nassif X, Oztas S, Petit MA, Pichon C, Rouy Z, Saint Ruf C, Schneider D, Tourret J, Vacherie B, Vallenet D, Medigue C, Rocha EPC, Denamur E.** 2009. Organised Genome Dynamics in the *Escherichia coli* Species Results in Highly Diverse Adaptive Paths. Plos Genetics **5**.
4. **Kaper JB, Nataro JP, Mobley HL.** 2004. Pathogenic *Escherichia coli*. Nature reviews Microbiology **2:**123-140.
5. **Tenaillon O, Skurnik D, Picard B, Denamur E.** 2010. The population genetics of commensal *Escherichia coli*. Nature Reviews Microbiology **8:**207-217.
6. **Smith HW.** 1965. Observations on the Flora of the Alimentary Tract of Animals and Factors Affecting Its Composition. J Pathol Bacteriol **89:**95-122.
7. **Shulman ST, Friedmann HC, Sims RH.** 2007. Theodor Escherich: the first pediatric infectious diseases physician? Clin Infect Dis **45:**1025-1029.
8. **Mitsuoka T, Hayakawa K, Kimura N.** 1975. [The fecal flora of man. III. Communication: The composition of Lactobacillus flora of different age groups (author's transl)]. Zentralblatt fur Bakteriologie, Parasitenkunde, Infektionskrankheiten und Hygiene Erste Abteilung Originale Reihe A: Medizinische Mikrobiologie und Parasitologie **232:**499-511.
9. **Savageau MA.** 1983. *Escherichia-Coli* Habitats, Cell-Types, and Molecular Mechanisms of Gene-Control. American Naturalist **122:**732-744.

10. **Unden G, Bongaerts J.** 1997. Alternative respiratory pathways of *Escherichia coli*: energetics and transcriptional regulation in response to electron acceptors. Biochimica et biophysica acta **1320:**217-234.
11. **Jones SA, Chowdhury FZ, Fabich AJ, Anderson A, Schreiner DM, House AL, Autieri SM, Leatham MP, Lins JJ, Jorgensen M, Cohen PS, Conway T.** 2007. Respiration of *Escherichia coli* in the mouse intestine. Infection and immunity **75:**4891-4899.
12. **Jones SA, Gibson T, Maltby RC, Chowdhury FZ, Stewart V, Cohen PS, Conway T.** 2011. Anaerobic respiration of *Escherichia coli* in the mouse intestine. Infection and immunity **79:**4218-4226.
13. **Winfield MD, Groisman EA.** 2003. Role of nonhost environments in the lifestyles of *Salmonella* and *Escherichia coli*. Appl Environ Microbiol **69:**3687-3694.
14. **Ishii S, Ksoll WB, Hicks RE, Sadowsky MJ.** 2006. Presence and growth of naturalized *Escherichia coli* in temperate soils from Lake Superior watersheds. Appl Environ Microbiol **72:**612-621.
15. **Ferens WA, Hovde CJ.** 2011. *Escherichia coli* O157:H7: animal reservoir and sources of human infection. Foodborne pathogens and disease **8:**465-487.
16. **Orth D, Grif K, Zimmerhackl LB, Wurzner R.** 2008. Prevention and treatment of enterohemorrhagic *Escherichia coli* infections in humans. Expert Review of Anti-Infective Therapy **6:**101-108.
17. **Gyles CL.** 2007. Shiga toxin-producing *Escherichia coli*: an overview. Journal of animal science **85:**E45-62.
18. **Laven RA, Ashmore A, Stewart CS.** 2003. *Escherichia coli* in the rumen and colon of slaughter cattle, with particular reference to E. coli O157. Veterinary journal **165:**78-83.
19. **Widiasih DA, Ido N, Omoe K, Sugii S, Shinagawa K.** 2004. Duration and magnitude of faecal shedding of Shiga toxin-producing *Escherichia coli* from naturally infected cattle. Epidemiology and infection **132:**67-75.
20. **Fegan N, Vanderlinde P, Higgs G, Desmarchelier P.** 2004. The prevalence and concentration of *Escherichia coli* O157 in faeces of cattle from different production systems at slaughter. Journal of applied microbiology **97:**362-370.
21. **Kudva IT, Blanch K, Hovde CJ.** 1998. Analysis of *Escherichia coli* O157:H7 survival in ovine or bovine manure and manure slurry. Applied and environmental microbiology **64:**3166-3174.
22. **Locking ME, O'Brien SJ, Reilly WJ, Wright EM, Campbell DM, Coia JE, Browning LM, Ramsay CN.** 2001. Risk factors for sporadic cases of *Escherichia coli* O157 infection: the importance of contact with animal excreta. Epidemiology and infection **127:**215-220.
23. **Solomon EB, Yaron S, Matthews KR.** 2002. Transmission of *Escherichia coli* O157:H7 from contaminated manure and irrigation water to lettuce plant tissue and its subsequent internalization. Applied and environmental microbiology **68:**397-400.
24. **Islam M, Doyle MP, Phatak SC, Millner P, Jiang X.** 2004. Persistence of enterohemorrhagic *Escherichia coli* O157:H7 in soil and on leaf lettuce and parsley grown in fields treated with contaminated manure composts or irrigation water. Journal of food protection **67:**1365-1370.

25. **Jablasone J, Warriner K, Griffiths M.** 2005. Interactions of *Escherichia coli* O157:H7, *Salmonella* typhimurium and *Listeria monocytogenes* plants cultivated in a gnotobiotic system. International journal of food microbiology **99:**7-18.
26. **Sivick KE, Mobley HL.** 2010. Waging war against uropathogenic *Escherichia coli*: winning back the urinary tract. Infect Immun **78:**568-585.
27. **Chen SL, Wu M, Henderson JP, Hooton TM, Hibbing ME, Hultgren SJ, Gordon JI.** 2013. Genomic diversity and fitness of E. coli strains recovered from the intestinal and urinary tracts of women with recurrent urinary tract infection. Science translational medicine **5:**184ra160.
28. **Manges AR, Johnson JR.** 2012. Food-borne origins of *Escherichia coli* causing extraintestinal infections. Clinical infectious diseases : an official publication of the Infectious Diseases Society of America **55:**712-719.
29. **Yamamoto S, Tsukamoto T, Terai A, Kurazono H, Takeda Y, Yoshida O.** 1997. Genetic evidence supporting the fecal-perineal-urethral hypothesis in cystitis caused by *Escherichia coli*. The Journal of urology **157:**1127-1129.
30. **Johnson JR, Kuskowski MA, Smith K, O'Bryan TT, Tatini S.** 2005. Antimicrobial-resistant and extraintestinal pathogenic *Escherichia coli* in retail foods. The Journal of infectious diseases **191:**1040-1049.
31. **Phillips I, Eykyn S, King A, Gransden WR, Rowe B, Frost JA, Gross RJ.** 1988. Epidemic multiresistant *Escherichia coli* infection in West Lambeth Health District. Lancet **1:**1038-1041.
32. **Manges AR, Johnson JR, Foxman B, O'Bryan TT, Fullerton KE, Riley LW.** 2001. Widespread distribution of urinary tract infections caused by a multidrug-resistant *Escherichia coli* clonal group. N Engl J Med **345:**1007-1013.
33. **Mulvey MA, Schilling JD, Hultgren SJ.** 2001. Establishment of a persistent *Escherichia coli* reservoir during the acute phase of a bladder infection. Infect Immun **69:**4572-4579.
34. **Wright KJ, Seed PC, Hultgren SJ.** 2007. Development of intracellular bacterial communities of uropathogenic *Escherichia coli* depends on type 1 pili. Cell Microbiol **9:**2230-2241.
35. **Blango MG, Mulvey MA.** 2010. Persistence of uropathogenic *Escherichia coli* in the face of multiple antibiotics. Antimicrob Agents Chemother **54:**1855-1863.
36. **Jorgensen I, Seed PC.** 2012. How to Make It in the Urinary Tract: A Tutorial by *Escherichia coli*. PLoS Pathog **8**.
37. **Stewart PS, Franklin MJ.** 2008. Physiological heterogeneity in biofilms. Nat Rev Microbiol **6:**199-210.
38. **Hall-Stoodley L, Costerton JW, Stoodley P.** 2004. Bacterial biofilms: From the natural environment to infectious diseases. Nature Reviews Microbiology **2:**95-108.
39. **Wilson M.** 2001. Bacterial biofilms and human disease. Sci Prog **84:**235-254.
40. **Vidal O, Longin R, Prigent-Combaret C, Dorel C, Hooreman M, Lejeune P.** 1998. Isolation of an *Escherichia coli* K-12 mutant strain able to form biofilms on inert surfaces: Involvement of a new *ompR* allele that increases curli expression. J Bacteriol **180:**2442-2449.
41. **Zogaj X, Nimtz M, Rohde M, Bokranz W, Romling U.** 2001. The multicellular morphotypes of *Salmonella* typhimurium and *Escherichia coli* produce cellulose as the second component of the extracellular matrix. Mol Microbiol **39:**1452-1463.

42. **Whitchurch CB, Tolker-Nielsen T, Ragas PC, Mattick JS.** 2002. Extracellular DNA required for bacterial biofilm formation. Science **295:**1487-1487.
43. **Beloin C, Roux A, Ghigo JM.** 2008. *Escherichia coli* biofilms. Current topics in microbiology and immunology **322:**249-289.
44. **Bachmann BJ.** 1972. Pedigrees of Some Mutant Strains of *Escherichia-Coli* K-12. Bacteriological Reviews **36:**525-557.
45. **Fux CA, Shirtliff M, Stoodley P, Costerton JW.** 2005. Can laboratory reference strains mirror 'real-world' pathogenesis? Trends Microbiol **13:**58-63.
46. **Depas WH, Hufnagel DA, Lee JS, Blanco LP, Bernstein HC, Fisher ST, James GA, Stewart PS, Chapman MR.** 2013. Iron induces bimodal population development by *Escherichia coli*. Proc Natl Acad Sci U S A **110:**2629-2634.
47. **Hadjifrangiskou M, Gu AP, Pinkner JS, Kostakioti M, Zhang EW, Greene SE, Hultgren SJ.** 2012. Transposon mutagenesis identifies uropathogenic *Escherichia coli* biofilm factors. J Bacteriol **194:**6195-6205.
48. **Uhlich GA, Cooke PH, Solomon EB.** 2006. Analyses of the red-dry-rough phenotype of an *Escherichia coli* O157:H7 strain and its role in biofilm formation and resistance to antibacterial agents. Appl Environ Microbiol **72:**2564-2572.
49. **Liu NT, Nou X, Lefcourt AM, Shelton DR, Lo YM.** 2014. Dual-species biofilm formation by *Escherichia coli* O157:H7 and environmental bacteria isolated from fresh-cut processing facilities. Int J Food Microbiol **171:**15-20.
50. **Reisner A, Krogfelt KA, Klein BM, Zechner EL, Molin S.** 2006. *In vitro* biofilm formation of commensal and pathogenic *Escherichia coli* strains: impact of environmental and genetic factors. J Bacteriol **188:**3572-3581.
51. **Serra DO, Richter AM, Klauck G, Mika F, Hengge R.** 2013. Microanatomy at cellular resolution and spatial order of physiological differentiation in a bacterial biofilm. mBio **4:**e00103-00113.
52. **Boles BR, Singh PK.** 2008. Endogenous oxidative stress produces diversity and adaptability in biofilm communities. Proc Natl Acad Sci U S A **105:**12503-12508.
53. **Chai Y, Chu F, Kolter R, Losick R.** 2008. Bistability and biofilm formation in *Bacillus subtilis*. Molecular microbiology **67:**254-263.
54. **Boles BR, Thoendel M, Singh PK.** 2004. Self-generated diversity produces "insurance effects" in biofilm communities. Proceedings of the National Academy of Sciences of the United States of America **101:**16630-16635.
55. **Xu KD, Stewart PS, Xia F, Huang CT, McFeters GA.** 1998. Spatial physiological heterogeneity in *Pseudomonas aeruginosa* biofilm is determined by oxygen availability. Applied and environmental microbiology **64:**4035-4039.
56. **Williamson KS, Richards LA, Perez-Osorio AC, Pitts B, McInnerney K, Stewart PS, Franklin MJ.** 2012. Heterogeneity in *Pseudomonas aeruginosa* biofilms includes expression of ribosome hibernation factors in the antibiotic-tolerant subpopulation and hypoxia-induced stress response in the metabolically active population. Journal of bacteriology **194:**2062-2073.
57. **Lewis K.** 2008. Multidrug tolerance of biofilms and persister cells. Current topics in microbiology and immunology **322:**107-131.
58. **Pratt LA, Kolter R.** 1998. Genetic analysis of *Escherichia coli* biofilm formation: roles of flagella, motility, chemotaxis and type I pili. Molecular microbiology **30:**285-293.

59. **Hung C, Zhou YZ, Pinkner JS, Dodson KW, Crowley JR, Heuser J, Chapman MR, Hadjifrangiskou M, Henderson JP, Hultgren SJ.** 2013. *Escherichia coli* Biofilms Have an Organized and Complex Extracellular Matrix Structure. Mbio **4**.
60. **Wang X, Preston JF, 3rd, Romeo T.** 2004. The *pgaABCD* locus of *Escherichia coli* promotes the synthesis of a polysaccharide adhesin required for biofilm formation. Journal of bacteriology **186:**2724-2734.
61. **Cegelski L, Pinkner JS, Hammer ND, Cusumano CK, Hung CS, Chorell E, Aberg V, Walker JN, Seed PC, Almqvist F, Chapman MR, Hultgren SJ.** 2009. Small-molecule inhibitors target *Escherichia coli* amyloid biogenesis and biofilm formation. Nat Chem Biol **5:**913-919.
62. **Bokranz W, Wang X, Tschape H, Romling U.** 2005. Expression of cellulose and curli fimbriae by *Escherichia coli* isolated from the gastrointestinal tract. Journal of Medical Microbiology **54:**1171-1182.
63. **Zhou Y, Smith DR, Hufnagel DA, Chapman MR.** 2013. Experimental manipulation of the microbial functional amyloid called curli. Methods Mol Biol **966:**53-75.
64. **Hammar M, Arnqvist A, Bian Z, Olsen A, Normark S.** 1995. Expression of two *csg* operons is required for production of fibronectin- and Congo red-binding curli polymers in *Escherichia coli* K-12. Mol Microbiol **18:**661-670.
65. **Jubelin G, Vianney A, Beloin C, Ghigo JM, Lazzaroni JC, Lejeune P, Dorel C.** 2005. CpxR/OmpR interplay regulates curli gene expression in response to osmolarity in *Escherichia coli*. J Bacteriol **187:**2038-2049.
66. **Zheng D, Constantinidou C, Hobman JL, Minchin SD.** 2004. Identification of the CRP regulon using in vitro and in vivo transcriptional profiling. Nucleic Acids Res **32:**5874-5893.
67. **Olsen A, Arnqvist A, Hammar M, Sukupolvi S, Normark S.** 1993. The RpoS sigma factor relieves H-NS-mediated transcriptional repression of *csgA*, the subunit gene of fibronectin-binding curli in *Escherichia coli*. Molecular microbiology **7:**523-536.
68. **Hufnagel DA, DePas WH, Chapman MR.** 2014. The Disulfide Bonding System Suppresses CsgD-independent Cellulose Production in E. coli. J Bacteriol doi:10.1128/JB.02019-14.
69. **Wu C, Lim JY, Fuller GG, Cegelski L.** 2012. Quantitative analysis of amyloid-integrated biofilms formed by uropathogenic *Escherichia coli* at the air-liquid interface. Biophysical Journal **103:**464-471.
70. **Wai SN, Mizunoe Y, Takade A, Kawabata SI, Yoshida SI.** 1998. *Vibrio cholerae* O1 strain TSI-4 produces the exopolysaccharide materials that determine colony morphology, stress resistance, and biofilm formation. Applied and environmental microbiology **64:**3648-3655.
71. **Yildiz FH, Dolganov NA, Schoolnik GK.** 2001. VpsR, a Member of the Response Regulators of the Two-Component Regulatory Systems, Is Required for Expression of vps Biosynthesis Genes and EPS(ETr)-Associated Phenotypes in *Vibrio cholerae* O1 El Tor. Journal of bacteriology **183:**1716-1726.
72. **Yildiz FH, Liu XS, Heydorn A, Schoolnik GK.** 2004. Molecular analysis of rugosity in a *Vibrio cholerae* O1 El Tor phase variant. Molecular microbiology **53:**497-515.
73. **Asally M, Kittisopikul M, Rue P, Du Y, Hu Z, Cagatay T, Robinson AB, Lu H, Garcia-Ojalvo J, Suel GM.** 2012. Localized cell death focuses mechanical forces during

3D patterning in a biofilm. Proceedings of the National Academy of Sciences of the United States of America **109:**18891-18896.

74. **Dietrich LE, Okegbe C, Price-Whelan A, Sakhtah H, Hunter RC, Newman DK.** 2013. Bacterial community morphogenesis is intimately linked to the intracellular redox state. Journal of bacteriology **195:**1371-1380.
75. **Epstein AK, Pokroy B, Seminara A, Aizenberg J.** 2011. Bacterial biofilm shows persistent resistance to liquid wetting and gas penetration. Proc Natl Acad Sci U S A **108:**995-1000.
76. **Kolodkin-Gal I, Elsholz AK, Muth C, Girguis PR, Kolter R, Losick R.** 2013. Respiration control of multicellularity in *Bacillus subtilis* by a complex of the cytochrome chain with a membrane-embedded histidine kinase. Genes & development **27:**887-899.
77. **Romling U, Sierralta WD, Eriksson K, Normark S.** 1998. Multicellular and aggregative behaviour of *Salmonella* typhimurium strains is controlled by mutations in the *agfD* promoter. Mol Microbiol **28:**249-264.
78. **Romling U.** 2005. Characterization of the rdar morphotype, a multicellular behaviour in Enterobacteriaceae. Cellular and Molecular Life Sciences **62:**1234-1246.
79. **Lim JY, May JM, Cegelski L.** 2012. Dimethyl sulfoxide and ethanol elicit increased amyloid biogenesis and amyloid-integrated biofilm formation in *Escherichia coli*. Appl Environ Microbiol **78:**3369-3378.
80. **McCrate OA, Zhou X, Reichhardt C, Cegelski L.** 2013. Sum of the parts: composition and architecture of the bacterial extracellular matrix. Journal of molecular biology **425:**4286-4294.
81. **White AP, Gibson DL, Kim W, Kay WW, Surette MG.** 2006. Thin aggregative fimbriae and cellulose enhance long-term survival and persistence of *Salmonella*. J Bacteriol **188:**3219-3227.
82. **Serra DO, Richter AM, Hengge R.** 2013. Cellulose as an Architectural Element in Spatially Structured *Escherichia coli* Biofilms. J Bacteriol **195:**5540-5554.
83. **Weiss-Muszkat M, Shakh D, Zhou Y, Pinto R, Belausov E, Chapman MR, Sela S.** 2010. Biofilm formation by and multicellular behavior of *Escherichia coli* O55:H7, an atypical enteropathogenic strain. Applied and environmental microbiology **76:**1545-1554.
84. **Lim JY, Pinkner JS, Cegelski L.** 2014. Community behavior and amyloid-associated phenotypes among a panel of uropathogenic *E. coli*. Biochemical and biophysical research communications **443:**345-350.
85. **Zogaj X, Bokranz W, Nimtz M, Romling U.** 2003. Production of cellulose and curli fimbriae by members of the family Enterobacteriaceae isolated from the human gastrointestinal tract. Infect Immun **71:**4151-4158.
86. **Romling U, Rohde M, Olsen A, Normark S, Reinkoster J.** 2000. AgfD, the checkpoint of multicellular and aggregative behaviour in *Salmonella* typhimurium regulates at least two independent pathways. Mol Microbiol **36:**10-23.
87. **Gao R, Mack TR, Stock AM.** 2007. Bacterial response regulators: versatile regulatory strategies from common domains. Trends in biochemical sciences **32:**225-234.
88. **Skerker JM, Perchuk BS, Siryaporn A, Lubin EA, Ashenberg O, Goulian M, Laub MT.** 2008. Rewiring the specificity of two-component signal transduction systems. Cell **133:**1043-1054.

89. **Stock AM, Robinson VL, Goudreau PN.** 2000. Two-component signal transduction. Annual review of biochemistry **69:**183-215.
90. **Zakikhany K, Harrington CR, Nimtz M, Hinton JCD, Romling U.** 2010. Unphosphorylated CsgD controls biofilm formation in *Salmonella enterica* serovar Typhimurium. Molecular Microbiology **77:**771-786.
91. **Wang L, Tian X, Wang J, Yang H, Fan K, Xu G, Yang K, Tan H.** 2009. Autoregulation of antibiotic biosynthesis by binding of the end product to an atypical response regulator. Proceedings of the National Academy of Sciences of the United States of America **106:**8617-8622.
92. **Sitnikov DM, Schineller JB, Baldwin TO.** 1995. Transcriptional regulation of bioluminesence genes from Vibrio fischeri. Molecular microbiology **17:**801-812.
93. **Evans ML, Chapman MR.** 2013. Curli biogenesis: Order out of disorder. Biochim Biophys Acta doi:10.1016/j.bbamcr.2013.09.010.
94. **Mika F, Hengge R.** 2013. Small Regulatory RNAs in the Control of Motility and Biofilm Formation in *E. coli* and *Salmonella*. International journal of molecular sciences **14:**4560-4579.
95. **Olsen A, Jonsson A, Normark S.** 1989. Fibronectin binding mediated by a novel class of surface organelles on *Escherichia coli*. Nature **338:**652-655.
96. **Romling U, Bian Z, Hammar M, Sierralta WD, Normark S.** 1998. Curli fibers are highly conserved between *Salmonella* typhimurium and *Escherichia coli* with respect to operon structure and regulation. J Bacteriol **180:**722-731.
97. **Romling U, Gomelsky M, Galperin MY.** 2005. C-di-GMP: the dawning of a novel bacterial signalling system. Mol Microbiol **57:**629-639.
98. **Simm R, Morr M, Kader A, Nimtz M, Romling U.** 2004. GGDEF and EAL domains inversely regulate cyclic di-GMP levels and transition from sessility to motility. Mol Microbiol **53:**1123-1134.
99. **Sommerfeldt N, Possling A, Becker G, Pesavento C, Tschowri N, Hengge R.** 2009. Gene expression patterns and differential input into curli fimbriae regulation of all GGDEF/EAL domain proteins in *Escherichia coli*. Microbiology-Sgm **155:**1318-1331.
100. **Weber H, Pesavento C, Possling A, Tischendorf G, Hengge R.** 2006. Cyclic-di-GMP-mediated signalling within the sigma network of *Escherichia coli*. Molecular microbiology **62:**1014-1034.
101. **Hengge R.** 2009. Principles of c-di-GMP signalling in bacteria. Nature Reviews Microbiology **7:**263-273.
102. **Brombacher E, Dorel C, Zehnder AJ, Landini P.** 2003. The curli biosynthesis regulator CsgD co-ordinates the expression of both positive and negative determinants for biofilm formation in *Escherichia coli*. Microbiology **149:**2847-2857.
103. **Gualdi L, Tagliabue L, Landini P.** 2007. Biofilm formation-gene expression relay system in *Escherichia coli*: modulation of sigmaS-dependent gene expression by the CsgD regulatory protein via sigmaS protein stabilization. Journal of bacteriology **189:**8034-8043.
104. **Ogasawara H, Yamamoto K, Ishihama A.** 2011. Role of the biofilm master regulator CsgD in cross-regulation between biofilm formation and flagellar synthesis. J Bacteriol **193:**2587-2597.

105. **Collinson SK, Emody L, Muller KH, Trust TJ, Kay WW.** 1991. Purification and characterization of thin, aggregative fimbriae from *Salmonella* enteritidis. J Bacteriol **173:**4773-4781.
106. **Arnqvist A, Olsen A, Pfeifer J, Russell DG, Normark S.** 1992. The Crl protein activates cryptic genes for curli formation and fibronectin binding in *Escherichia coli* HB101. Mol Microbiol **6:**2443-2452.
107. **Chapman MR, Robinson LS, Pinkner JS, Roth R, Heuser J, Hammar M, Normark S, Hultgren SJ.** 2002. Role of *Escherichia coli* curli operons in directing amyloid fiber formation. Science **295:**851-855.
108. **Fowler DM, Koulov AV, Balch WE, Kelly JW.** 2007. Functional amyloid--from bacteria to humans. Trends Biochem Sci **32:**217-224.
109. **Schwartz K, Syed AK, Stephenson RE, Rickard AH, Boles BR.** 2012. Functional amyloids composed of phenol soluble modulins stabilize *Staphylococcus aureus* biofilms. PLoS Pathog **8:**e1002744.
110. **Romero D, Aguilar C, Losick R, Kolter R.** 2010. Amyloid fibers provide structural integrity to *Bacillus subtilis* biofilms. Proc Natl Acad Sci U S A **107:**2230-2234.
111. **Alteri CJ, Xicohtencatl-Cortes J, Hess S, Caballero-Olin G, Giron JA, Friedman RL.** 2007. *Mycobacterium tuberculosis* produces pili during human infection. Proc Natl Acad Sci U S A **104:**5145-5150.
112. **Larsen P, Nielsen JL, Dueholm MS, Wetzel R, Otzen D, Nielsen PH.** 2007. Amyloid adhesins are abundant in natural biofilms. Environ Microbiol **9:**3077-3090.
113. **Dueholm MS, Albertsen M, Otzen D, Nielsen PH.** 2012. Curli functional amyloid systems are phylogenetically widespread and display large diversity in operon and protein structure. PLoS One **7:**e51274.
114. **White AP, Sibley KA, Sibley CD, Wasmuth JD, Schaefer R, Surette MG, Edge TA, Neumann NF.** 2011. Intergenic sequence comparison of *Escherichia coli* isolates reveals lifestyle adaptations but not host specificity. Appl Environ Microbiol **77:**7620-7632.
115. **Hammar M, Bian Z, Normark S.** 1996. Nucleator-dependent intercellular assembly of adhesive curli organelles in *Escherichia coli*. Proceedings of the National Academy of Sciences of the United States of America **93:**6562-6566.
116. **Bian Z, Normark S.** 1997. Nucleator function of CsgB for the assembly of adhesive surface organelles in *Escherichia coli*. The EMBO journal **16:**5827-5836.
117. **Abdallah AM, Van Pittius NCG, Champion PAD, Cox J, Luirink J, Vandenbroucke-Grauls CMJE, Appelmelk BJ, Bitter W.** 2007. Type VII secretion - mycobacteria show the way. Nature Reviews Microbiology **5:**883-891.
118. **Desvaux M, Hebraud M, Talon R, Henderson IR.** 2009. Secretion and subcellular localizations of bacterial proteins: a semantic awareness issue. Trends Microbiol **17:**139-145.
119. **Hammer ND, Schmidt JC, Chapman MR.** 2007. The curli nucleator protein, CsgB, contains an amyloidogenic domain that directs CsgA polymerization. Proc Natl Acad Sci U S A **104:**12494-12499.
120. **Epstein EA, Reizian MA, Chapman MR.** 2009. Spatial Clustering of the Curlin Secretion Lipoprotein Requires Curli Fiber Assembly. J Bacteriol **191:**608-615.
121. **Zhou Y, Smith D, Leong BJ, Brannstrom K, Almqvist F, Chapman MR.** 2012. Promiscuous cross-seeding between bacterial amyloids promotes interspecies biofilms. The Journal of biological chemistry **287:**35092-35103.

122. **Robinson LS, Ashman EM, Hultgren SJ, Chapman MR.** 2006. Secretion of curli fibre subunits is mediated by the outer membrane-localized CsgG protein. Mol Microbiol **59:**870-881.
123. **Loferer H, Hammar M, Normark S.** 1997. Availability of the fibre subunit CsgA and the nucleator protein CsgB during assembly of fibronectin-binding curli is limited by the intracellular concentration of the novel lipoprotein CsgG. Molecular microbiology **26:**11-23.
124. **Goyal G KP, Van Gerven N, Gubellini F, Van den Broeck I, Troupoiotis-Tsailaki A, Jonkheere W, Pejau-Arnaudet G, Pinkner JS, Chapman MR, Hultgren SJ, Howorka S, Fronzes R, and Remaut H.** 2014. Structural and mechanistic insights into the bacterial amyloid secretion channel CsgG. Nature **In Press**.
125. **Nenninger AA, Robinson LS, Hammer ND, Epstein EA, Badtke MP, Hultgren SJ, Chapman MR.** 2011. CsgE is a curli secretion specificity factor that prevents amyloid fibre aggregation. Mol Microbiol **81:**486-499.
126. **Andersson EK, Bengtsson C, Evans ML, Chorell E, Sellstedt M, Lindgren AE, Hufnagel DA, Bhattacharya M, Tessier PM, Wittung-Stafshede P, Almqvist F, Chapman MR.** 2013. Modulation of curli assembly and pellicle biofilm formation by chemical and protein chaperones. Chemistry & Biology **20:**1245-1254.
127. **Evans ML, Chorell E, Taylor JD, Aden J, Gotheson A, Li F, Koch M, Sefer L, Matthews SJ, Wittung-Stafshede P, Almqvist F, Chapman MR.** 2015. The bacterial curli system possesses a potent and selective inhibitor of amyloid formation. Mol Cell **57:**445-455.
128. **Horvath I, Weise CF, Andersson EK, Chorell E, Sellstedt M, Bengtsson C, Olofsson A, Hultgren SJ, Chapman M, Wolf-Watz M, Almqvist F, Wittung-Stafshede P.** 2012. Mechanisms of protein oligomerization: inhibitor of functional amyloids templates alpha-synuclein fibrillation. Journal of the American Chemical Society **134:**3439-3444.
129. **Kuner P, Bohrmann B, Tjernberg LO, Naslund J, Huber G, Celenk S, Gruninger-Leitch F, Richards JG, Jakob-Roetne R, Kemp JA, Nordstedt C.** 2000. Controlling polymerization of beta-amyloid and prion-derived peptides with synthetic small molecule ligands. Journal of Biological Chemistry **275:**1673-1678.
130. **Pinkner JS, Remaut H, Buelens F, Miller E, Aberg V, Pemberton N, Hedenstrom M, Larsson A, Seed P, Waksman G, Hultgren SJ, Almqvist F.** 2006. Rationally designed small compounds inhibit pilus biogenesis in uropathogenic bacteria. Proc Natl Acad Sci U S A **103:**17897-17902.
131. **Aberg V, Norman F, Chorell E, Westermark A, Olofsson A, Sauer-Eriksson AE, Almqvist F.** 2005. Microwave-assisted decarboxylation of bicyclic 2-pyridone scaffolds and identification of Abeta-peptide aggregation inhibitors. Org Biomol Chem **3:**2817-2823.
132. **Haass C, Selkoe DJ.** 2007. Soluble protein oligomers in neurodegeneration: lessons from the Alzheimer's amyloid beta-peptide. Nat Rev Mol Cell Biol **8:**101-112.
133. **Brown AJ.** 1887. Note on the cellulose formed by *Bacterium xylinum*. J Chem Soc **51:**643.
134. **Romling U.** 2002. Molecular biology of cellulose production in bacteria. Res Microbiol **153:**205-212.
135. **Ross P, Mayer R, Benziman M.** 1991. Cellulose biosynthesis and function in bacteria. Microbiol Rev **55:**35-58.

136. **Da Re S, Ghigo JM.** 2006. A CsgD-independent pathway for cellulose production and biofilm formation in *Escherichia coli*. J Bacteriol **188:**3073-3087.
137. **Ryjenkov DA, Simm R, Romling U, Gomelsky M.** 2006. The PilZ domain is a receptor for the second messenger c-di-GMP: the PilZ domain protein YcgR controls motility in enterobacteria. Journal of Biological Chemistry **281:**30310-30314.
138. **Amikam D, Galperin MY.** 2006. PilZ domain is part of the bacterial c-di-GMP binding protein. Bioinformatics **22:**3-6.
139. **Omadjela O, Narahari A, Strumillo J, Melida H, Mazur O, Bulone V, Zimmer J.** 2013. BcsA and BcsB form the catalytically active core of bacterial cellulose synthase sufficient for in vitro cellulose synthesis. Proc Natl Acad Sci U S A **110:**17856-17861.
140. **Malone JG, Jaeger T, Spangler C, Ritz D, Spang A, Arrieumerlou C, Kaever V, Landmann R, Jenal U.** 2010. YfiBNR mediates cyclic di-GMP dependent small colony variant formation and persistence in *Pseudomonas aeruginosa*. PLoS Pathog **6:**e1000804.
141. **Morgan JLW, Strumillo J, Zimmer J.** 2013. Crystallographic snapshot of cellulose synthesis and membrane translocation. Nature **493:**181-U192.
142. **Morgan JL, McNamara JT, Zimmer J.** 2014. Mechanism of activation of bacterial cellulose synthase by cyclic di-GMP. Nat Struct Mol Biol **21:**489-496.
143. **Pontes MH, Lee EJ, Choi J, Groisman EA.** 2015. *Salmonella* promotes virulence by repressing cellulose production. Proc Natl Acad Sci U S A **112:**5183-5188.
144. **Kai-Larsen Y, Luthje P, Chromek M, Peters V, Wang X, Holm A, Kadas L, Hedlund KO, Johansson J, Chapman MR, Jacobson SH, Romling U, Agerberth B, Brauner A.** 2010. Uropathogenic *Escherichia coli* modulates immune responses and its curli fimbriae interact with the antimicrobial peptide LL-37. PLoS Pathog **6:**e1001010.
145. **Al-Hasan MN, Eckel-Passow JE, Baddour LM.** 2010. Bacteremia complicating gram-negative urinary tract infections: a population-based study. J Infect **60:**278-285.
146. **Hung C, Marschall J, Burnham CAD, Byun AS, Henderson JP.** 2014. The Bacterial Amyloid Curli Is Associated with Urinary Source Bloodstream Infection. PLoS One **9**.
147. **Bian Z, Brauner A, Li Y, Normark S.** 2000. Expression of and cytokine activation by *Escherichia coli* curli fibers in human sepsis. J Infect Dis **181:**602-612.
148. **Danese PN, Pratt LA, Dove SL, Kolter R.** 2000. The outer membrane protein, antigen 43, mediates cell-to-cell interactions within *Escherichia coli* biofilms. Molecular microbiology **37:**424-432.
149. **Kjaergaard K, Schembri MA, Ramos C, Molin S, Klemm P.** 2000. Antigen 43 facilitates formation of multispecies biofilms. Environ Microbiol **2:**695-702.
150. **Anderson GG, Goller CC, Justice S, Hultgren SJ, Seed PC.** 2010. Polysaccharide capsule and sialic acid-mediated regulation promote biofilm-like intracellular bacterial communities during cystitis. Infect Immun **78:**963-975.
151. **Saldana Z, Xicohtencatl-Cortes J, Avelino F, Phillips AD, Kaper JB, Puente JL, Giron JA.** 2009. Synergistic role of curli and cellulose in cell adherence and biofilm formation of attaching and effacing *Escherichia coli* and identification of Fis as a negative regulator of curli. Environ Microbiol **11:**992-1006.
152. **Wang X, Rochon M, Lamprokostopoulou A, Lunsdorf H, Nimtz M, Romling U.** 2006. Impact of biofilm matrix components on interaction of commensal *Escherichia coli* with the gastrointestinal cell line HT-29. Cellular and Molecular Life Sciences **63:**2352-2363.

153. **Rapsinski GJ, Newman TN, Oppong GO, van Putten JP, Tukel C.** 2013. CD14 protein acts as an adaptor molecule for the immune recognition of *Salmonella* curli fibers. Journal of Biological Chemistry **288:**14178-14188.
154. **Tukel C, Nishimori JH, Wilson RP, Winter MG, Keestra AM, van Putten JP, Baumler AJ.** 2010. Toll-like receptors 1 and 2 cooperatively mediate immune responses to curli, a common amyloid from enterobacterial biofilms. Cell Microbiol **12:**1495-1505.
155. **Oppong GO, Rapsinski GJ, Newman TN, Nishimori JH, Biesecker SG, Tukel C.** 2013. Epithelial cells augment barrier function via activation of the Toll-like receptor 2/phosphatidylinositol 3-kinase pathway upon recognition of *Salmonella enterica* serovar Typhimurium curli fibrils in the gut. Infect Immun **81:**478-486.
156. **Nishimori JH, Newman TN, Oppong GO, Rapsinski GJ, Yen JH, Biesecker SG, Wilson RP, Butler BP, Winter MG, Tsolis RM, Ganea D, Tukel C.** 2012. Microbial amyloids induce interleukin 17A (IL-17A) and IL-22 responses via Toll-like receptor 2 activation in the intestinal mucosa. Infect Immun **80:**4398-4408.
157. **Lundmark K, Westermark GT, Olsen A, Westermark P.** 2005. Protein fibrils in nature can enhance amyloid protein A amyloidosis in mice: Cross-seeding as a disease mechanism. Proc Natl Acad Sci U S A **102:**6098-6102.
158. **Hartman K, Brender JR, Monde K, Ono A, Evans ML, Popovych N, Chapman MR, Ramamoorthy A.** 2013. Bacterial curli protein promotes the conversion of PAP248-286 into the amyloid SEVI: cross-seeding of dissimilar amyloid sequences. PeerJ **1:**e5.
159. **Gerstel U, Romling U.** 2001. Oxygen tension and nutrient starvation are major signals that regulate *agfD* promoter activity and expression of the multicellular morphotype in *Salmonella* typhimurium. Environ Microbiol **3:**638-648.
160. **Olsen A, Arnqvist A, Hammar M, Normark S.** 1993. Environmental regulation of curli production in *Escherichia coli*. Infect Agents Dis **2:**272-274.
161. **Reshamwala SM, Noronha SB.** 2011. Biofilm formation in *Escherichia coli cra* mutants is impaired due to down-regulation of curli biosynthesis. Arch Microbiol **193:**711-722.
162. **Gottesman S, Stout V.** 1991. Regulation of capsular polysaccharide synthesis in *Escherichia coli* K12. Mol Microbiol **5:**1599-1606.
163. **Hanna A, Berg M, Stout V, Razatos A.** 2003. Role of capsular colanic acid in adhesion of uropathogenic *Escherichia coli*. Appl Environ Microbiol **69:**4474-4481.
164. **Danese PN, Pratt LA, Kolter R.** 2000. Exopolysaccharide production is required for development of *Escherichia coli* K-12 biofilm architecture. J Bacteriol **182:**3593-3596.
165. **Matthysse AG, Deora R, Mishra M, Torres AG.** 2008. Polysaccharides cellulose, poly-beta-1,6-N-acetyl-D-glucosamine, and colanic acid are required for optimal binding of *Escherichia coli* O157 : H7 strains to alfalfa sprouts and K-12 strains to plastic but not for binding to epithelial cells. Appl Environ Microbiol **74:**2384-2390.
166. **Cookson AL, Cooley WA, Woodward MJ.** 2002. The role of type 1 and curli fimbriae of Shiga toxin-producing *Escherichia coli* in adherence to abiotic surfaces. Int J Med Microbiol **292:**195-205.
167. **Macarisin D, Patel J, Bauchan G, Giron JA, Sharma VK.** 2012. Role of curli and cellulose expression in adherence of *Escherichia coli* O157:H7 to spinach leaves. Foodborne Pathog Dis **9:**160-167.

168. **Jeter C, Matthysse AG.** 2005. Characterization of the binding of diarrheagenic strains of *E. coli* to plant surfaces and the role of curli in the interaction of the bacteria with alfalfa sprouts. Mol Plant Microbe Interact **18:**1235-1242.
169. **Patel J, Sharma M, Ravishakar S.** 2011. Effect of curli expression and hydrophobicity of *Escherichia coli* O157:H7 on attachment to fresh produce surfaces. J Appl Microbiol **110:**737-745.
170. **Hou Z, Fink RC, Black EP, Sugawara M, Zhang Z, Diez-Gonzalez F, Sadowsky MJ.** 2012. Gene expression profiling of *Escherichia coli* in response to interactions with the lettuce rhizosphere. J Appl Microbiol **113:**1076-1086.
171. **Chen Y, Cao S, Chai Y, Clardy J, Kolter R, Guo JH, Losick R.** 2012. A *Bacillus subtilis* sensor kinase involved in triggering biofilm formation on the roots of tomato plants. Mol Microbiol **85:**418-430.
172. **Zhou Y.** 2012. Promiscuous cross-seeding between bacterial amyloids promotes interspecies biofilms.
173. **Zhou YZ, Smith D, Leong BJ, Brannstrom K, Almqvist F, Chapman MR.** 2012. Promiscuous Cross-seeding between Bacterial Amyloids Promotes Interspecies Biofilms. Journal of Biological Chemistry **287:**35092-35103.

Chapter 2

The Disulfide Bonding System Suppresses CsgD-Independent Cellulose Production in *E. coli*

Abstract

The bacterial extracellular matrix encases cells and protects them from host-related and environmental insults. The *Escherichia coli* master biofilm regulator, CsgD, is required for production of the matrix components curli and cellulose. CsgD activates the diguanylate cyclase AdrA, which in turn stimulates cellulose production through cyclic-di-GMP (c-di-GMP). Here, we identified and characterized a CsgD- and AdrA-independent cellulose production pathway that was maximally active when cultures were grown under reducing conditions or when the disulfide bonding system (DSB) was compromised. The CsgD-independent cellulose activation pathway was dependent on a second diguanylate cyclase called YfiN. C-di-GMP production by YfiN was repressed by the periplasmic protein YfiR, and deletion of *yfiR* promoted CsgD-independent cellulose production. Conversely, when YfiR was overexpressed, cellulose production was decreased. Finally, we found that YfiR was oxidized by DsbA, and that intra-protein YfiR disulfide bonds stabilized YfiR in the periplasm. Altogether, we showed that reducing conditions and mutations in the DSB system caused hyper activation of YfiN and subsequent CsgD-independent cellulose production.

Introduction

Organisms often cluster together into homotypic aggregates that help the population resist environmental pressures (1). Similarly, bacteria form communities known as biofilms, in which cells are encased in a protective extracellular matrix (ECM) composed of proteins, polysaccharides, and DNA (2-5). The ECM provides bacteria with resistance to environmental insults like antimicrobial compounds, desiccation, and host immune responses (6-8).

Curli and cellulose are structural components of *E. coli* and *Salmonella* spp. biofilms. Amyloid fibers are a common component of natural biofilms (9). Curli are also abundantly represented, as homologs of the curli genes are found in four different bacterial phyla (10). Expression of curli and cellulose requires the master biofilm regulator, CsgD (3, 11). The regulation of CsgD involves upwards of 13 transcriptional regulators, multiple sRNAs, and post-translational phosphorylation (12). The complex regulation of *csgD* allows for precise control of curli and cellulose production in low glucose, low temperature, and low salt environments (13-15). CsgD induces *csgBAC* transcription, leading to production of the major and minor curli subunits, CsgA and CsgB (11). CsgD also positively regulates *adrA,* which encodes an inner membrane diguanylate cyclase (3). Diguanylate cyclases produce the secondary messenger cyclic-di-GMP (c-di-GMP) which activates the cellulose synthase, BcsA, in a concentration dependent manner by binding to the RXXXR residues in the PilZ domain (3, 16, 17). Activated BcsA links UDP-D-glucose molecules together via a β-1,4 linkage, forming bacterial cellulose (3, 16).

When *E. coli* produces curli and cellulose on agar plates the bacteria form a wrinkled colony that spreads away from the original inoculation site. These colonies are called rugose or

rdar (red, dry and rough) biofilms. Various bacterial species form rugose biofilms including: *Salmonella spp., Escherichia coli, Citrobacter koseri, Pseudomonas aeruginosa, Bacillus subtilis,* etc (18-22). The uropathogenic *Escherichia coli* (UPEC) isolate, UTI89, forms curli and cellulose-dependent rugose biofilms (19). The major ECM components in *E. coli* and *Salmonella spp.* rugose biofilms are the proteinaceous amyloid fiber curli, and the polysaccharide, cellulose (23). Within UTI89 rugose biofilms, matrix production occurs at the air-colony interface, and the air-exposed matrix-encased cells demonstrate increased resistance to H_2O_2 compared to interior, non-matrix-encased cells (19). Curli and cellulose bind the dye Congo red (CR), leading to red (curli only or curli and cellulose) or pink (cellulose only) colonies (3, 18). Genetic disruption of curli or cellulose production in *S. enterica* or *E. coli* results in colonies that spread less and have a smaller colony diameter (3, 7). Deletion of *csgD* leads to smooth colonies that do not bind CR, due to the absence of curli and cellulose (3). While most *E. coli* strains, including UTI89, produce cellulose through the CsgD-dependent pathway, exceptions have been reported (19). For instance, *E. coli* 1094 produces cellulose in a CsgD-independent manner that is reliant on the diguanylate cyclase, YedQ (24).

We discovered a CsgD- and AdrA-independent cellulose activation pathway that is linked to the disulfide bonding (DSB) machinery in *E. coli*. DsbB and DsbA coordinate disulfide bond formation in periplasmic proteins (25). DsbB is an inner membrane protein that oxidizes the periplasmic oxidoreductase, DsbA, and DsbA in turn oxidizes periplasmic proteins by catalyzing disulfide bond formation (26, 27). Deletion of *dsbA* or *dsbB* results in a non-functional DSB system (25). We report here that DSB mutant colonies have increased colony diameter in comparison to WT and produce cellulose in a CsgD- and AdrA-independent manner. Unlike CsgD-dependent cellulose production, the CsgD-independent pathway that is active in

DSB mutants promotes cellulose production under many growth conditions. The CsgD-independent pathway requires the diguanylate cyclase YfiN. The periplasmic protein YfiR regulates YfiN and is a direct target of the DSB system.

Results

Disulfide bonding mutants form hyper biofilms

Many enteric bacteria, including UTI89, require an extracellular matrix (ECM) that contains both curli and cellulose for rugose colony formation. *E. coli* rugose colonies are typified by a wrinkled morphology and increased diameter compared to a colony that does not produce curli or cellulose (3, 7, 19). Therefore, colony diameter can be a simple proxy for curli and cellulose production within a colony. To identify additional components of the genetic network controlling ECM production in UTI89, a Tn*5* mutant library was screened for hyper-spreading strains. Using the mariner Tn*5* conjugation system (28), an unsaturated screen of approximately 20,000 UTI89 transposon mutants revealed three isolates that had increased colony diameter in comparison to WT; two *dsbA* mutants and a *dsbB* mutant (data not shown). Clean deletions of the *dsbA* and *dsbB* coding regions via lambda red mutagenesis were constructed in UTI89. *dsb* mutant colonies (Δ*dsbA* and Δ*dsbB*) had increased colony diameter compared to WT, but were less wrinkled (Figure 2.1A and 2.1B). Since Δ*dsbA* and Δ*dsbB* colony phenotypes were similar, we focused on the Δ*dsbB* strain for most of the subsequent experiments.

Because disulfide bonding (DSB) mutants had increased colony diameter in comparison to WT, we hypothesized that mutations in the DSB system caused an upregulation of curli or cellulose. However, western blot analysis revealed that *dsbA* and *dsbB* mutants had similar CsgA

and CsgD protein levels as compared to WT, suggesting that curli production was not significantly changed (Figure 2.1C). We measured *adrA* transcription levels as a proxy for cellulose induction. *adrA* transcription levels as measured by β-galactosidase assays were similar in WT and Δ*dsbB* colonies (Figure 2.1D). These data suggested that CsgD-regulated curli and cellulose production were not increased in the DSB mutants.

We next tested how mutations in DSB affected biofilm formation in other environmental conditions. UTI89 WT forms a pellicle biofilm at the air-liquid interface when grown in YESCA CR at 26°C in static culture for 48 hours (Figure 2.1E) (29). Like rugose colonies, pellicle biofilms are dependent on both curli and cellulose (30). A Δ*dsbB* mutant formed a more robust and wrinkled pellicle than WT (Figure 2.1E). We quantified pellicle integrity by measuring the ability of the pellicle to hold weight using a modified glass bead assay (31). The top panel of Figure 1F shows glass beads held by the pellicle above the culture, while the panel on the bottom shows a pellicle that collapsed and sank into the culture from glass bead addition (Figure 1F). Δ*dsbB* pellicles held an average of 14 glass beads, while WT pellicles held fewer than 6 glass beads on average (Figure 2.1G). A *bcsA* cellulose synthase mutant did not form a pellicle and could not support glass beads (Figure 2.1G).

CsgD-independent activation of cellulose synthesis

We next investigated which components of the CsgD-dependent matrix production pathway were necessary for the DSB mutant colony morphotype, since curli protein levels and *adrA* transcription were not dramatically different between DSB mutants and WT. Mutating the curli biosynthetic genes in a *dsbB* background (Δ*dsbB*Δ*csgBA*) produced colonies that were light

red on CR, wrinkled, but had had a small colony diameter (Figure 2.2A), suggesting that cellulose was still being produced. Mutating the cellulose synthase in a DSB mutant (Δ*dsbB*Δ*bcsA*) yielded colonies that had a small colony diameter and did not wrinkle, but did bind CR (Figure 2.2A), suggesting that curli were still being produced. Unexpectedly, mutating the master biofilm regulator CsgD in a DSB mutant (Δ*csgD*Δ*dsbB*) resulted in colonies that wrinkled in a similar manner to Δ*dsbB*Δ*csgBA* (Figure 2.2A). We hypothesized that the ability of the Δ*csgD*Δ*dsbB* strains to form wrinkled colonies was dependent on cellulose production. Indeed, mutation of the cellulose synthase in a Δ*csgD*Δ*dsbB* background (Δ*csgD*Δ*dsbB*Δ*bcsA*) led to smooth, small-diameter colonies that failed to bind CR (Figure 2.2A). Curli did not contribute to CR binding by Δ*csgD*Δ*dsbB* strains, as the Δ*csgD*Δ*dsbB* strain did not produce the major curli subunit, CsgA (Figure 2.2B). To confirm cellulose production in DSB mutant backgrounds, colonies were probed with the cellulose specific stain Pontamine Fast Scarlet 4B (S4B) (32). S4B bound Δ*csgBA,* Δ*dsbB*Δ*csgBA,* and Δ*csgD*Δ*dsbB* at similar levels (Figure 2.3A). S4B did not significantly bind to Δ*csgBA*Δ*bcsA* or Δ*csgD*Δ*dsbB*Δ*bcsA*, as these strains were unable to produce cellulose (Figure 2.3A).

CsgD in WT *E. coli* promotes cellulose production by upregulating expression of the diguanylate cyclase AdrA (3). However, since cellulose production in DSB mutants was CsgD-independent, we tested if it was also AdrA-independent. Δ*dsbB*Δ*adrA* colonies were similar in appearance to Δ*dsbB* colonies, suggesting that the CsgD-independent pathway did not require AdrA (Figure 2.2A). Furthermore, mutation of *adrA* did not affect colony formation of Δ*csgD*Δ*dsbB* colonies (Figure 2.2A).

DSB mutants produce cellulose in many growth conditions

We next tested if CsgD-independent cellulose production occurred under diverse growth conditions. WT colonies grown on plates that were amended with 0.4% glucose did not wrinkle and had a small colony diameter (Figure 2.4A), likely because Cra and Crp-cAMP are activated in low sugar conditions, and both positively regulate *csgD* expression (13, 33). Interestingly, Δ*dsbB* and Δ*csgD*Δ*dsbB* colonies wrinkled and bound to CR on glucose-supplemented media (Figure 2.4A). High osmolarity and salt conditions also inhibit *csgD* transcription (15) and on LB CR plates, which have increased salt compared to YESCA media, WT UTI89 colonies do not bind to CR and do not wrinkle (Figure 2.4A). In contrast, Δ*dsbB* and Δ*csgD*Δ*dsbB* colonies wrinkled when grown on LB CR plates (Figure 2.4A). S4B staining confirmed that Δ*dsbB* and Δ*csgD*Δ*dsbB* colonies were producing cellulose on LB plates (Figure 2.3B). Finally, *E. coli* cellulose production is temperature dependent and maximal at 26°C (34). WT UTI89 colonies grown at 37°C were smooth, while Δ*csgD*Δ*dsbB* colonies wrinkled (Figure 2.4B).

Transposon screen for factors that affect the CsgD-independent cellulose activation pathway

The CsgD-mediated cellulose production pathway requires c-di-GMP, and we therefore asked if the CsgD-independent pathway was also dependent on c-di-GMP. c-di-GMP levels were manipulated by overexpressing the phosphodiesterase, *yoaD.* YoaD is proposed to break down the pool of c-di-GMP that activates BcsA (35). *yoaD* expressed from an inducible *tac* promoter in Δ*dsbB* resulted in decreased colony diameter and wrinkling (Figure 2.5A), implying that c-di-GMP is involved in the CsgD-independent cellulose activation pathway.

To identify the diguanylate cyclase responsible for producing AdrA-independent c-di-GMP in the DSB mutant, we performed a transposon screen. A transposon library of ~20,000 mutants was created in a UTI89 Δ*csgD*Δ*dsbB* background (28). The mutants were plated on YESCA CR and incubated at 26°C until colonies were visually screened for the failure to wrinkle or bind to Congo red. We isolated 32 mutants that were white and unwrinkled (Table 2.1), including *bcsA*, *bcsB*, *bcsC*, *bcsE*, and *galU*, which had all been shown to be involved in cellulose production (36-38). We also isolated mutations in genes that had not previously been associated with cellulose production in *E. coli*. These genes included: *nhaA,* a sodium antiporter; *nrdB,* a ribonucleoside-diphosphate reductase; and *seqA,* a protein involved in the regulation of DNA replication (39-42). Finally, one of the mutants that failed to bind Congo red and wrinkle was in a gene encoding a diguanylate cyclase called *yfiN* (43). We therefore hypothesized that the CsgD-independent cellulose production present in DSB mutants was activated through the diguanylate cyclase, YfiN.

YfiN and YfiR can control cellulose production in UTI89.

YfiN is a diguanylate cyclase encoded within the *yfiRNB* operon that, when activated, contributes to biofilm formation via production of c-di-GMP (44, 45). A clean deletion of *yfiN* was constructed in the UTI89 Δ*csgD*Δ*dsbB* background. This triple mutant (Δ*csgD*Δ*dsbB*Δ*yfiN)* formed smooth and white colonies on YESCA at 26°C and 37°C (Figure 2.6A). Additionally, deletion of *yfiN* in UTI89 (Δ*yfiN*) resulted in decreased CR binding and wrinkling, suggesting that YfiN was required for cellulose production by both the CsgD-independent pathway and the canonical CsgD-dependent pathway (Figure 2.6A). The Δ*yfiN* strain had lower levels of CsgD

protein by western blot (Figure 2.5B), which might account for the lack of CR binding and wrinkling by this strain (Figure 2.6A).

YfiN's role in cellulose production prompted an investigation of the periplasmic regulator, YfiR, which inhibits YfiN activity in *P. aeruginosa* (45). We expected that deletion of *yfiR* in *E. coli* would result in greater ci-di-GMP production by YfiN and increased cellulose production. Indeed, Δ*yfiR* colonies had an increased colony diameter compared to WT at 26°C, and wrinkled at 37°C (Figure 2.6A). Also, Δ*csgD*Δ*yfiR* colonies wrinkled with a small colony diameter at 26°C and 37°C (Figure 2.6A), which suggested that the CsgD-independent cellulose production pathway was active in the *yfiR* deletion strain. In *P. aeruginosa,* YfiR can be inactivated by an outer membrane protein called YfiB (45). However, *yfiB* didn't appear to play a role in in UTI89 cellulose production, as Δ*yfiB* and WT had similar colony phenotypes at 26°C and 37°C (Figure 2.6A). In concert with this result, overexpression of *yfiB,* did not appear to affect the WT colony morphotype (Figure 2.6B). These results suggested YfiR, but not YfiB, played a role in UTI89 cellulose production.

Because deletion of *yfiR* activated CsgD-independent cellulose production, we tested whether overexpression of YfiR inhibited cellulose production and rugose colony formation. WT, Δ*dsbB*, and Δ*csgD*Δ*dsbB* were transformed with a plasmid that overexpressed *yfiR* (p*yfiR*), or with the same plasmid that was missing the *yfiR* gene (pEV). Δ*dsbB* overexpressing *yfiR* displayed decreased colony spreading at 26°C and decreased CR binding at 37°C (Figure 2.7A and 2.7B). Δ*csgD*Δ*dsbB* overexpressing *yfiR* had decreased CR binding and wrinkling at 37°C and at 26°C (Figure 2.7A). WT overexpressing *yfiR* had decreased wrinkling and colony diameter at 26°C compared to WT colonies transformed with pEV but still bound CR (Figure 2.7A and 2.7B). CsgD levels were decreased when *yfiR* was overexpressed in WT, and *yfiR*

overexpression led to a minor decrease in CsgA levels in WT (Figure 2.8A). Additionally, Δ*yfiR* strains were attenuated in their swimming motility (Figure 2.8B), similar to results seen in *E. coli* CFT073 (44).

The result that YfiN induced the CsgD-independent cellulose production in a DSB mutant background was interesting because of the prospect that the DSB system could directly act on the periplasmic YfiN repressor YfiR. In *P. aeruginosa* YfiR whole cell protein levels are decreased in DSB mutant strains (46). Furthermore, YfiR contains four cysteine residues at positions 55, 92, 127, & 134. To directly test whether DSB oxidizes YfiR, UTI89 WT and Δ*dsbA* were transformed with pCKR101 (pEV) and pCKR101 with a *tac* promoter driving expression of *yfiR* with a His-tag on the C-terminal of YfiR (p*yfiR*^{His}) so that YfiR could be monitored by western blotting. UTI89 WT pEV and p*yfiR*^{His} along with Δ*dsbA* pEV and p*yfiR*^{His} were plated on YESCA IPTG plates and incubated at 37°C for 24 hours. Periplasmic extracts were isolated and incubated in SDS-sample buffer with or without the reducing agent dithiothreitol (DTT) and incubated for 10min. Western blot analysis revealed that YfiR-His was not present in Δ*dsbA* periplasmic extracts, suggesting that YfiR was not stable and was degraded in the absence of the DSB system (Figure 2.7C). Furthermore, DTT caused a mobility shift in YfiR-His (Figure 2.7C). Interestingly, there is a 'spur' on the left side of the YfiR-His band without DTT (→* Figure 5C). Spurs are commonly attributed to diffusion of the reducing agent present in the adjacent lane (47, 48). The spur and the higher molecular weight shift due to reduction is indicative of an oxidized protein that contains disulfide bonds (48). We therefore conclude that mutation of the DSB system results in YfiR degradation and causes YfiN mediated activation of the cellulose synthase.

Lastly, we considered environmental conditions that could activate the DSB mutant induced cellulose production pathway in WT UTI89. Since oxidation of YfiR is necessary for its periplasmic stability, we hypothesized that growth under reducing conditions would result in YfiR destabilization and production of cellulose via YfiN mediated cellulose synthase activation. Colonies were spotted near a sterile paper disk that contained buffer or the reducing agent DTT. After incubation at 37°C both WT and Δ*csgD* cells wrinkled and bound CR when spotted 1.5 cm from the DTT disk (Figure 2.7D). YfiN was required for cellulose production in the presence of DTT, as Δ*yfiN* colonies were smooth and did not bind CR (Figure 2.7D). Cellulose synthase mutants, Δ*bcsA,* were also smooth and did not bind CR (Figure 2.7D). These experiments demonstrate that reducing conditions induce the YfiN mediated cellulose production in WT *E. coli.*

Discussion

Here, we describe a YfiN-mediated cellulose synthase activation pathway in *E. coli*. The YfiN-mediated pathway is dependent on the cellulose synthase, BcsA, but is independent of CsgD and the previously described BcsA activator, AdrA. YfiN is a diguanylate cyclase that is repressed by YfiR. We found that YfiN is active in DSB mutants because YfiR is unstable.

YfiN was identified by a transposon screen done in a Δ*csgD*Δ*dsbB* background. We isolated 32 transposon mutants that appeared white on CR plates (Table 2.1). The Δ*csgD*Δ*dsbB* strain was used in the screen because we wanted to focus on the CsgD-independent cellulose production pathway. Many of the mutants identified in the screen could have been predicted *a priori*. For example, the *bcs* genes (*A, B, C* and *E*) are required for cellulose synthesis in *E. coli*

and are required for the CsgD-independent cellulose production pathway (Table 2.1) (3, 37). *galU* is required, as it is necessary for the production of the building block of bacterial cellulose, UDP-D-glucose (38). However, a few additional genes were identified in the screen that will require further work to fully understand their role in cellulose production. These genes include *nhaA,* a sodium antiporter*; nrdB* a ribonucleoside diphosphate reductase; and *seqA,* a regulator of DNA replication. *nhaA, nrdB,* and *seqA* were not previously identified in a UTI89 transposon screen for genes affecting biofilms in UTI89, suggesting that they may not affect the CsgD-mediated cellulose production pathway (49).

YfiN plays an important role across species in the regulation of matrix production. YfiN (or TpbA) in *P. aeruginosa* leads to increased production of EPS and the development of small colony variants (45, 50). *P. aeruginosa* YfiN is localized to the inner membrane and is activated via homodimerization to produce the second messenger ci-di-GMP (45, 46). YfiN homodimerization is inhibited by the periplasmic protein, YfiR (45, 46). *yfiRNB* are in a single operon in *E. coli*, and YfiR and YfiN have similar activities in *E. coli* as that in *P. aeruginosa* (43-45, 51). Previous work has also shown that the YfiN homolog AwsR controls *Pseudomonas fluorescens* cellulose and biofilm formation (52), and in *Yersinia pestis* the YfiN and YfiR homologs, HmsD and HmsC respectively, contribute to biofilm formation and blockage of blood intake in the rat flea *Xenopsylla cheopis (53, 54)*. The inhibition of YfiN by YfiR can be overcome in *P. aeruginosa* via overexpression of the outer membrane protein YfiB, which sequesters YfiR away from YfiN (45). Interestingly, our results showed that deletion or overexpression of *yfiB* had little to no effect on cellulose production in UTI89 (Figure 2.6A and 2.6B). In *Y. pestis,* biofilm formation was only modestly affected by deletion or overexpression of the YfiB homolog HmsE (53, 54). In the UPEC strain CFT073, *yfiR* deletion leads to an

increase in cellulose and curli production along with attenuation of bladder and kidney titers in a murine UTI model (44). In UTI89, a *yfiLR*::Tn mutant has decreased bladder titers, intracellular bacterial communities, and a decrease in motility (49).

The periplasmic protein, YfiR, tempers YfiN-dependent cellulose production. YfiR has four cysteine residues that are available for disulfide bonding. Previous work in *P. aeruginosa* showed that YfiR whole cell protein levels are decreased in a Δ*dsbA* background (46). Similarly, we show here that the stability of YfiR in *E. coli* is dependent on a functioning DSB system (Figure 2.7C). Furthermore, we expanded this analysis by closely monitoring the migration of oxidized and reduced YfiR by SDS-PAGE. YfiR migrated slower on an SDS-PAGE gel when it was reduced by DTT (Figure 2.7C), which is indicative of proteins that have a redox sensitive disulfide bond (47, 48). Interestingly, we observed a 'spur' in the lane containing oxidized YfiR that was directly adjacent to the DTT reduced lane (Figure 2.7C). Spurs are a distinguishing characteristic of disulfide bonded proteins that are partially reduced by the DTT in the adjacent lane (47, 48). These results indicate that the DSB system normally oxidizes YfiR and that in the absence of the DSB system YfiR is unstable and degraded (Figure 2.7C and Figure 2.9).

Δ*yfiR* colonies have increased colony diameter similar to Δ*dsb*, and Δ*csgD*Δ*yfiR* colonies phenocopy Δ*csgD*Δ*dsbB* (Figure 2.6A). Overexpression of *yfiR* in Δ*dsbB* and Δ*csgD*Δ*dsbB* inhibits the CsgD-independent cellulose production, as these colonies no longer bind CR at 37°C (Figure 2.7A). Also, *yfiR* expression in Δ*dsbB* decreases colony diameter at 26°C, and *yfiR* expression in Δ*csgD*Δ*dsbB* decreases colony diameter and binding to CR at 26°C (Figure 2.7A and 2.7B). These data support a model where YfiR quells the cellulose production by inhibiting YfiN (Figure 2.9).

Since YfiR requires oxidative folding for protein stability we reasoned that YfiN and cellulose production would be induced under reducing conditions. Indeed, the addition of DTT to colonies promoted CsgD-independent cellulose production at 37°C (Figure 2.7D). Thus, it is possible that anaerobic or reducing environments, such as those in the lower intestinal tract, may induce cellulose production through YfiN activation.

There is at least one additional instance of CsgD-independent cellulose activation. YedQ is the primary cellulose activator in WT *E. coli* 1094 and is independent of the CsgD-mediated activation pathway (24). UTI89 *E. coli* in contrast utilizes the CsgD-dependent diguanylate cyclase, AdrA, for WT cellulose activation (19). YfiN is similar to YedQ activation as it is CsgD independent, however it is an alternate or secondary diguanylate cyclase that only activates cellulose in specific reducing conditions.

YfiN is not only required for CsgD-independent cellulose production in DSB mutants, but it also plays a role in the CsgD-dependent canonical cellulose production pathway in UTI89 WT. Deletion of *yfiN* led to smooth and white colonies in UTI89 (Figure 2.6A) and decreased CsgD protein levels in comparison to WT (Figure 2.5B). DSB mutations in *yfiN* mutants cause an increase in CsgD and CsgA proteins levels in comparison to *yfiN* single mutants (Figure 2.5B). This could be due to DSB mutations activating additional diguanylate cyclases, which then produce enough c-di-GMP to increase CsgD protein levels. C-di-GMP and diguanylate cyclases have been previously implicated in controlling *csgD* transcription levels (55, 56). Furthermore, *yfiR* overexpression in WT leads to decreased CsgD protein levels (Figure 2.7 and Figure 2.8A). *yfiR* overexpression in DSB mutants did not decrease CsgD or CsgA protein levels. This phenomenon could also be explained by multiple diguanylate cyclases being activated by DSB mutation. *yfiR* overexpression could quell YfiN activation in DSB mutants, but

other diguanylate cyclases might help maintain CsgD at WT levels (Figure 2.8A).The ability of YfiR to modulate CsgD protein levels and cellulose production in WT UTI89 demonstrates that it has roles in both canonical cellulose production and in the CsgD-independent pathway (Figure 2.9).

Besides cellulose production, the DSB system is also important for many other *E. coli* virulence traits. The *E. coli* flagellar machinery (57), P pili (58), the type III secretion system (59), and enterotoxin production (60) all require the DSB system for proper function. The necessity of DSB for these virulence traits has led to suggestion that DSB might be a promising drug target (61). However, because cellulose production and biofilm formation by *E. coli* can confer resistance to host factors and environmental insults (62), targeting the DSB system might promote cellulose production and unwanted outcomes. Cellulose expression in DSB mutants may not have been noticed in other studies since cellulose is not produced in K12 strains due to a mutation in the *bcs* operon (63).

The CsgD-independent cellulose production may provide a means for industrial production of cellulose. Cellulose is widely utilized in industrial applications (textiles, dietary supplements, gauze, scaffolds for tissue regeneration, and even in headphones) (64, 65). Microbial cellulose is coveted because of its purity and is typically harvested from *Gluconacetobacter xylinus* (65, 66). One of the largest problems with industrial production of microbial cellulose from *G. xylinus* is the high production costs (66). Glucose based media is used for *G. xylinus* growth and cellulose production, and the metabolic byproducts produced during growth actually inhibit cellulose production (66). CsgD-independent cellulose production allows *E. coli* to produce cellulose in many conditions including high temperature, high glucose, and high salt (Figure 4). Genetically modifying *E. coli* has been proposed as a tractable method

for producing microbial cellulose (66), in part due to the ability of *E. coli* to flourish in a variety of nutrient sources. Cellulose could be harvested by feeding a DSB or YfiR mutant, mutant with a variety of inexpensive and environmentally friendly nutrients (such as waste from various industrial processes). Similar types of studies have already been attempted in *G. xylinus* (67, 68). The work presented here might increase the financial feasibility of microbial cellulose production and helps further the understanding of matrix production in microbial biofilms.

Materials and Methods

Strains and growth conditions

Starting cultures were grown with agitation at 37°C overnight in Luria Broth (LB) media. UTI89 mutants were constructed using the lambda Red recombinase technique (69). The primers used for mutations can be found in the Primer Table (Table 2.3). The mutant strain names can be found in the strain list (Table 2.4). In the manuscript, we refer to the strains by the mutations constructed.

Colony biofilms were grown from 4µl dots of a 1.0 OD_{600} cell suspension. Bacterial pellets were washed twice in YESCA media (10 g Casamino acids, 1 g yeast extract/L) before plating onto YESCA Congo red (CR) media plates (50 µg CR/mL & 20 g agar/L). Pellicles were grown in liquid YESCA CR (1.67 µg CR/mL). Bacteria were then incubated for 48 hours at 26°C and the colony images were captured using an Olympus SZX16 microscope with an Olympus DP72 camera. Glucose plates contained 0.4% (w/v) dextrose (D-glucose) and were buffered with 15 mM MES (pH 6.6). Increased acetic acid production from glucose metabolism is most likely the cause of this darker pigment, as CR is a pH indicator which can darken in low

pH environments (70). Motility plates contained 0.25% agar with LB or YESCA media. To inoculate motility plates, pipette tips were dipped into an overnight culture and then into the plate. Motility plates were incubated at 37°C for five hours prior to imaging. For the DTT addition assay, 20 µL of 200 mM Tris buffer (pH 8.6) with or without 500 mM DTT was added to a sterile paper filter disk. Colony biofilms were grown as before 1.5 cm from the sterile filter paper disk at 37°C for 24 hours.

Pellicle Bead assay

The pellicle bead assay was adapted from Montiero *et al.* (31). Sterile 3mm glass beads were added via tweezers to pellicles that had grown for 48 hours at 26°C. After 5 seconds, the next glass bead was added. Only beads that were held for the complete duration of 5 seconds were counted as held by the pellicle.

S4B staining and Cellulose quantification

Recent work in *Arabidopsis thaliana* showed that Pontamine Fast Scarlet 4B (S4B) binds more specifically to cellulose than does calcofluor, and that S4B fluoresces more brightly in the presence of cellulose than Solophenyl Flavine 7GFE and calcofluor (71). To quantitate cellulose using S4B, 4 µL colonies were grown as indicated and collected in 800 µL of 50mM potassium phosphate buffer (KPi) (pH 7.2). Cells were tissue homogenized for 15 seconds on setting 3 with a Fisher Tissuemizer. Cells were incubated with 0.05 mg/mL S4B (32), briefly vortexed, and incubated for 10 minutes at RT on a rocking shaker at 200 RPM. Cells were then centrifuged at 13,000 RPM for 1 minute and washed twice with KPi and then resuspended in 100 µL of KPi. Cell suspensions were diluted 1:10 into a 96 well plate and read on a Tecan Infinite 200 plate reader, at excitation 535nm and emission 595nm. Readings from unstained cell suspensions were

subtracted from the stained cell suspensions. Cells suspensions were normalized by OD_{600}. Error bars represent standard deviation from biological triplicate samples.

β-galactosidase assay

β-galactosidase activity assays were adapted from Miller *et al.*1972 and DePas *et al.,* 2013 (19, 72). Colonies were grown for 48 hours and resuspended in 1 mL 50 mM KPi (pH 7.2). Cells were tissue homogenized for 15 seconds at setting 3 and allowed to incubate for 3 minutes. Cells at the top of the mixture were diluted 1:10 and 100 µL of this dilution was added to a 96 well plate. Reaction buffer (90 µL) and cell dilutions (7 µL) were incubated for 20 minutes at 30°C prior to adding 2 0µL of 4 mg/mL ortho-Nitrophenyl-β-galactoside (ONPG). In order to stop the reaction, 50 µL of 1 M Na_2CO_3 were added after the reaction reached a light yellow color. OD_{600} absorbance of the cell and KPi dilutions were recorded, along with absorbance at 420nm and 550nm readings of the reaction on a Tecan Infinite 200 plate reader. Assays were performed on 3 biological triplicates of strains with pRJ800 empty vector (EV) (pRJ800 without a promoter upstream of *lacZ*) and were averaged. The average EV reading was subtracted from each biological triplicate strain carrying pRJ800-*adrA* or pRJ800-16s. Averages and standard deviations were determined from the biological triplicates with the EV values subtracted.

Transposon Screen

The transposon screen was adapted from Rubin *et al.* (28). WT UTI89 or UTI89 Δ*csgD*Δ*dsbB* was grown in streptomycin to select for antibiotic resistant isolates. These isolates were conjugated with a donor strain BW25113 transformed with pFD1 containing the Isopropyl β-D-1-thiogalactopyranoside (IPTG) inducible transposase (NDH587).Cultures of both BW25113 NDH 587 and UTI89 Δ*csgD*Δ*dsbB* (750 µL each) were mixed, pelleted and resuspended in 50 µL YESCA media. All 50 µL were added to a cellulose filter that was placed

on top of a YESCA media plate. The bacteria on the plate were incubated at 37°C for 2.5 hours. The cellulose filter was then removed from the plate and the cells were removed by washing this filter with 10 mL liquid YESCA media containing streptomycin and 1mM IPTG and collected into a 15 mL tube. The cells were then incubated at 37°C for 3 hours. The cells were then pelleted and resuspended in 10mL fresh YESCA media containing streptomycin and kanamycin for 1 hour at 37°C. Cells were then diluted 1:10,000 and were plated on YESCA Congo red media plates containing streptomycin and kanamycin. Transposons were verified using random primed sequencing. Colony PCR with mariner 1 and mariner 2 primers yielded the DNA flanking the transposon. Nested PCR of this DNA fragment with mariner 3 and mariner 4 then amplified this DNA segment. Sanger sequencing was then performed at the University of Michigan Seqencing Core using the primer Mariner 4. Sequences were then aligned to the genome of UTI89 to reveal the location of the mutations in the genome. Whole gene deletions were made via the lambda red recombinase method.

Western Blot analysis

Western blots were performed adapting the procedure from (73). CsgA western blots), Colony biofilms were grown at 26°C for 48 hours. Colonies were then resuspended in 50 mM Potassium Phosphate buffer (KPi) (pH 7.2). Cells were homogenized with a Fisher Tissuemizer tissue homogenizer on setting 3 for 20 seconds. Colony debris was then able to settle for 3 minutes prior to spectrophotometric measurement to normalize cells at 1-$OD_{600..}$ 150 μL of normalized cells were resuspended in 2x SDS-running buffer or hexa-fluoroisporopanol (HFIP). HFIP treated cells had HFIP removed via 45 minutes in a Thermo Savant SPD SpeedVac at 45°C. Samples were then resuspended in 2x SDS-running buffer. All samples were then heated at 95°C for 10 minutes prior to loading and electrophoresing 8 μL onto a 15% SDS-PAGE gel

for 45 minutes at 25 mAmps. The samples were then transferred to a PVDF membrane via transfer on a semi-dry transfer apparatus at 10V for 25 minutes at room temperature. Blots were blocked overnight in 5% milk with Tris-buffered saline in Tween 20 (TBST) buffer at 4°C. Primary antibody treatment was for 1 hour (1:8000 αCsgA (74) 5% milk in TBST) followed by 3 x 5 minute TBST washes. Secondary antibody treatment was for 1 hour (1:15000 Licor α Rabbit or α Mouse IRDYE). Blots were then dried and imaged on a Licor Odyssey CLX imager. α-CsgD (1:5000 anti-rabbit a generous gift from *Ute Römling*), α-His (1:5000 anti-mouse ABGENT Inc San Diego, CA), and α-σ70 (1:10000 anti-mouse Santa Cruz RNA pol σ D antibody) blots had an altered procedure. The SDS-PAGE gel was prepared in the same manner without the HFIP treatment. Samples were wet-transferred to a nitrocellulose membrane in 25 mM CAPS transfer buffer in 10% methanol (pH 11.2) at 12V overnight at 4°C.

α-His and α-MBP (1:10,000 anti-mouse a generous gift from Jim Bardwell, New England BioLabs, Ipswich, MA) western blots contained periplasmic protein samples which were normalized by protein concentration via the Pierce BCA protein assay (Thermo Scientific). Samples were incubated with 2x SDS-sample buffer containing no β-mercaptoethanol with or without 5mM of the reducing agent dithiothreitol (DTT) for 10 minutes shaking at room temperature prior to loading onto an SDS-PAGE gel.

Periplasmic Protein Isolation

We isolated periplasmic proteins following an adapted procedure from Quan *et al*. (75). 200 µL of 1-OD_{600} cells were evenly spread on YESCA plates amended with 10 µM IPTG and incubated at 37°C for 24 hours. Cells were harvested, resuspended in osmotic shock buffer (30mM Tris pH 7.2, 40% sucrose, 2mM EDTA), and incubated at room temperature for 10

minutes. Cells were centrifuged at 13,000 RPM for 10 minutes. The supernatant was removed and the pellet was resuspended with 450µL ice-cold water followed by addition of 50 µL of 20 mM $MgCl_2$. Samples were incubated on ice for three minutes prior to centrifugation at 4°C at 13,000RPM for 10 min. The periplasmic extract is the supernatant fraction. Protein concentrations of the periplasmic extracts were normalized via the Pierce BCA protein assay (Thermo Scientific) (76). Anti-MBP Western blots were used to ensure that there were no aberrations in periplasmic protein isolated between samples.

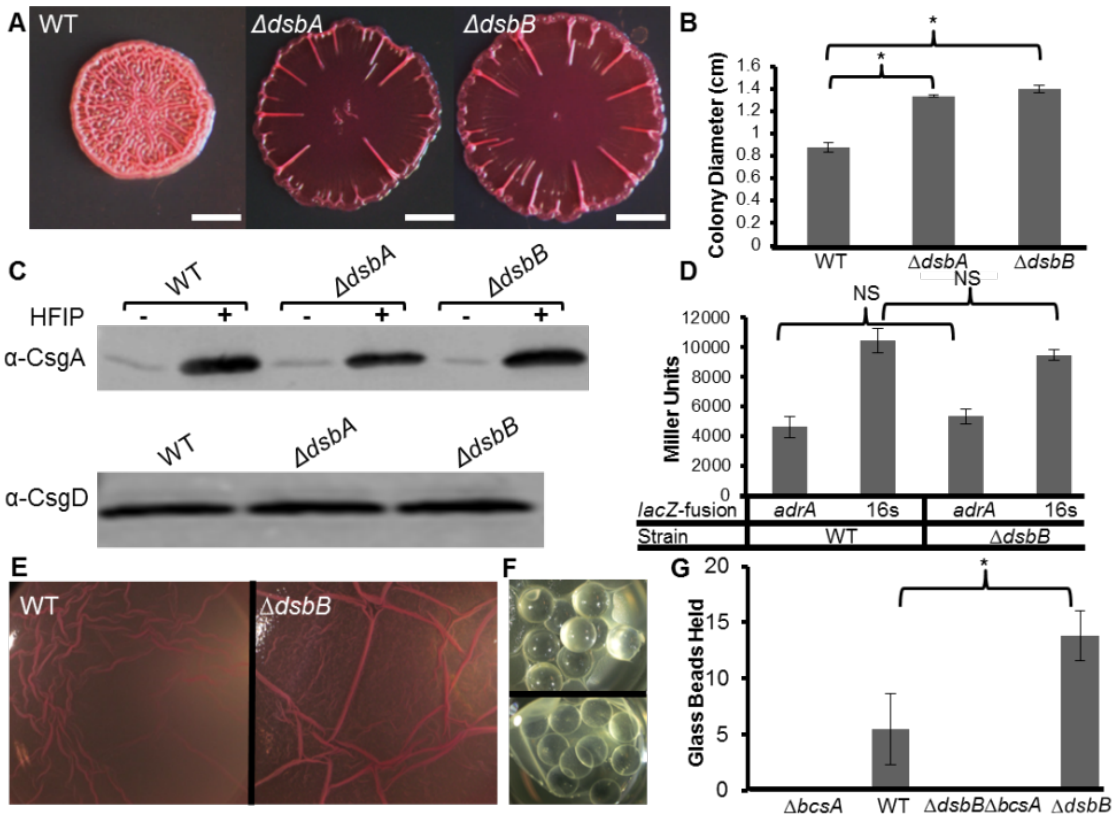

Figure 2.1- Δ*dsb* colonies had increased spreading but similar curli levels and *adrA* transcription to WT. A) UTI89 colonies were grown on YESCA CR plates for 48 hours at 26°C. Δ*dsbB* and Δ*dsbA* colonies formed hyper spreading colonies that had a lack of wrinkling in the center of the colony. Scale bars are 0.25cm. B) Δ*dsbB* and Δ*dsbA* had increased colony diameter compared to WT. Colony diameters were measured in biological triplicate, error bars represent standard deviation of biological triplicates. Significance was determined by the student's two-tailed t-test (* P-value> 0.01). C) CsgA Western blot showed that WT, Δ*dsbA,* and Δ*dsbB* had similar levels of CsgA when grown at 26°C for 48 hours. *Hexafluoroisopropanol (HFIP) is a strong denaturant that was added to monomerize the aggregated curli fibers.* CsgD Western blot analysis was performed on colonies that were grown at 26°C for 24 hours. D) β-galactosidase assays were performed on WT and Δ*dsbB* transformed with prj800, prj800-*adrA,* or prj800-16s (*rrsA)*. The average of biological triplicate readings from prj800 was subtracted from readings from strains containing prj800-*adrA* (*adrA* promoter upstream of *lacZ*) *&* prj800-16s (16s promoter upstream of *lacZ*). *adrA* and 16s transcription were similar between WT and Δ*dsbB.* Error bars are the standard deviation of Miller Units from biological triplicates. Significance was determined using the student's two-tailed t-test. E) UTI89 derivatives were grown statically in 24 well plates after 2 µL of an overnight culture was inoculated into 2ml YESCA broth that contained 1.67 µg/mL of CR. Pellicles formed at the air-liquid interface with WT UTI89 and DSB mutants. F) Glass beads were added to WT and Δ*dsbB* pellicles every 5 seconds, until the pellicle could no longer hold the glass beads. The image on top shows a pellicle holding glass beads, while the image on the bottom shows a collapsed pellicle. G) WT pellicles held ~5 glass beads in YESCA CR media at 48 hours, while Δ*dsbB* pellicles held ~13 glass beads. Mutation of the cellulose synthase, BcsA, in WT and Δ*dsbB* yielded cultures that could not produce pellicles or hold glass beads. Error bars represent standard deviation of six biological replicates. P-value was calculated using a student's two-tailed t-test (P-value<0.01).

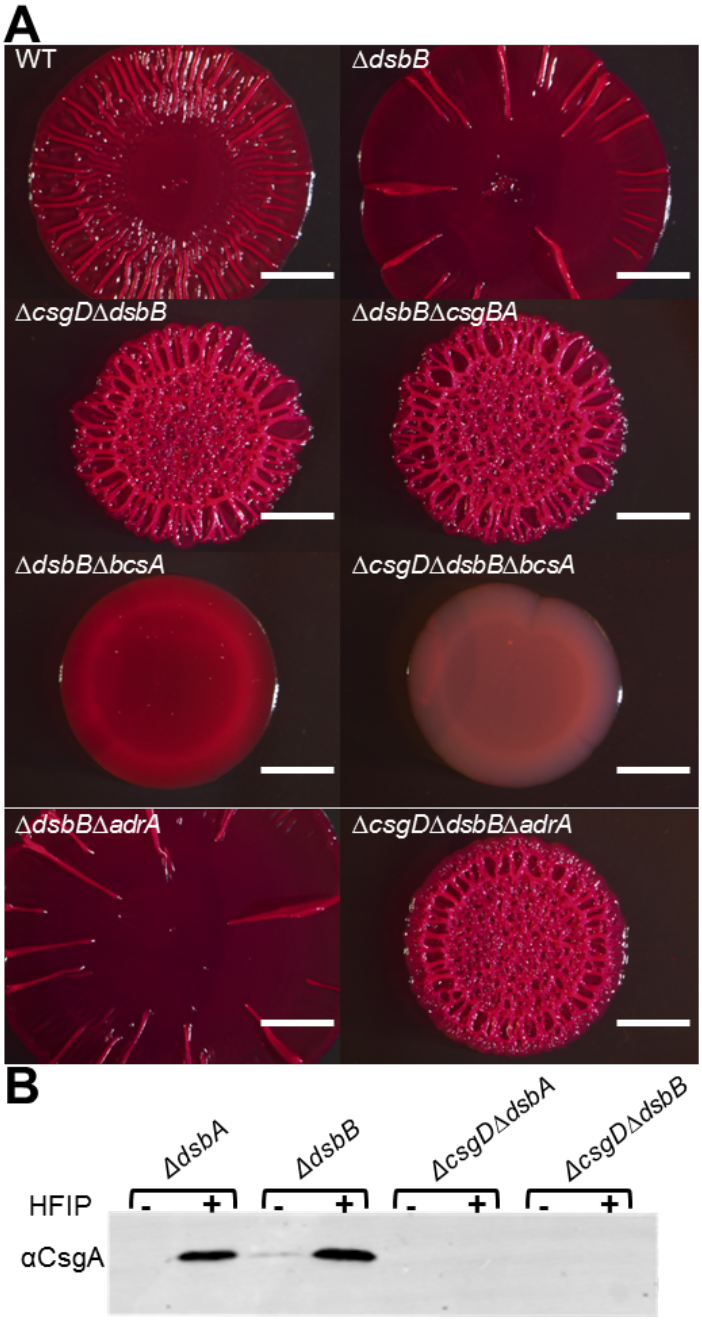

Figure 2.2- Δ*dsb* colonies wrinkle due to *csgD* and *adrA* independent cellulose production. A) Colonies were grown in YESCA media for 48 hours on YESCA CR plates at 26°C. Scale bars are 0.25 cm. B) CsgA protein levels were assessed via Western Blot analysis. Samples were treated with HFIP to solubilize CsgA fibers. Colonies that were photographed were grown as above, but on YESCA CR, Δ*csgD*Δ*dsbA* colonies wrinkled but did not spread, similar to Δ*csgD*Δ*dsbB* colonies.

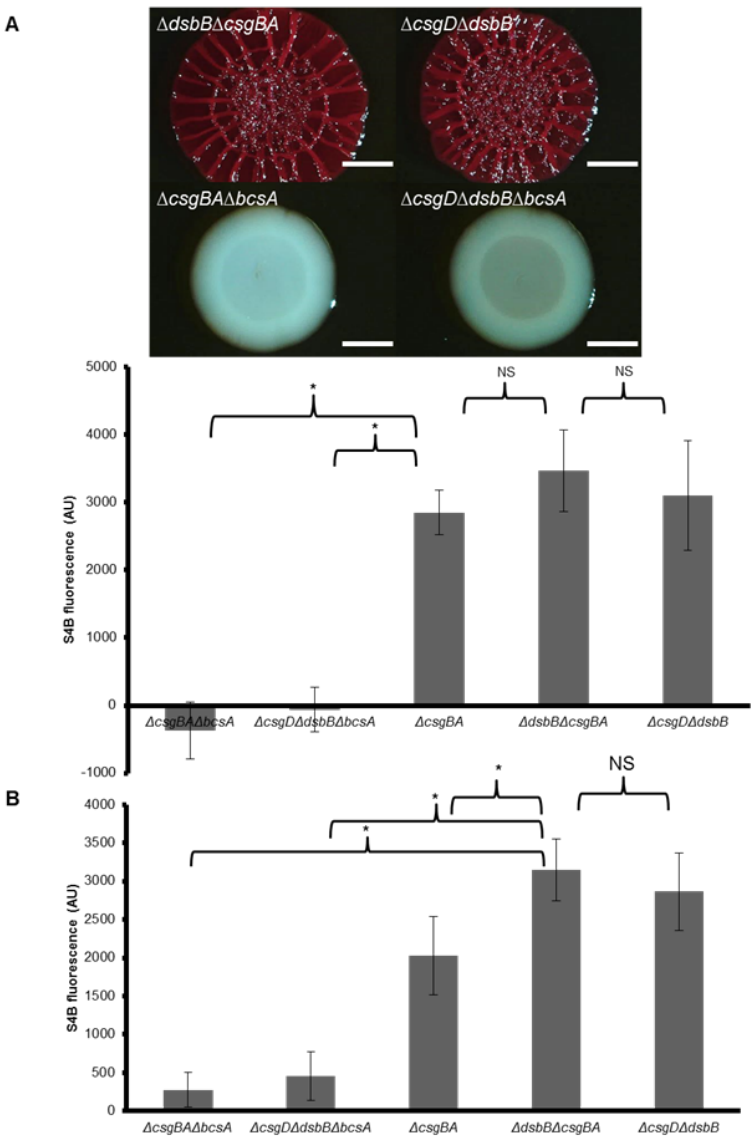

Figure 2.3- UTI89 WT, Δ*dsbB,* and Δ*csgD*Δ*dsbB* have increased binding to the cellulose stain S4B even on LB plates. A) In the top images, colonies were grown for 48 hours at 26°C on YESCA CR. Scale bars are 0.25cm. In the graph, the colonies were grown on YESCA for 48 hours at 26°C were stained with 100x Pontamine Fast Scarlet 4B (S4B). Fluorescence readings were normalized by OD_{600} and unstained cells fluorescence were subtracted from the stained cells fluorescence. Error bars are the standard deviation from biological triplicate samples. P-values were calculated using the student's two-tailed t-test (*P-value<0.04). B) Colonies grown on LB plates at 26°C for 48 hours were stained with S4B. Fluorescence readings were normalized by OD_{600} and unstained cells fluorescence were subtracted from the stained cells fluorescence. Error bars are the standard deviation from biological triplicate samples. P-values were calculated using the student's two-tailed t-test (P-value<0.03).

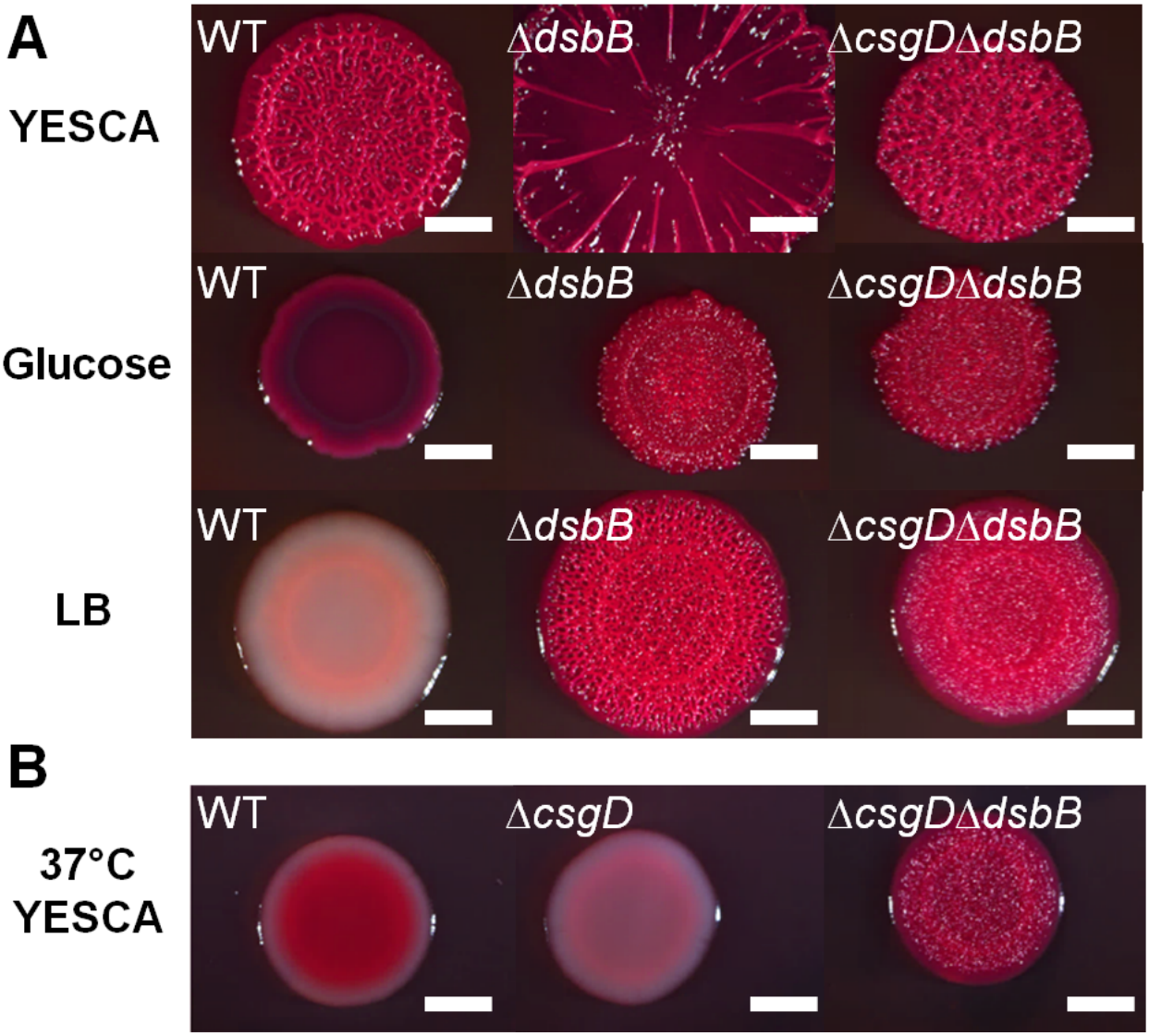

Figure 2.4- UTI89 Δ*dsb* colonies wrinkle at 37°C, on dextrose, and on LB plates. A) Strains were grown on YESCA media buffered with 15 mM MES to pH 6.6 at 26°C for 48 hours. WT, Δ*dsbB,* and Δ*csgD*Δ*dsbB* colony morphotypes were not affected by buffering of the plates. In the second row colonies were grown on YESCA media with 0.4% dextrose buffered with 15 mM MES to pH 6.6 at 26°C for 48 hours. In the third row strains were grown on LB CR (1:200) plates at 26°C for 48 hours. WT colonies were white and non-spreading or wrinkling on LB, while Δ*dsbB* and Δ*csgD*Δ*dsbB* both wrinkled on LB. B) Colonies were grown for 24 hours at 37°C on YESCA CR plates. Scale bars are 0.25 cm.

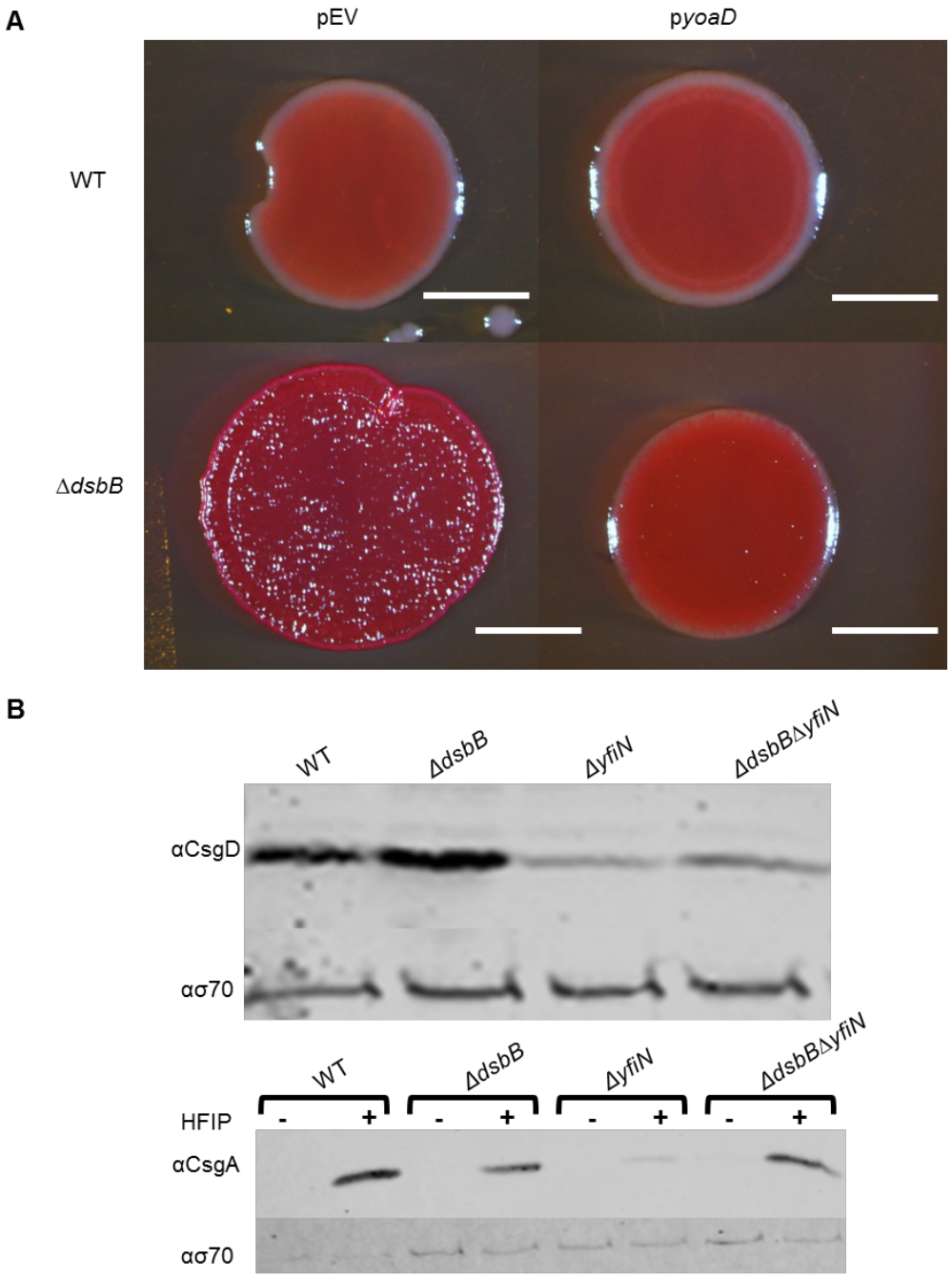

Figure 2.5- Δ*dsb* phenotype is dependent on c-di-GMP, and YfiN is necessary for normal CsgD expression. A) WT and Δ*dsbB* were transformed with pCKR101-EV and pCKR101-*yoaD*. Colonies were grown on YESCA CR plates with 100µM IPTG at 26°C for 24 hours. B) Colonies were grown at 26°C for 48 hours for αCsgA and 24 hours for αCsgD Western blots.

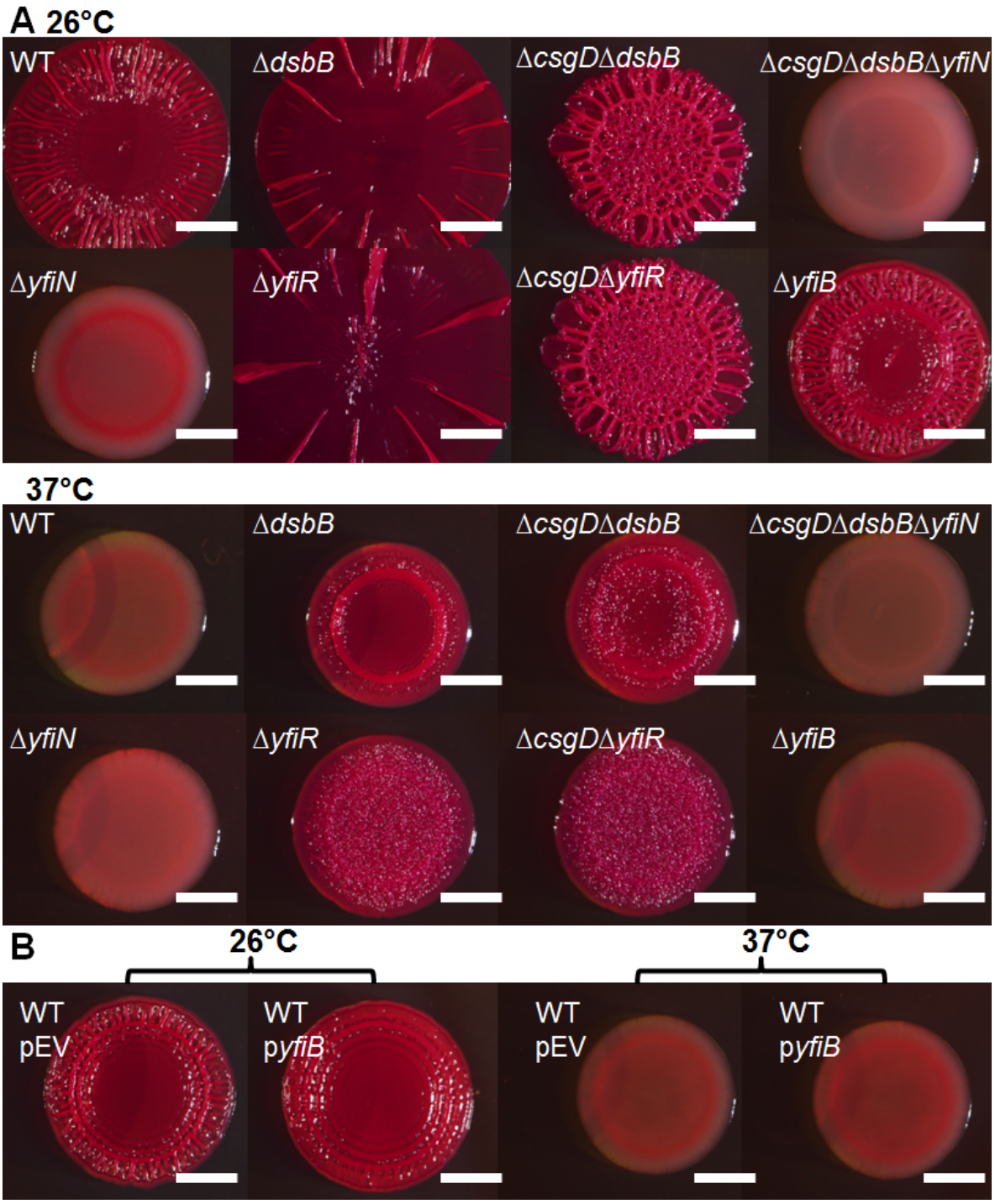

Figure 2.6- Cellulose production in Δ*csgD*Δ*dsbB* is dependent on the diguanylate cyclase, YfiN. A) Strains were grown on YESCA CR media. The top row of strains were grown at 26°C for 48 hours, and the bottom row of strains were grown at 37°C for 24 hours. B) Strains were grown on YESCA CR media supplemented with 15 µM IPTG for 48 hours at 26°C or for 24 hours at 37°C. Scale bars are 0.25 cm.

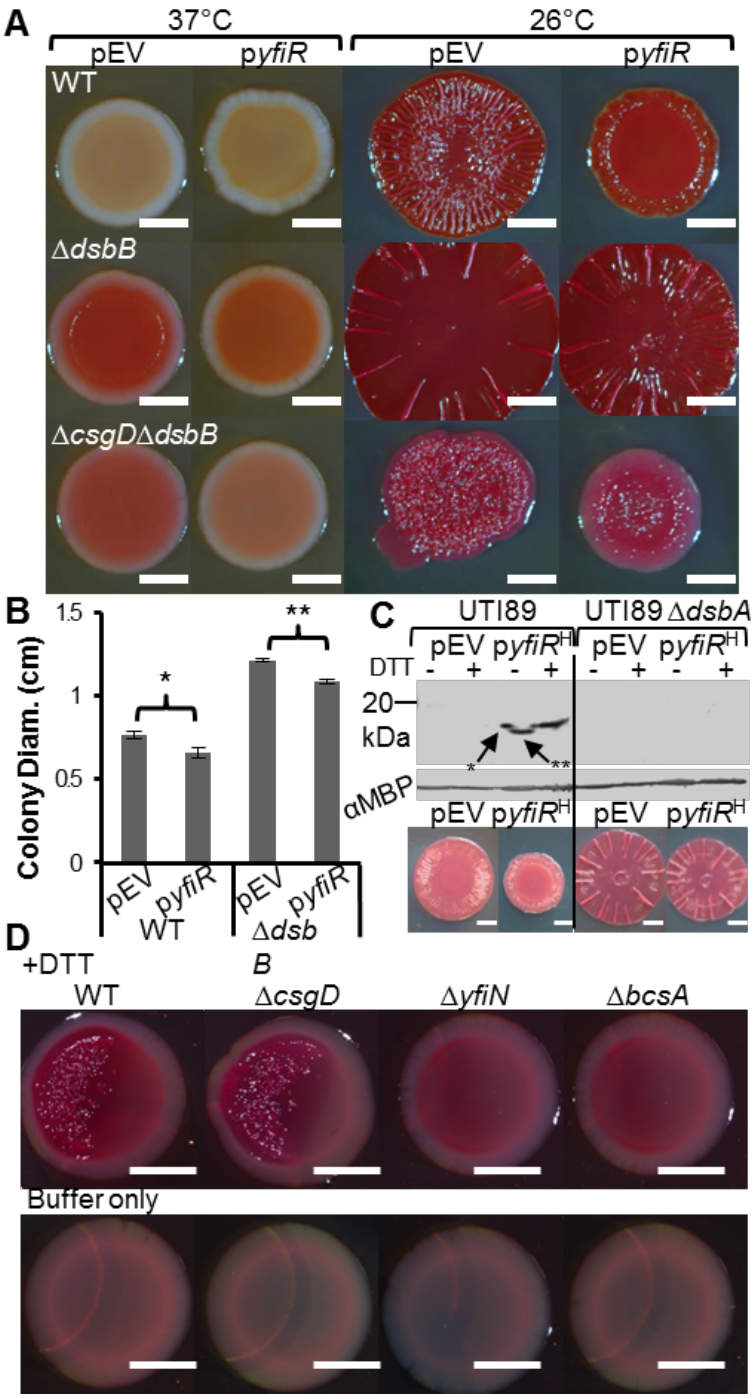

Figure 2.7- *yfiR* overexpression inhibits alternate cellulose expression. A) WT, Δ*dsbB*, and Δ*csgD*Δ*dsbB* strains were transformed with pckr101-EV (pEV) or pckr101-*yfiR (*p*yfiR*). Colonies were grown on YESCA CR 10 µM IPTG plates. The colonies on the left were grown at 37°C for 24 hours, and the plates on the right were grown at 26°C for 48 hours. B) Colony diameter measurements were taken from biological triplicate colonies that were grown on YESCA media at 26°C for 48 hours. Error bars show the standard deviation of the measured diameters. P-values represent student's two-tailed t-test (*P-Value <0.04 **P-Value<0.01). C) UTI89 WT and Δ*dsbA* were transformed with pEV and p*yfiR*^{His} and grown for 24 hours at 37°C on YESCA IPTG plates. Periplasms were isolated from the cells and were incubated with non-reducing SDS-sample buffer with or without 5 mM DTT for 10 minutes. α-His western blot analysis revealed that YfiR was oxidized in UTI89 WT, as DTT treatment led to reduced YfiR with decreased migration through the gel. Without DTT YfiR ran further on the gel (**), however there was a spur on the left side of the band (*). Spurs develop from reducing agent diffusion from adjacent lanes causing reduction of the protein on one side of the protein band and are indicative of proteins containing disulfide bonds (48). MBP levels were assayed to ensure similar periplasmic protein concentration was loaded in each sample. Underneath the western blot are pictures of WT pEV and pCKR101-*yfiR*^{His} and Δ*dsbA* pEV and pCKR101-*yfiR*^{His} colonies grown on YESCA CR plates for 48 hours at 26°C. D) Colonies were grown at 37°C for 24 hours 1.5 cm away from a filter paper disk containing 20 µL of 500 mM DTT suspended in 200 mM Tris buffer (pH 8.6) or buffer alone. Scale bars are 0.25 cm.

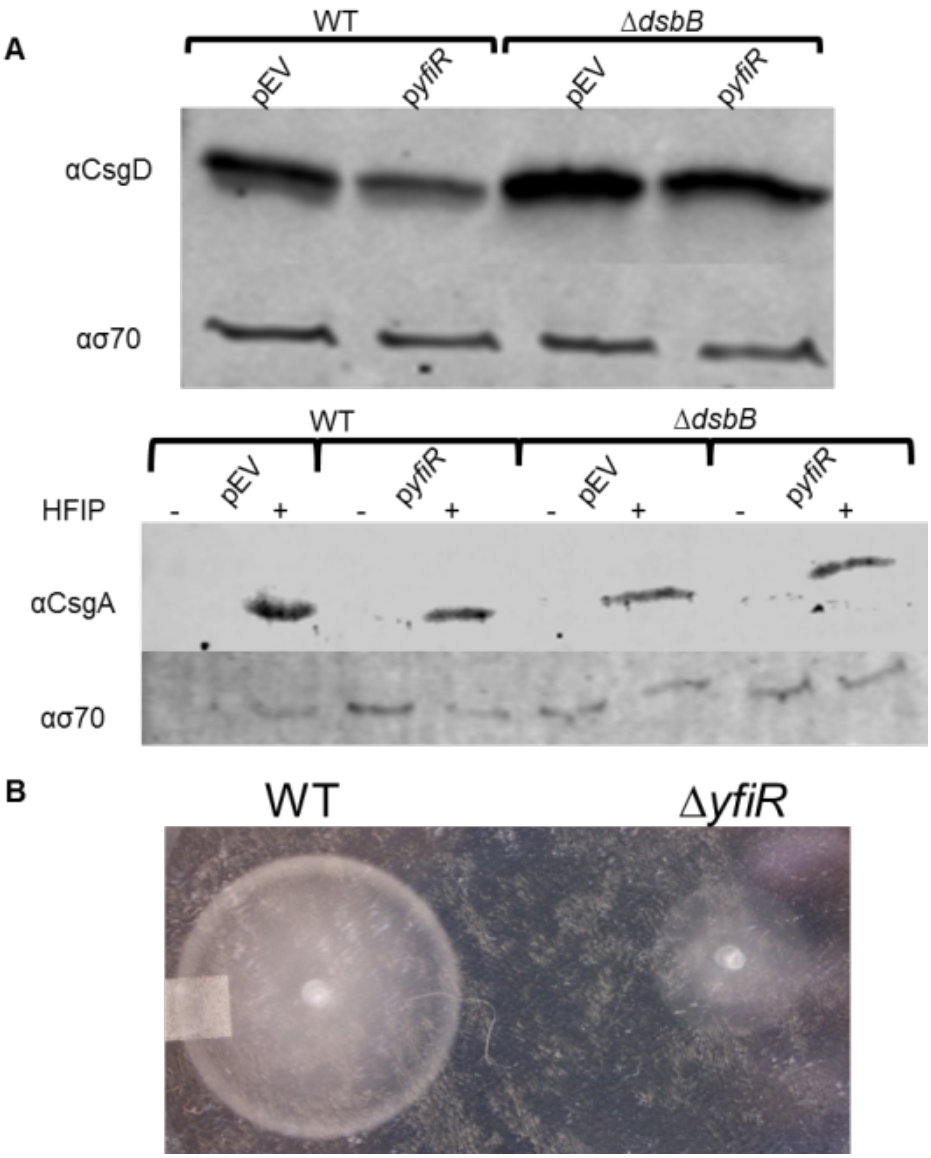

Figure 2.8- *yfiR* overexpression decreases CsgD levels in WT and Δ*dsbB* colonies. A) Western Blot analysis was performed on colonies grown at 26°C on YESCA plates. Colonies used to analyze CsgA protein levels were grown for 48 hours, while Western Blots used to analyze CsgD levels were grown for 24 hours. CsgA colony preps were treated with HFIP in order to solubilize CsgA fibers. ασ70 blots were used as loading controls. B) 1 µL of culture was inoculated into .25% YESCA motility agar. Plates were incubated at 37°C for 5 hours.

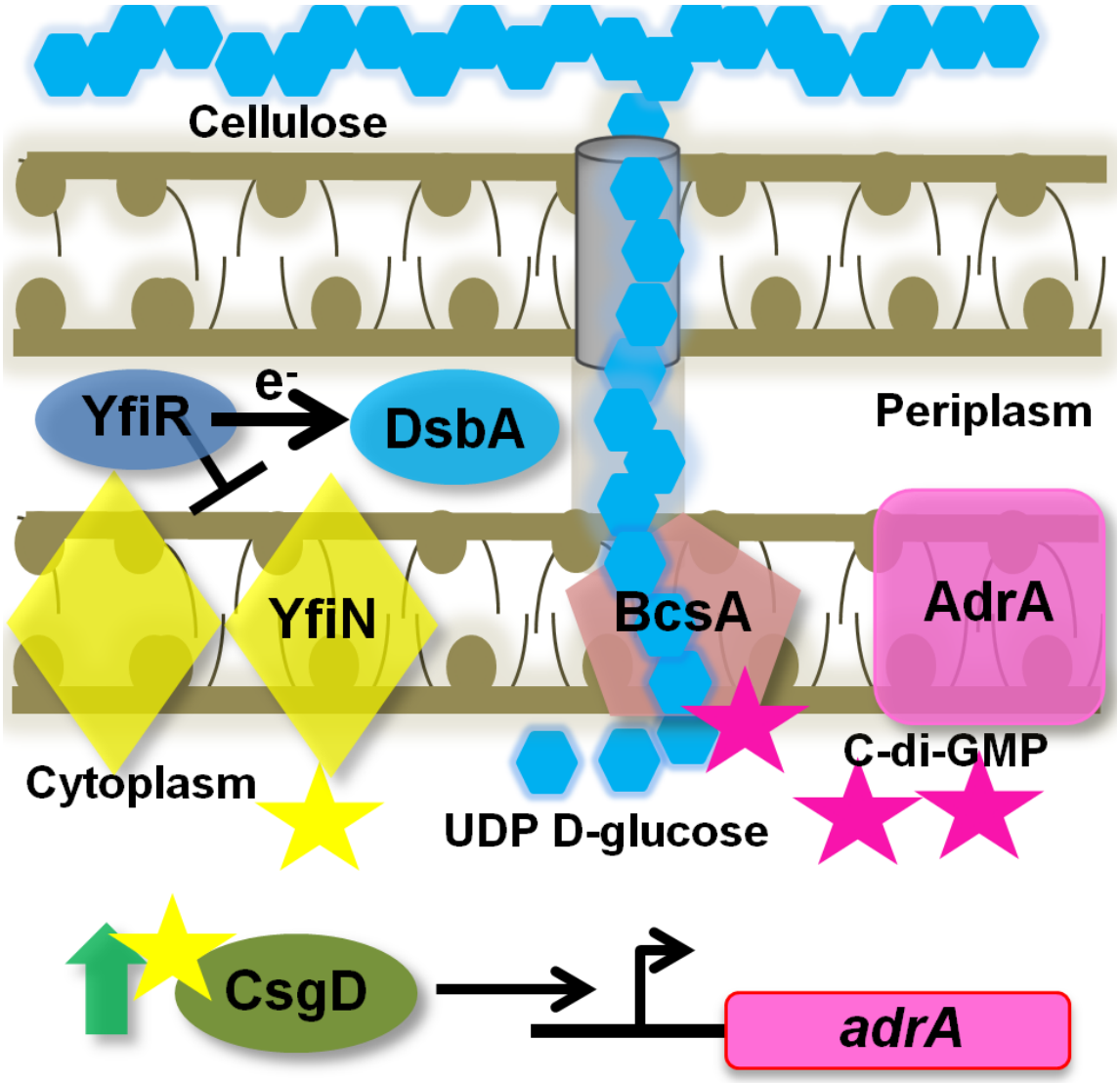

Figure 2.9- Updated model of cellulose production in UTI89. YfiN is inhibited by YfiR, which requires the DSB system to properly fold. YfiN produces small amounts of c-di-GMP (yellow stars) that are required for normal CsgD protein levels. CsgD positively regulates *adrA,* which encodes the diguanylate cyclase that produces c-di-GMP (pink stars) to bind to the PilZ of BcsA and activate the cellulose synthase complex. UDP-D-glucose are the monomers of cellulose production. In the absence of the DSB system or YfiR, YfiR is not present, and YfiN dimerizes and leads to uninhibited production of c-di-GMP. YfiN produces c-di-GMP that leads to BcsA activation, even in the absence of CsgD or AdrA.

Tables:

Table 2.1- Genes required for CsgD-independent cellulose production

Gene	Number	Encoded protein's function
bcsA	4	Cellulose synthase (3)
bcsB	8	Involved in biosynthesis of cellulose (3)
bcsC	11	Involved in biosynthesis of cellulose (3)
bcsE	2	Involved in biosynthesis of cellulose (3)
galU	3	UTP-glucose-1-phosphate uridylyltransferase, which produces UDP-D-glucose, the building block of cellulose (40)
nhaA	1	Sodium antiporter (41)
nrdB	1	B2 protein of ribonucleoside-diphosphate reductase. Involved in production of deoxynucleotides from nucleotides (42)
seqA	1	Involved in the regulation of DNA replication (44)
yfiN	1	Inner membrane diguanylate cyclase (46, 47)

Table 2.2- Plasmid list Chapter 2

Plasmids	Reference	Notes
pRJ800	DePas *et al.* 2013	
pRJ800-*adrA*	DePas *et al.* 2013	
pRJ800-16s	DePas *et al.* 2013	
pCKR101	DePas *et al.* 2013(20)	
pCKR101-*yfiR*	This study	*yfIR* amplified with primers DH165 and DH166 subcloned into pCKR101 at the KpnI and XbaI sites.
pCKR101-*yfiR*^{His}	This study	*yfIR* amplified with primers DH165 and DH167 subcloned into pCKR101 at the KpnI and XbaI sites.
pCKR101-*yoaD*	This study	*yoaD* amplified with primers DH62 and DH63 subcloned into pCKR101 at the KpnI and XbaI sites.
pCKR101-*bcsA*^{WT}	This study	*bcsA* amplified with primers DH36 and DH37 subcloned into pCKR101 at the KpnI and XbaI sites.
pCKR101-*bcsA*^{1}	This study	*bcsA* PilZ *mutant 1* initially amplified with primers DH36&DH45 and DH37&DH44 followed by amplification of first PCR products with

		primers DH36 and DH37 subcloned into pCKR101 at the KpnI and XbaI sites.
pCKR101-*bcsA*^{2}	This study	*bcsA* PilZ *mutant 2* initially amplified with primers DH36&DH47 and DH37&DH46 followed by amplification of first PCR products with primers DH36 and DH37 subcloned into pCKR101 at the KpnI and XbaI sites.
pFD1	Rubin *et al.* 1999	
pCKR101-*yfiB*	This study	*yfiB* amplified with primers DH168 and DH169 subcloned into pCKR101 at the KpnI and XbaI sites.

Table 2.3- Primer list Chapter 2

name	description	sequence
DH32	pRJ800 lacZ 16s F	GAT CGG ATC CTA TAC CGA TTG GGA GCA GGT
DH33	pRJ800 lacZ 16s R	GAT CTC TAG AAA AAG TTT GAT GCT CGT GAA TTA AA
DH34	pRJ800 lacZ *adrA* F	GAT CGG ATC CCA AAA GAT GCG CGA ATG TAA TAA TC
DH35	pRJ800 lacZ *adrA* R	GAT CTC TAG ATC AGA AAC AAT TTT CCC AAA TTA TA
DH36	*bcsA* F KpnI pCKR101 SOE	GAT CGG TAC CAT GAG TAT CCT GAC CCG GTG
DH37	*bcsA* R XbaI pCKR101 SOE	GAT CTC TAG ATC ATT GTT GAG CCA AAG CCT
DH44	*bcsA* pilZ pckr101 mut1 C F	GCA AAC AGG TAG ACC GAT CGC ACC G
DH45	*bcsA* pilZ pckr101 mut1 B R	CGG TGC GAT CGG TCT ACC TGT TTG C
DH46	*bcsA* pilZ pckr101 mut2 C F	GCC GAT CGC ACG ACG TGG AGA TGA C
DH47	*bcsA* pilZ pckr101 mut2 B R	GTC ATC TCC ACG TCG TGC GAT CGG C
DH62	*yoaD* F KpnI pckr101	GAT CGG TAC CTT GTC GCC ATA CGC TTA CAG
DH63	*yoaD* R XbaI pckr101	GAT CTC TAG ATT AAC GTA ACG GCA TAA TGG
DH74	prj800 *yoaD* F BamHI	GAT CGG ATC CTG CAG GGC AAG TTC AGG T
DH75	pRJ800 *yoaD* R XbaI	GAT CTC TAG AAC GCC TGA CGC AAC AGT GGA
DH149	UTI89 *yfiN* RS F	TCT TAA TAA GCG CCC CAC GTT TAA AAG AGC ATT ACG CAA CAT CAG TAT GAG TGT AGG CTG GAG CTG CTT C

DH150	UTI89 *yfiN* RS R	AGG TGC TTT ATC ATA TCG ATA TAT CCT TGT TAT CTC ACC AGC TTT TCG GCC ATA TGA ATA TCC TCC TTA G
DH151	UTI89 *yfiR* RS F	TGA AAA AAT ATC GAT GCA TTT CGA GCG AAG ATG GTG AGG ATC CCT GAA TGG TGT AGG CTG GAG CTG CTT C
DH152	UTI89 *yfiR* RS R	CGA GCA TTA AGA CAT CCG GGT TGA CTT TTA CAC CGC TAC GAG ATA AAG CAC ATA TGA ATA TCC TCC TTA G
DH157	UTI89 *yfiB* RS F	CAA GGA TAT ATC GAT ATG ATA AAG CAC CTG CTA GCA CCC CTG ATT TTC ACG TGT AGG CTG GAG CTG CTT C
DH158	UTI89 *yfiB* RS R	GCT GGC CCT TTT TTT GTC TGT TTG CTC GTG TTT TAA GGG GTT GTA ATC ACC ATA TGA ATA TCC TCC TTA G
DH165	UTI89 pckr101 KpnI *yfiR* F	GAT CGG TAC CAT GCG TTT TTC TCA CCG ACT
DH166	UTI89 pckr101 XbaI *yfiR* R	GAT CTC TAG ATT ATC CAT CAT TTT TCT TCC
DH167	UTI89 pckr101 XbaI yfiR R HisT	GAT CTC TAG ATT AGT GAT GGT GAT GGT GAT GTC CAT CAT TTT TCT TCC
DH168	UTI89 pckr101 KpnI *yfiB* F	GAT CGG TAC CAT GAT AAA GCA CCT GCT AGC
DH169	UTI89 pckr101 XbaI *yfiB* R	GAT CTC TAG ATT AAG GGG TTG TAA TCA CCA
WD277	UTI89 *dsbA* RS left	TTC ACG GGC TTT ATG TAA TTT ACA TTG AAT TAT TTT TTC TCG GAC AGA TAG TGT AGG CTG GAG CTG CTT C
WD278	UTI89 *dsbA* RS right	ACC CCC TTT GCA ATT AAC ACC TAT GTA TTA ATC GGA GAG AGT AGA TCA TGC ATA TGA ATA TCC TCC TTA G
WD273	UTI89 *dsbB* RS left	AAA GCG CTC CCG CAG GAG CGC CGA ATG GAT TAG CGA CCG AAC AGG TCA CGC ATA TGA ATA TCC TCC TTA G
WD274	UTI89 *dsbB* RS right	GAA TTG GTT TAA ACT GCG CAC TCT ATG CAT ATT GCA GGG AAA TGA TTA TGG TGT AGG CTG GAG CTG CTT C
WD99	*adrA* Red swap left. Use w/ WD100 in UTI89.	CTT CTG CCT TTA GCC CCG TCT CTA TAA TTT GGG AAA ATT GTT TCT GAA TGG TGT AGG CTG GAG CTG CTT C
WD100	adrA Red swap right. Use w/ WD99 in UTI89.	CAG CAA ATC CTG ATG GCT TTT GCC GGA CGT CAG GCC GCC ACT TCG GTG CGC ATA TGA ATA TCC TCC TTA G
WD36	UTI89 *csgD* Red swap primer F. Use w/ pKD4	CAA TCC AGC GTA AAT AAC GTT TCA TGG CTT TAT CGC CTG AGG TTA TCG TTC

	and WD 37.	ATA TGA ATA TCC TCC TTA
WD37	UTI89 *csgD* Red swap primer R. Use w/ pKD4 and WD36	GAG GCA GCT GTC AGG TGT GCG ATC AAT AAA AAA AGC GGG GTT TCA TCA TGG TGT AGG CTG GAG CTG CTT C
WD6	Red swap F primer for deleting *csgBA* in UTI89.	AAA TAC AGG TTG CGT TAA CAA CCA AGT TGA AAT GAT TTA ATT TCT TAA GTG TGT AGG CTG GAG CTG CTT
WD7	Red swap R primer for deleting *csgBA* in UTI89.	CGA AAA AAA ACA GGG CTT GCG CCC TGT TTC TTT AAT ACA GAG GAT GTA TAT GAA TAT CCT CCT TAG
WD349	*bcsA* UTI89 RS F	TGC CTG TTA AAC TAT TCC GGG CTG AAA ATG CCA GTC GGG AGT GCA TCA TGC ATA TGA ATA TCC TCC TTA G
WD350	*bcsA* UTI89 RS R	AGA ATA TTT TTC TTT TCA TCG CGT TAT CAT CAT TGT TGA GCC AAA GCC TGG TGT AGG CTG GAG CTG CTT C
NDH89	Mariner 1	GGC CAC GCG TGC ACT AGT ACN NNN NNN NNN TAC NG
NDH90	Mariner 2	ATG CAT TTA ATA CTA GCG ACG C
NDH91	Mariner 3	GGC CAC GCG TGC ACT AGT AC
NDH92	Mariner 4	GCG ATC TAT GTG TCA GAC CGG

Table 2.4- Strain list Chapter 2

Strain Name	Strain Genotype	Reference	Notes
	UTI89	Mulvey *et al.* 2001	
	UTI89 Δ*csgD*	DePas *et al.* 2013	
	UTI89 Δ*csgBA*	DePas *et al.* 2013	
	UTI89 Δ*bcsA*	DePas *et al.* 2013	
CL-1484	UTI89 Δ*dsbA*	This study	Red Swap mutagenesis of UTI89 with primers WD277 and WD288 followed by electroporation with the recombinase PCP20 to remove kanamycin cassette
CL-1291	UTI89Δ*dsbB*	This study	Red Swap mutagenesis of UTI89 with primers WD273 and WD274 followed by electroporation with the recombinase PCP20 to remove kanamycin cassette
CL-1413	UTI89 Δ*dsbB* pRJ800-*adrA*	This study	UTI89 ΔdsbB electroporated with prj800-*adrA*
CL-1414	UTI89 Δ*dsbB* pRJ800-16s	This study	UTI89 ΔdsbB electroporated with prj800-16s

CL-1415	UTI89 Δ*dsbB* pRJ800	This study	UTI89 ΔdsbB electroporated with prj800
	UTI89 pRJ800-*adrA*	DePas *et al.* 2013	
	UTI89 pRJ800-16s	DePas *et al.* 2013	
	UTI89 pRJ800	DePas *et al.* 2013	
CL-1869	UTI89 Δ*dsbB*Δ*csgBA*	This study	Red Swap mutagenesis of UTI89 Δ*dsbB* with primers WD6 and WD7 followed by electroporation with the recombinase PCP20 to remove kanamycin cassette
CL-1866	UTI89 Δ*dsbB*Δ*bcsA*	This study	Red Swap mutagenesis of UTI89 Δ*dsbB* with primers WD349 and WD350 followed by electroporation with the recombinase PCP20 to remove kanamycin cassette
CL-1354	UTI89 Δ*csgD*Δ*dsbB*	This study	Red Swap mutagenesis of UTI89 Δ*csgD* with primers WD273 and WD274 followed by electroporation with the recombinase PCP20 to remove kanamycin cassette
CL-1394	UTI89 Δ*csgD*Δ*dsbB*Δ*bcsA*	This study	Red Swap mutagenesis of UTI89 Δ*csgD*Δ*dsbB* with primers WD349 and WD350 followed by electroporation with the recombinase PCP20 to remove kanamycin cassette
CL-1543	UTI89 Δ*dsbB*Δ*adrA*	This study	Red Swap mutagenesis of UTI89 Δ*dsbB* with primers WD99 and WD100 followed by electroporation with the recombinase PCP20 to remove kanamycin cassette
CL-1393	UTI89 Δ*csgD*Δ*dsbB*Δ*adrA*	This study	Red Swap mutagenesis of UTI89 Δ*csgD*Δ*dsbB* with primers WD99 and WD100 followed by electroporation with the recombinase PCP20 to remove kanamycin cassette
CL-1355	UTI89 Δ*csgD*Δ*dsbA*	This study	Red Swap mutagenesis of UTI89 Δ*csgD* with primers WD277 and WD278 followed by electroporation with the recombinase PCP20 to remove kanamycin cassette
CL-1827	UTI89 Δ*csgD*Δ*dsbB*Δ*yfiN*	This study	Red Swap mutagenesis of UTI89 Δ*csgD*Δ*dsbB* with primers DH149 and DH150 followed by electroporation with the recombinase PCP20 to remove kanamycin cassette
CL-1825	UTI89 Δ*yfiN*	This study	Red Swap mutagenesis of UTI89 with primers DH149 and DH150 followed by electroporation with the recombinase PCP20 to remove kanamycin cassette

CL-1826	UTI89 Δ*yfiR*	This study	Red Swap mutagenesis of UTI89 with primers DH151and DH152 followed by electroporation with the recombinase PCP20 to remove kanamycin cassette
CL-1837	UTI89 Δ*csgD*Δ*yfiR*	This study	Red Swap mutagenesis of UTI89 Δ*csgD* with primers DH151and DH152 followed by electroporation with the recombinase PCP20 to remove kanamycin cassette
CL-1828	UTI89 Δ*yfiB*	This study	Red Swap mutagenesis of UTI89 with primers DH157 and DH158 followed by electroporation with the recombinase PCP20 to remove kanamycin cassette
	UTI89 pCKR101	DePas *et al.* 2013	
CL-1840	UTI89 pCKR101-*yfiR*	This study	UTI89 electroporated with pCKR101-*yfiR*
CL-1883	UTI89 pCKR101-*yfiR*^{His}	This study	UTI89 electroporated with pCKR101-*yfiR*^{His}
CL-1646	UTI89 Δ*dsbA* pCKR101	This study	UTI89 Δ*dsbA* electroporated with pCKR101
CL-1884	UTI89 Δ*dsbA* pCKR101-yfiR^{His}	This study	UTI89 Δ*dsbA* electroporated with pCKR101-*yfiR*^{His}
CL-1532	UTI89 Δ*dsbB* pCKR101	This study	UTI89 Δ*dsbB* electroporated with pCKR101
CL-1841	UTI89 Δ*dsbB* pCKR101-*yfiR*	This study	UTI89 Δ*dsbB* electroporated with pCKR101-*yfiR*
CL-1539	UTI89 Δ*csgD*Δ*dsbB* pCKR101	This study	UTI89 Δ*csgD*Δ*dsbB* electroporated with pCKR101
CL-1842	UTI89 Δ*csgD*Δ*dsbB* pCKR101-*yfiR*	This study	UTI89 Δ*csgD*Δ*dsbB* electroporated with pCKR101-*yfiR*
	UTI89 Δ*csgBA*Δ*bcsA*	DePas *et al.* 2013	
CL-1394	UTI89 Δ*csgD*Δ*dsbB*Δ*bcsA*	This study	Red Swap mutagenesis of UTI89 Δ*csgD*Δ*dsbB* with primers DH349 and DH350
CL-1525	UTI89 pckr101-*yoaD*	This study	UTI89 electorporated with pCKR101-*yoaD*
CL-1526	UTI89 Δ*dsbB* pCKR101-*yoaD*	This study	UTI89 Δ*dsbB* electroporated with pCKR101-*yoaD*
CL-1473	UTI89 Δ*csgD*Δ*dsbB*Δ*bcsA* pCKR101-	This study	UTI89 electorporated with pCKR101-*bcsA*^{WT}

	bcsA^{WT}		
CL-1471	UTI89 Δ*csgD*Δ*dsbB*Δ*bcsA* pCKR101-*bcsA*^{1}	This study	UTI89 electorporated with pCKR101-*bcsA*^{1}
CL-1472	UTI89 Δ*csgD*Δ*dsbB*Δ*bcsA* pCKR101-*bcsA*^{2}	This study	UTI89 electorporated with pCKR101-*bcsA*^{2}
CL-1470	UTI89 Δ*csgD*Δ*dsbB*Δ*bcsA* pCKR101	This study	UTI89 electroporated with pCKR101
CL-1914	UTI89 pCKR101-*yfiB*	This study	UTI89 electroporated with pCKR101-*yfiB*

Acknowledgements

This manuscript was published in *Journal of Bacteriology* (Hufnagel *et al.* 2014). Will DePas helped with the experimental design in this project.

References

1. **Dittmer CG.** 1931. Animal Aggregations: A Study in General Sociology. Journal of Educational Sociology **5:**130-130.
2. **Vidal O, Longin R, Prigent-Combaret C, Dorel C, Hooreman M, Lejeune P.** 1998. Isolation of an *Escherichia coli* K-12 mutant strain able to form biofilms on inert surfaces: Involvement of a new ompR allele that increases curli expression. J Bacteriol **180:**2442-2449.
3. **Zogaj X, Nimtz M, Rohde M, Bokranz W, Romling U.** 2001. The multicellular morphotypes of *Salmonella* typhimurium and *Escherichia coli* produce cellulose as the second component of the extracellular matrix. Mol Microbiol **39:**1452-1463.
4. **Wu JF, Xi CW.** 2009. Evaluation of Different Methods for Extracting Extracellular DNA from the Biofilm Matrix. Appl Environ Microbiol **75:**5390-5395.
5. **Whitchurch CB, Tolker-Nielsen T, Ragas PC, Mattick JS.** 2002. Extracellular DNA required for bacterial biofilm formation. Science **295:**1487-1487.
6. **Epstein AK, Pokroy B, Seminara A, Aizenberg J.** 2011. Bacterial biofilm shows persistent resistance to liquid wetting and gas penetration. Proc Natl Acad Sci U S A **108:**995-1000.
7. **White AP, Gibson DL, Kim W, Kay WW, Surette MG.** 2006. Thin aggregative fimbriae and cellulose enhance long-term survival and persistence of *Salmonella*. J Bacteriol **188:**3219-3227.
8. **Kai-Larsen Y, Luthje P, Chromek M, Peters V, Wang X, Holm A, Kadas L, Hedlund KO, Johansson J, Chapman MR, Jacobson SH, Romling U, Agerberth B, Brauner A.** 2010. Uropathogenic *Escherichia coli* modulates immune responses and its curli fimbriae interact with the antimicrobial peptide LL-37. PLoS Pathog **6:**e1001010.
9. **Larsen P, Nielsen JL, Dueholm MS, Wetzel R, Otzen D, Nielsen PH.** 2007. Amyloid adhesins are abundant in natural biofilms. Environ Microbiol **9:**3077-3090.
10. **Dueholm MS, Albertsen M, Otzen D, Nielsen PH.** 2012. Curli functional amyloid systems are phylogenetically widespread and display large diversity in operon and protein structure. PLoS One **7:**e51274.
11. **Hammar M, Arnqvist A, Bian Z, Olsen A, Normark S.** 1995. Expression of two *csg* operons is required for production of fibronectin- and Congo red-binding curli polymers in *Escherichia coli* K-12. Mol Microbiol **18:**661-670.

12. **Evans ML, Chapman MR.** 2013. Curli biogenesis: Order out of disorder. Biochim Biophys Acta doi:10.1016/j.bbamcr.2013.09.010.
13. **Reshamwala SM, Noronha SB.** 2011. Biofilm formation in *Escherichia coli cra* mutants is impaired due to down-regulation of curli biosynthesis. Arch Microbiol **193:**711-722.
14. **Bougdour A, Lelong C, Geiselmann J.** 2004. Crl, a low temperature-induced protein in *Escherichia coli* that binds directly to the stationary phase sigma subunit of RNA polymerase. Journal of Biological Chemistry **279:**19540-19550.
15. **Jubelin G, Vianney A, Beloin C, Ghigo JM, Lazzaroni JC, Lejeune P, Dorel C.** 2005. CpxR/OmpR interplay regulates curli gene expression in response to osmolarity in *Escherichia coli*. J Bacteriol **187:**2038-2049.
16. **Ryjenkov DA, Simm R, Romling U, Gomelsky M.** 2006. The PilZ domain is a receptor for the second messenger c-di-GMP: the PilZ domain protein YcgR controls motility in enterobacteria. Journal of Biological Chemistry **281:**30310-30314.
17. **Omadjela O, Narahari A, Strumillo J, Melida H, Mazur O, Bulone V, Zimmer J.** 2013. BcsA and BcsB form the catalytically active core of bacterial cellulose synthase sufficient for in vitro cellulose synthesis. Proc Natl Acad Sci U S A **110:**17856-17861.
18. **Romling U, Sierralta WD, Eriksson K, Normark S.** 1998. Multicellular and aggregative behaviour of *Salmonella* typhimurium strains is controlled by mutations in the *agfD* promoter. Mol Microbiol **28:**249-264.
19. **Depas WH, Hufnagel DA, Lee JS, Blanco LP, Bernstein HC, Fisher ST, James GA, Stewart PS, Chapman MR.** 2013. Iron induces bimodal population development by *Escherichia coli*. Proc Natl Acad Sci U S A **110:**2629-2634.
20. **Proctor RA, von Eiff C, Kahl BC, Becker K, McNamara P, Herrmann M, Peters G.** 2006. Small colony variants: a pathogenic form of bacteria that facilitates persistent and recurrent infections. Nat Rev Microbiol **4:**295-305.
21. **Dietrich LEP, Okegbe C, Price-Whelan A, Sakhtah H, Hunter RC, Newman DK.** 2013. Bacterial Community Morphogenesis Is Intimately Linked to the Intracellular Redox State. J Bacteriol **195:**1371-1380.
22. **Branda SS, Gonzalez-Pastor JE, Ben-Yehuda S, Losick R, Kolter R.** 2001. Fruiting body formation by *Bacillus subtilis*. Proc Natl Acad Sci U S A **98:**11621-11626.
23. **McCrate OA, Zhou XX, Reichhardt C, Cegelski L.** 2013. Sum of the Parts: Composition and Architecture of the Bacterial Extracellular Matrix. J Mol Biol **425:**4286-4294.
24. **Da Re S, Ghigo JM.** 2006. A CsgD-independent pathway for cellulose production and biofilm formation in *Escherichia coli*. J Bacteriol **188:**3073-3087.
25. **Bardwell JC, Lee JO, Jander G, Martin N, Belin D, Beckwith J.** 1993. A pathway for disulfide bond formation in vivo. Proc Natl Acad Sci U S A **90:**1038-1042.
26. **Nakamoto H, Bardwell JC.** 2004. Catalysis of disulfide bond formation and isomerization in the *Escherichia coli* periplasm. Biochim Biophys Acta **1694:**111-119.
27. **Bardwell JC.** 1994. Building bridges: disulphide bond formation in the cell. Mol Microbiol **14:**199-205.
28. **Rubin EJ, Akerley BJ, Novik VN, Lampe DJ, Husson RN, Mekalanos JJ.** 1999. *In vivo* transposition of mariner-based elements in enteric bacteria and mycobacteria. Proc Natl Acad Sci U S A **96:**1645-1650.

29. **Cegelski L, Pinkner JS, Hammer ND, Cusumano CK, Hung CS, Chorell E, Aberg V, Walker JN, Seed PC, Almqvist F, Chapman MR, Hultgren SJ.** 2009. Small-molecule inhibitors target *Escherichia coli* amyloid biogenesis and biofilm formation. Nat Chem Biol **5:**913-919.
30. **Hung C, Zhou YZ, Pinkner JS, Dodson KW, Crowley JR, Heuser J, Chapman MR, Hadjifrangiskou M, Henderson JP, Hultgren SJ.** 2013. *Escherichia coli* Biofilms Have an Organized and Complex Extracellular Matrix Structure. Mbio **4**.
31. **Monteiro C, Papenfort K, Hentrich K, Ahmad I, Le Guyon S, Reimann R, Grantcharova N, Romling U.** 2012. Hfq and Hfq-dependent small RNAs are major contributors to multicellular development in *Salmonella enterica* serovar Typhimurium. RNA Biol **9:**489-502.
32. **Hoch HC, Galvani CD, Szarowski DH, Turner JN.** 2005. Two new fluorescent dyes applicable for visualization of fungal cell walls. Mycologia **97:**580-588.
33. **Zheng D, Constantinidou C, Hobman JL, Minchin SD.** 2004. Identification of the CRP regulon using in vitro and in vivo transcriptional profiling. Nucleic Acids Res **32:**5874-5893.
34. **Gualdi L, Tagliabue L, Bertagnoli S, Ierano T, De Castro C, Landini P.** 2008. Cellulose modulates biofilm formation by counteracting curli-mediated colonization of solid surfaces in *Escherichia coli*. Microbiology **154:**2017-2024.
35. **Brombacher E, Baratto A, Dorel C, Landini P.** 2006. Gene expression regulation by the Curli activator CsgD protein: modulation of cellulose biosynthesis and control of negative determinants for microbial adhesion. J Bacteriol **188:**2027-2037.
36. **Ross P, Mayer R, Benziman M.** 1991. Cellulose biosynthesis and function in bacteria. Microbiol Rev **55:**35-58.
37. **Solano C, Garcia B, Valle J, Berasain C, Ghigo JM, Gamazo C, Lasa I.** 2002. Genetic analysis of *Salmonella* enteritidis biofilm formation: critical role of cellulose. Mol Microbiol **43:**793-808.
38. **Weissborn AC, Liu Q, Rumley MK, Kennedy EP.** 1994. UTP: alpha-D-glucose-1-phosphate uridylyltransferase of *Escherichia coli*: isolation and DNA sequence of the galU gene and purification of the enzyme. J Bacteriol **176:**2611-2618.
39. **Taglicht D, Padan E, Schuldiner S.** 1991. Overproduction and purification of a functional Na+/H+ antiporter coded by *nhaA* (*ant*) from *Escherichia coli*. Journal of Biological Chemistry **266:**11289-11294.
40. **Mao SS, Yu GX, Chalfoun D, Stubbe J.** 1992. Characterization of C439SR1, a mutant of *Escherichia coli* ribonucleotide diphosphate reductase: evidence that C439 is a residue essential for nucleotide reduction and C439SR1 is a protein possessing novel thioredoxin-like activity. Biochemistry **31:**9752-9759.
41. **Lu M, Campbell JL, Boye E, Kleckner N.** 1994. SeqA: a negative modulator of replication initiation in E. coli. Cell **77:**413-426.
42. **Waldminghaus T, Skarstad K.** 2009. The *Escherichia coli* SeqA protein. Plasmid **61:**141-150.
43. **Sanchez-Torres V, Hu H, Wood TK.** 2011. GGDEF proteins YeaI, YedQ, and YfiN reduce early biofilm formation and swimming motility in *Escherichia coli*. Appl Microbiol Biotechnol **90:**651-658.
44. **Raterman EL, Shapiro DD, Stevens DJ, Schwartz KJ, Welch RA.** 2013. Genetic analysis of the role of *yfiR* in the ability of *Escherichia coli* CFT073 to control cellular

cyclic dimeric GMP levels and to persist in the urinary tract. Infect Immun **81:**3089-3098.

45. **Malone JG, Jaeger T, Spangler C, Ritz D, Spang A, Arrieumerlou C, Kaever V, Landmann R, Jenal U.** 2010. YfiBNR mediates cyclic di-GMP dependent small colony variant formation and persistence in *Pseudomonas aeruginosa*. PLoS Pathog **6:**e1000804.
46. **Malone JG, Jaeger T, Manfredi P, Dotsch A, Blanka A, Bos R, Cornelis GR, Haussler S, Jenal U.** 2012. The YfiBNR Signal Transduction Mechanism Reveals Novel Targets for the Evolution of Persistent *Pseudomonas aeruginosa* in Cystic Fibrosis Airways. PLoS Pathog **8**.
47. **Zander T, Phadke ND, Bardwell JC.** 1998. Disulfide bond catalysts in *Escherichia coli*. Methods Enzymol **290:**59-74.
48. **Allore RJ, Barber BH.** 1984. A recommendation for visualizing disulfide bonding by one-dimensional sodium dodecyl sulfate--polyacrylamide gel electrophoresis. Anal Biochem **137:**523-527.
49. **Hadjifrangiskou M, Gu AP, Pinkner JS, Kostakioti M, Zhang EW, Greene SE, Hultgren SJ.** 2012. Transposon mutagenesis identifies uropathogenic *Escherichia coli* biofilm factors. J Bacteriol **194:**6195-6205.
50. **Ueda A, Wood TK.** 2009. Connecting quorum sensing, c-di-GMP, pel polysaccharide, and biofilm formation in *Pseudomonas aeruginosa* through tyrosine phosphatase TpbA (PA3885). PLoS Pathog **5:**e1000483.
51. **Girgis HS, Liu Y, Ryu WS, Tavazoie S.** 2007. A comprehensive genetic characterization of bacterial motility. PLoS Genet **3:**1644-1660.
52. **Giddens SR, Jackson RW, Moon CD, Jacobs MA, Zhang XX, Gehrig SM, Rainey PB.** 2007. Mutational activation of niche-specific genes provides insight into regulatory networks and bacterial function in a complex environment. Proc Natl Acad Sci U S A **104:**18247-18252.
53. **Ren GX, Yan HQ, Zhu H, Guo XP, Sun YC.** 2014. HmsC, a periplasmic protein, controls biofilm formation via repression of HmsD, a diguanylate cyclase in *Yersinia pestis*. Environ Microbiol **16:**1202-1216.
54. **Bobrov AG KO, Vadyvaloo V, Koestler BJ, Hinz AK, Mack D, Waters CM, and Perry RD.** 2014. The *Yersinia pestis* HmsCDE regulatory system is essential for blockage of the oriental rat flea (*Xenopsylla cheopis*), a classic plague vector. Environmental Microbiology doi:DOI: 10.1111/1462-2920.12419.
55. **Kader A, Simm R, Gerstel U, Morr M, Romling U.** 2006. Hierarchical involvement of various GGDEF domain proteins in rdar morphotype development of *Salmonella enterica* serovar Typhimurium. Mol Microbiol **60:**602-616.
56. **Weber H, Pesavento C, Possling A, Tischendorf G, Hengge R.** 2006. Cyclic-di-GMP-mediated signalling within the sigma(S) network of *Escherichia coli*. Mol Microbiol **62:**1014-1034.
57. **Dailey FE, Berg HC.** 1993. Mutants in disulfide bond formation that disrupt flagellar assembly in *Escherichia coli*. Proc Natl Acad Sci U S A **90:**1043-1047.
58. **Jacob-Dubuisson F, Pinkner J, Xu Z, Striker R, Padmanhaban A, Hultgren SJ.** 1994. PapD chaperone function in pilus biogenesis depends on oxidant and chaperone-like activities of DsbA. Proc Natl Acad Sci U S A **91:**11552-11556.

59. **Miki T, Okada N, Kim Y, Abe A, Danbara H.** 2008. DsbA directs efficient expression of outer membrane secretin EscC of the enteropathogenic *Escherichia coli* type III secretion apparatus. Microb Pathog **44:**151-158.
60. **Wulfing C, Rappuoli R.** 1997. Efficient production of heat-labile enterotoxin mutant proteins by overexpression of *dsbA* in a *degP*-deficient *Escherichia coli* strain. Arch Microbiol **167:**280-283.
61. **Heras B, Shouldice SR, Totsika M, Scanlon MJ, Schembri MA, Martin JL.** 2009. DSB proteins and bacterial pathogenicity. Nat Rev Microbiol **7:**215-225.
62. **Hufnagel DA, Tukel C, Chapman MR.** 2013. Disease to dirt: the biology of microbial amyloids. PLoS Pathog **9:**e1003740.
63. **Serra DO, Richter AM, Hengge R.** 2013. Cellulose as an Architectural Element in Spatially Structured *Escherichia coli* Biofilms. J Bacteriol **195:**5540-5554.
64. **Meftahi A, Khajavi R, Rashidi A, Sattari M, Yazdanshenas ME, Torabi M.** 2010. The effects of cotton gauze coating with microbial cellulose. Cellulose **17:**199-204.
65. **Czaja WK, Young DJ, Kawecki M, Brown RM.** 2007. The future prospects of microbial cellulose in biomedical applications. Biomacromolecules **8:**1-12.
66. **Lin SP, Calvar IL, Catchmark JM, Liu JR, Demirci A, Cheng KC.** 2013. Biosynthesis, production and applications of bacterial cellulose. Cellulose **20:**2191-2219.
67. **Cavka A, Guo X, Tang SJ, Winestrand S, Jonsson LJ, Hong F.** 2013. Production of bacterial cellulose and enzyme from waste fiber sludge. Biotechnology for Biofuels **6**.
68. **Thompson DN, Hamilton MA.** 2001. Production of bacterial cellulose from alternate feedstocks. Applied Biochemistry and Biotechnology **91-3:**503-513.
69. **Datsenko KA, Wanner BL.** 2000. One-step inactivation of chromosomal genes in *Escherichia coli* K-12 using PCR products. Proc Natl Acad Sci U S A **97:**6640-6645.
70. **Steensma DP.** 2001. "Congo" red: out of Africa? Arch Pathol Lab Med **125:**250-252.
71. **Anderson CT, Carroll A, Akhmetova L, Somerville C.** 2010. Real-time imaging of cellulose reorientation during cell wall expansion in Arabidopsis roots. Plant Physiol **152:**787-796.
72. **Miller J.** 1972. Experiments in Molecular Genetics. Cold Spring Harbor Lab Press, Cold Spring Harbor, NY.
73. **Zhou Y, Smith DR, Hufnagel DA, Chapman MR.** 2013. Experimental manipulation of the microbial functional amyloid called curli. Methods Mol Biol **966:**53-75.
74. **Barnhart MM, Lynem J, Chapman MR.** 2006. GlcNAc-6P levels modulate the expression of Curli fibers by *Escherichia coli*. J Bacteriol **188:**5212-5219.
75. **Quan S, Hiniker A, Collet JF, Bardwell JC.** 2013. Isolation of bacteria envelope proteins. Methods Mol Biol **966:**359-366.
76. **Sorensen K, Brodbeck U.** 1986. A Sensitive Protein Assay-Method Using Micro-Titer Plates. Experientia **42:**161-162.

Chapter 3

Cysteine Auxotrophy Uncouples the UPEC Extracellular Matrix

Abstract

A hallmark of bacterial biofilms is the production of an extracellular matrix (ECM) that encases the cells. In uropathogenic *Escherichia coli* (UPEC) the ECM is composed of the amyloid curli and the polysaccharide cellulose, whose expression is intimately choreographed by the biofilm master regulator CsgD. Multiple metabolites involved in cysteine biosynthesis have been implicated in *E. coli* and *Vibrio fischeri* biofilm formation. Additionally, in UPEC and other enterobacteriaceael infections cysteine auxotrophs are isolated ~ 1.5% of the time and are correlated with mecillinam resistance, leading us to investigate how cysteine impacts the UPEC isolate's (UTI89) biofilm formation and the production of the ECM. We found that cysteine auxotrophs over-produced curli and under-produced cellulose. WT levels of ECM components were produced by cysteine auxotrophs if they were grown in the presence of surplus cysteine. Time-lapse photography of wrinkled colony (rugose) biofilms revealed that WT cells produce both curli and cellulose at the same time, whereas cysteine auxotrophs produce curli before cellulose. Transposon mutagenesis revealed YfiR, the periplasmic regulator of the diguanylate cyclase YfiN, controls the cellulose defect in *ΔcysE* biofilms. We also found that UPEC cysteine auxotrophs (UTI89 Δ*cysE* and 7 patient isolates) produced curli at 37°C, unlike WT UTI89 that only produced detectable curli at 26°C. High curli, low cellulose production, and mecillinam resistance in cysteine auxotrophs occurred because of hyper-oxidation, as both cysteine and

glutathione, restored WT biofilm phenotypes to strains unable to produce cysteine and glutathione. Interestingly, we found that sub-lethal concentrations of mecillinam and Bactrim inhibit curli production; however cysteine auxotrophs are resistant to the curli-inhibitory activity.

Introduction

Escherichia coli is the most common etiologic agent of urinary tract infections (UTIs) and accounts for over 6 billion in healthcare costs in premenopausal women according to the American Urological Association (1). The uropathogenic *E. coli* (UPEC) that cause UTIs are commonly derived from the patient's own intestinal tract (2, 3). However, clonal UPEC outbreaks require UPEC to survive outside the host (4, 5). To survive outside of the host, UPEC must protect itself from predation and oxidative stress, which can be achieved by biofilm formation (6-9).

Biofilms are characterized as communities of bacteria that are associated with a surface and produce an extracellular matrix (ECM) composed of polysaccharide, protein, and DNA (10). The biofilm formation process of *E. coli* occurs in low salt, low temperature, and low nutrient conditions and is dependent on transcription of *csgD* (11-13). CsgD upregulates production of both ECM components, curli and cellulose (14, 15). CsgD activates *csgBAC* transcription, which encodes the minor and major subunits of the curli fiber (14, 16). Certain isolates of *E. coli* have been found to produce curli at higher temperatures (17-19). CsgD transcriptionally up-regulates *adrA* which encodes a diguanylate cyclase that produces the secondary messenger, c-di-GMP (15). C-di-GMP binds to the cellulose synthase, BcsA, leading to cellulose synthase activation (15, 20). WT CsgD protein levels require c-di-GMP from YfiN and Ydam (21, 22). The cellulose synthase, BcsA, binds c-di-GMP, activates, and then produces cellulose from UDP-glucose (15,

23). High levels of c-di-GMP also act to inhibit motility , as the molecular brake, YcgR acts to inhibit flagellar rotation when c-di-GMP levels are high (23, 24).

Multiple cysteine biosynthesis and catabolic products have been implicated in biofilm formation and development (25-28). O-acetylated serine (OAS) is a precursor to cysteine produced by serine acetyl transferase, CysE (Figure 3.1A), and was found to be a biofilm inhibiting compound in *E. coli* and *Providencia stuartii* (25). Δ*cysE* strains that can not produce OAS form hyper-biofilms, and exogenous OAS addition led to WT biofilm inhibition (25). Additionally, Δ*cysB* strains produce hyper-biofilms, and CysB is regulated by NAS, a product of OAS (28). Phosphoadenosine 59-Phosphosulfate (PAPS), which is produced by CysC in the sulfur assimilation pathway, is another cysteine precursor that is a biofilm-activating compound that can increase production of curli (26). Additionally, work in *Vibrio fischeri* has found that cysteine auxotrophs are defective at forming wrinkled colonies (29).

Cysteine auxotrophs are commonly isolated from patients with an active UTI. In 1952 Gillespie discovered 6 UPEC strains that were cysteine auxotrophs (30). In 1978 and 2002, two different studies found that around 1.5-2% of UPEC strains were cysteine auxotrophs (31, 32). Lastly, in 2015 *Thulin et al.* screened a Swedish UPEC collection for mecillinam resistance and found 12 mecillinam resistant strains that were all cysteine auxotrophs (33). This suggests a niche for cysteine auxotrophs in the host, especially during chronic infections.

Our current study seeks to detail the biofilm phenotype and molecular pathways of cysteine auxotrophs. Our work detailed here found that UPEC cysteine auxotrophs had increased curli and decreased cellulose production. UPEC cysteine auxotrophs formed smooth colony biofilms similar to that seen in *V. fischeri* (29). We've found that the lack of thiol reducing agents such as cysteine or glutathione were the cause of increased curli and decreased cellulose

production and could restore sensitivity of cysteine auxotrophs to mecillinam. We found that sub-inhibitory concentrations of mecillinam inhibited curli biogenesis, and this may be a wide-spread mode of action, as the antibiotic Bactrim (Trimethoprim/sulfamethoxazole) also inhibits curli production. Cysteine auxotrophs are resistant to the curli-inhibition of both antibiotics. In summary cysteine biosynthesis is necessary for the coupling of curli and cellulose production in UPEC biofilms.

Results

We characterized UPEC biofilm formation by WT UTI89 and the cysteine auxotrophic strains Δ*cysE* and *ΔcsyKΔcysM* (see Figure 3.1A for the cysteine biogenesis pathway). We found that both cysteine auxotrophic strains bound Congo red (CR), but did not wrinkle or spread (Figure 3.1B). Addition of 20µL 10% (w/v) cysteine to a sterile paper disk on YESCA media restored colony wrinkling to both cysteine auxotroph colonies, however addition of OAS only restored wrinkling to Δ*cysE* and not to Δ*cysK*Δ*cysM* (Figure 3.1B). Since OAS was unable to restore colony wrinkling to Δ*cysK*Δ*cysM* it suggests that the smooth colony morphotype of cysteine auxotrophs was due to the lack of cysteine not OAS. CFU per rugose colony of Δ*cysE* grown on YESCA and YESCA cys were unchanged (Figure 3.1C), and Δ*cysE* and *ΔcsyKΔcysM* wrinkled when complemented *in trans* (Figure 3.1D).

ECM of Cysteine Auxotrophs

The production of the extracellular matrix (ECM) components curli and cellulose was investigated in the cysteine auxotrophs. A *csgBA* mutant strain Δc*ysE*Δ*csgBA* bound CR at 26°C

wrinkled in the presence of cysteine, showing *ΔcysE* CR binding by a separate ECM component from curli (Figure 3.2A). UTI89 *csgBA* mutants bind CR and stain red due to cellulose production (6, 21). The *cysE* mutant was analyzed with the cellulose specific stain Pontamine Fast Scarlet 4B(S4B) to determine its cellulose production compared to WT. S4B staining revealed decreased cellulose production in Δ*cysE* than WT (Figure 3.2B).

Western blots showed similar CsgD levels between WT and Δ*cysE,* although there were modestly higher CsgA protein levels in Δ*cysE* strains (Figure 3.2C). The addition of 250μM of cysteine to YESCA plates induced colony wrinkling by Δ*cysE* strains and also brought CsgA protein levels to WT levels (Figure 3.2C). Expression of CsgA was completely dependent on CsgD, as Δ*cysE*Δ*csgD* strains did not bind CR or produce CsgA (Figure 3.2C).

We next looked at the temporal control of curli and cellulose production in our WT and Δ*cysE* colonies. We grew WT, Δ*cysE*, and Δ*cysE*Δ*csgBA* at 26°C on YESCA CR in a stage incubator (Figure 3.3A). Time-lapse photography allowed for temporal observation of curli and cellulose production, as both ECM components bind CR and Δ*csgBA*Δ*bcsA* strains do not bind CR (Figure 3.3A). WT and Δ*cysE* were stained with CR at 12 hours (Figure 3.3A), whereas Δ*cysE*Δ*csgBA* remained white until the 18 hour mark suggesting that the Δ*cysE*Δ*csgBA* strain was defective in synthesizing cellulose until this timepoint. To view WT timing of cellulose and curli production, we used Δ*csgBA* (cellulose+, curli$^-$) and Δ*bcsA* (curli+, cellulose). We found that both Δ*csgBA* and Δ*bcsA* strains were stained with CR at the 12 hour time point, demonstrating that curli and cellulose production was temporally coordinated. Mutation of both curli and cellulose abolished CR binding at all timepoints (Figure 3.3A). Together these data showed Δ*cysE* colonies had partially uncoupled the temporal regulation of curli and cellulose production.

Dark CR staining at the 12 hour mark led us to think that expression of *csgBA* was elevated at early timepoints. *csgBAC-mCHERRY* chromosomal transcriptional fusion strains were tracked by time-lapse fluorescence microscopy and revealed that despite early dark CR binding, *csgBA* expression was not increased in Δ*cysE* at any timepoint (Figure 3.3B). IPTG inducible expression of GFP revealed no differences in transcription between WT and Δ*cysE* (data not shown). Additionally, we looked at *csgBAC* and *adrA* transcription via β-galactosidase transcriptional fusions (6, 34) and surprisingly found similar transcription of *csgBAC* in WT, *cysE,* and *cysKM* mutant cells (Figure 3.4A). Unsurprisingly, *adrA* transcription is decreased in *ΔcysE* and *ΔcysKΔcysM* strains compared to WT (3.4A). The transcriptional data led us to hypothesize that perhaps curli were upregulated via post-transcriptional control in Δ*cysE* colonies. PAPs is a described regulator of curli that is produced in the cysteine biosynthesis pathway, so we investigated whether PAPs was the cause of cellulose inhibition (26). However, mutation of *cysC* (encodes the enzyme that produces PAPs) did not restore wrinkling to *ΔcysE* (Figure 3.4B). Additionally, the curli biosynthesis regulator, CysB, didn't appear to affect cellulose production in Δ*cysE* (Figure 3.4B). This result is in concert with cysteine not OAS causing the Δ*cysE* smooth colony morphotype (Figure 3.1B), as a byproduct of OAS (Figure 3.1A), NAS, activates CysB.

Glutathione is a reducing agent of reactive oxygen species (ROS), participates in the glutaredoxin cytoplasmic disulfide reduction system (35), and is produced from cysteine (Figure 3.5A) (36, 37). Cysteine itself is also able to act as a reductant to disulfide bonds (38). We hypothesized cysteine auxotrophs were hyper-oxidized without pools of reduced thiols (cysteine or glutathione). We found that glutathione induced Δ*cysE* colonies to wrinkle and spread (Figure 3.5B). Because glutathione could be converted back into cysteine by GshA and GshB (Figure

3.5A), we constructed Δ*cysEgshA::kan* and Δ*cysEgshB::kan* strains. Δ*cysE/gshA::kan* and Δ*cysEgshB::kan* phenocopied Δ*cysE* colonies. Upon addition of cysteine or glutathione, colony wrinkling and spreading were restored to these strains (Figure 3.5C). These results suggest that hyper-oxidation of Δ*cysE* strains was the cause of the smooth non-spreading non-wrinkling colony morphotype.

C-di-GMP can upregulate CsgD protein levels (21, 22) so we tested whether c-di-GMP was the cause behind our hyper-curli production in cysteine auxotrophs. High c-di-GMP causes a motility defect through the flagellar brake YcgR (23, 24), so motility is used as a proxy for relative c-di-GMP levels. Despite high levels of CsgD, Δ*cysE* mutants displayed greater than WT levels of motility (Figure 3.6), showing this strain did not have high c-di-GMP production, despite a hyper-biofilm phenotype in respect to curli. Additionally, this result could explain the lack of cellulose production, as c-di-GMP activates the cellulose synthase in UTI89.

Δ*cysE* Cellulose Inhibition Factors

To better understand why *cysE* strains produced smooth colonies at 26°C transposon mutations were constructed in the *cysE* background. We screened the entire *cysE*+transposon library on CR-indicator plates grown at 26°C to identify strains that had gained the wrinkled colony phenotype (Table 3.1). The object of this screen was to identify mutations that would revert the smooth colony phenotype of *cysE* strains back to wrinkled. We predicted that transposons which interrupted phosphodiesterases that degrade c-di-GMP might restore wrinkling to *csyE* strains. Indeed, one transposon insertion was in *yciR,* which encodes a phosphodiesterase (39). A second transposon was found inserted into *yfiR,* whose gene product inhibits activation of the diguanylate cyclase YfiN (21, 40). A Δ*cysE yfiR::kan* and a Δ*cysE*

yciR::kan strain were constructed by lambda red genome editing. Δ*cysE yciR::kan* only partially restored wrinkling, while Δ*cysE yfiR::kan* had a robust wrinkled colony morphotype (Figure 3.7A). YfiR contains a disulfide bond that is sensitive to the oxidation state of the cell (21). Oxidized YfiR is more stable in the periplasm and would be able to quench the diguanylate cyclase activity of YfiN (21, 40). These results and the glutathione results, led us to hypothesize *cysE* strains had increased oxidation compared to WT and increased YfiR stability leading to decreased YfiN activation and cellulose production. Overexpression of *yfiR,* conferred a smooth CR binding morphotype to WT colonies similar to that of cysteine auxotrophs supporting our hypothesis that accumulation of YfiR causes the smooth and red colony of Δ*cysE* colonies (Figure 3.7b). The reducing agent, dithiothreitol (DTT), causes YfiR to lose its disulfide and misfold, leading to decreased YfiR levels in the periplasm (21). In agreement with cysteine auxotrophs having a smooth colony morphotype due to increased YfiR levels, DTT caused Δ*cysE* colony wrinkling at 26°C (Figure 3.7C).

There were several other transposon insertions in genes encoding interesting regulators that restored wrinkling to *cysE* strains. Since curli were upregulated without apparent increase in *csgBAC* transcription (Figure 3.3 and 3.4), we looked for small RNA modulators. Both *hfq* and *oxyR* were found in our screen. Hfq stabilizes small RNAs like *oxyS* (41), while OxyR is a cytoplasmic oxidation sensitive transcription factor that also regulates RpoS and the small RNA *oxyS* (42, 43). Δ*cysE hfq::kan* and Δ*cysE oxyR::kan* clean deletions both partially restored wrinkling to cysteine auxotrophs (Figure 3.7A).

Curli Dysregulation in Δ*cysE*

Increased curli production in cysteine auxotrophs, led us to hypothesize that perhaps curli were also made by *cysE* strains in normally non-permissive conditions like 37°C. Δ*cysE* and Δ*cysK*Δ*cysM* colonies stained bright red at 37°C (Figure 3.8A). Western blot analysis revealed slightly increased levels of CsgD and a large increase in CsgA in cysteine auxotrophs compared to WT (Figure 3.8A). To confirm this phenotype we grew Δ*cysE*Δ*csgBA* and Δ*cysE*Δ*csgD* strains at 37°C and found that both CR binding and CsgA production were abolished (Figure 3.8B). Furthermore, the addition of exogenous cysteine to cells grown at 37°C resulted in abolishment of curli production (Figure 3.8B).

The ability of cysteine mutants to produce curli at 37°C is interesting. There is evidence that certain *E. coli* strains express curli at 37°C and in human hosts (44-47). Additionally, cysteine auxotrophs are often found in enterobacteriaceae infections (31, 32). We screened a collection of patient UPEC isolates using CR-indicator plates to determine if they could express curli at 37°C. Of 52 strains tested, only 1 was able to bind CR at 37°C (1.89%) (Figure 3.8C). We then screened a collection of UPEC strains that were mecillinam (amdinocillin) resistant and, interestingly, all cysteine auxotrophs (33). In this collection of UPEC strains, 7 of 12 were able to bind CR at 37°C (58.83%) (Figure 3.8C). CsgA western blots were used to confirm that the 7 CR binding strains at 37°C were indeed producing CsgA (Figure 3.8D).

We took initial steps of identifying the culprit of curli dysregulation by screening the *cysE*+transposon mutant library on CR indicator plates at 37°C. We hypothesized that if the transposon interrupted a specific transcriptional activator that led to increased curli at 37°C that the mutant strains would be white at 37°C, but still red at the permissive temperature of 26°C. Although the transposon library was not saturated, we screened greater than 50,000 colonies

looking for white colonies on CR plates (Table 3.2). Several interesting genes could lead to the determination of the transcriptional regulator that induces curli production at 37°C. Lon and RelA are involved in the stringent response (48) and may induce *csgD* in the absence of cysteine. QseC is a sensor kinase that senses epinephrine, norepinephrine, and AI-3 (49) and its cognate transcriptional regulator QseB regulates curli (50).

Cysteine Auxotrophs and Antibiotics

The correlation of cysteine auxotrophy and mecillinam resistance led us to test the *cysE* strain of UTI89 for mecillinam resistance. When grown near mecillinam infused disks, we found UTI89 Δ*cysE* had an unobservable zone of clearing around mecillinam, whereas WT UTI89 had a large zone of clearing (Figure 3.9A). We hypothesized hyper-oxidation was the cause of the antibiotic resistance phenotype similar to the cause of the observed biofilm phenotype. Cysteine, glutathione, and DTT all increased the sensitivity of Δ*cysE* UTI89 to mecillinam (Figure 3.9B).

Various antibiotics have been implicated to cause oxidative stress in bacteria (51, 52). To test if sub-lethal doses of mecillinam could lead to oxidation of colonies and phenocopy the cysteine auxotroph biofilm, we performed a disk diffusion assay, but this time on YESCA CR plates at 26°C. Interestingly, WT CR binding was inhibited by sub-lethal concentrations of mecillinam, as a white line was clearly visible in the lawn of cells outside of the zone of clearing (Figure 3.9C). In contrast, Δ*cysE* bound CR in the sub-lethal zone of mecillinam (Figure 3.9C). Cells were scraped up from the lawn nearest to the zone of clearing and further away from it and were subjected to western blot analysis. CsgA was decreased in WT in the presence of sub-inhibitory concentrations of mecillinam, while Δ*cysE* appears to be resistant to CsgA inhibition by mecillinam (Figure 3.9C). Additionally, cells in the presence and absence of mecillinam were

normalized by OD_{600}, serial diluted, and plated to confirm consistent viability (Figure 3.10). Bactrim (Trimethoprim/sulfathoxazone) is the second most commonly prescribed antibiotic for UTIs in the US (53). Bactrim was also tested for its ability to quench matrix production, and once again we found that sub-lethal levels of Bactrim inhibit CR binding and production of curli in WT strains, whereas Δ*cysE* are resistant to the Bactrim-mediated curli inhibition (Figure 3.9D).

Discussion

Our findings here detail that cysteine auxotrophy causes an uncoupling of UPEC ECM production. The cause of these changes is due to the lack of reduced thiol pools, as glutathione and cysteine can both restore WT rugose colony formation to Δ*cysE*Δ*gsh* double mutants. Cysteine auxotrophs have inhibited cellulose production dependent on *yfiR* and produce curli independent of temperature.

The uncoupling of curli and cellulose in Δ*cysE* is a very surprising phenotype since these two ECM components are normally intertwined. Increased curli production was also seen in the Δ*cysK*Δ*cysM* strain (Figure 3.11A). CsgD controls both these components, but cysteine auxotrophs still produce CsgD (Figure 3.2C). Our time-lapse photography with Δ*bcsA* and Δ*csgBA* strains revealed that curli and cellulose are produced at similar time-points, whereas cysteine auxotrophs have delayed cellulose production (Figure 3.3A). In UTI89 both curli and cellulose are required for colony spreading, and Δ*cysE* mutants cannot spread despite producing both components. Mutation of *yfiR* in Δ*cysE* restores WT wrinkling, but not WT spreading. We hypothesize that an additional extracellular component is produced that inhibits colony spreading. In agreement, Rossi *et al.* saw increased extracellular levels of Flu, OmpX, and Slp in

cysteine auxotrophs (26). CsgD is at normal wild type levels in cysteine auxotrophs, but transcription of *adrA* is inhibited. AdrA inhibition could be due to: 1) a repressor of *adrA* transcription 2) low c-di-GMP changes CsgD behavior to favor *csgBAC* promoter binding instead of *adrA*. *In silico* analysis of CsgD does not reveal an observable PilZ domain or I site, motifs that are associated with c-di-GMP binding, however FleQ in *Pseudomonas aeruginosa* binds c-di-GMP via interaction with the Walker A motif (54). Perhaps CsgD is similar to FleQ and can bind c-di-GMP and modulate its behavior and have differential preferences for target promoters, or a secondary protein that responds to c-di-GMP alters CsgD promoter preference.

Many other community behaviors and biofilms are sculpted by various components of the cysteine biosynthesis pathway. Contact dependent growth inhibition in *E. coli* uses CysK in complex with CdiA in order to inhibit growth in the presence of other cells (55). A UTI89 *cysK* mutant alone forms a WT rugose colony (data not shown), and the smooth unwrinkled colony phenotype is only formed with the additional deletion of *cysM* (Figure 1B). This leads us to hypothesize that contact-dependent inhibition is not causing the cysteine auxotroph biofilm phenotype. The cysteine biosynthesis byproduct Phosphoadenosine 59-Phosphosulfate (PAPS) induces curli fiber production (26), so we tested whether PAPs caused our cysteine auxotroph biofilm phenotype. Due to a mutation in *bcsQ,* MC4100 does not produce cellulose (56), so the effect of PAPS on cellulose production was unobserved. However, a Δ*cysE*Δ*cysC* double mutant is unable to produce PAPs and still has the same phenotype as a Δ*cysE* strain (Figure 3.4). Additionally, OAS has been cited as a biofilm inhibitory compound, but Δ*cysK*Δ*cysM* mutants still have the smooth colony morphotype and still produce curli in the presence of OAS (Figure 3.1), showing that the smooth colony morphotype of cysteine auxotrophs is independent of the addition of OAS.

We think that the lack of thiol pools, not strictly cysteine auxotrophy, is responsible for our observed phenotype. Addition of the reducing agent glutathione restored colony wrinkling to Δ*cysE* (Figure 4B). GshA and GshB convert cysteine to glutathione (Figure 4A), so glutathione could be converted back to cysteine in Δ*cysE* colonies (Figure 4B). Mutation of *gshA* or *gshB* alone were unable to induce the cysteine auxotoroph smooth colony morphotype (Figure 3.11B). Δ*cysE gshB::kan* and Δ*cysE gshA::kan* double mutants are unable to convert glutathione back to cysteine and are induced to wrinkle and spread in the presence of both cysteine and glutathione. Glutathione functions as a reductant pool for glutaredoxins which reduce disulfides of multiple proteins like ribonucleotide reductase and PAPs reductase (36). PAPs reductase without an active glutaredoxin system should be inactive and may accumulate PAPs, similar to the result seen by Rossi *et al.* in *cysH* mutants (26). In UTI89 cysteine auxotrophs, PAPs doesn't cause cellulose inhibition (Figure 3.4B), and PAPs does not appear to affect the dysregulation of curli phenotype either, as *ΔcysEΔcysC* strains didn't produce curli at 37°C (Figure 3.11C). Perhaps a PAPs precursor, like adenosine 59-phosphosulfate (APS) accumulates in UTI89 cysteine auxotrophs leading to 37°C curli production. To test this, a Δ*cysEΔcysD* strain (defective in APS production) should be monitored for curli production at 37°C. Additionally, overexpression of *cysC* in a *cysE* mutant would decrease APS levels. Decreased curli production at 37°C with decreased APS in cysteine auxotrophs would implicate APS as a curli stimulatory compound.

The activator or de-repressor of curli production at 37°C still needs to be identified. The information in the transposon mutagenesis screening for white colonies at 37°C provides useful information for the cause of curli dysregulation in cysteine auxotrophs. *csgG, cyaA*, *rpoS, ompR* and *envZ* were expected to be white. *csg* locus expression even in strains that produce curli at 37°C is dependent on RpoS and OmpR/EnvZ (18). OmpC is regulated by OmpR, so if OmpR

were hyper-activated, we would see increased OmpC levels. To ensure that OmpR wasn't causing the dysregulation of curli, we probed for OmpC in WT and *ΔcysE* and found similar protein levels (Figure 3.12). *csgG* is required for curli secretion (57, 58), and CyaA produces cAMP which in concert with CRP activates *csgD* transcription (Chapter 4). Many genes hit in the transposon screen are involved in electron transfer (*aceF, aro, mdh, sdh,* and *suc*), so these mutations may decrease the hyper-oxidation phenotype seen in *cysE* mutant strains. Stringent response genes, *relA* and *lon,* popping up in the screen warrants investigation of the stringent response transcriptional regulator DksA (48) in cysteine auxotrophs, to determine if this is the factor that upregulates *csg* expression at 37°C. Identification of *qseC* mutation causing white *cysE* mutant colonies revealed another possible target, the transcriptional regulator QseB. QseB is activated via de-phosphorylation by QseC and regulates curli (50), but determination of why QseB is activated in cysteine auxotrophs would need to be determined. Epinephrine and norepinephrine are not produced by UTI89, and AI-3 is a yet to be identified compound. Perhaps AI-3 accumulates in cysteine auxotrophs leading to QseB activation (49, 59, 60). We believe APS and PAPs accumulate in cysteine auxotrophs, so perhaps AI-3 is a derivative of one of these compounds. Additional analysis of curli production at 37°C is needed.

Cysteine auxotrophs have recently been described to be resistant to the antibiotic mecillinam. *Thulin et al.* 2015 screened a collection of UPEC for mecillinam resistance and found that all resistant strains isolated were cysteine auxotrophs (33). Our UTI89 Δ*cysE* strain also showed greatly increased resistance to mecillinam in comparison to WT (Figure 3.9A). Δ*cysE* mecillinam resistance appears to be due to hyper-oxidation, as cysteine, glutathione, and DTT addition restore sensitivity of Δ*cysE* to mecillinam (Figure 3.9B). The cause of mecillinam resistance could be due to a number of pathways that are suppressors of the Δ*cysE* biofilm

phenotype hit in our transposon screens. In parallel, Tapsall and McIver found glutathione can rescue the small-colony phenotype of cysteine auxotrophs in *Klebsiella* and UPEC (61, 62). Sub-inhibitory concentrations of mecillinam and Bactrim inhibit production of curli in WT UPEC, however cysteine auxotrophs are resistant to the curli-inhibitory effect (Figure 3.9C and 3.9D). Perhaps, curli inhibition by mecillinam and Bactrim are part of the reason why these antibiotics are so effective against bacteria *in vivo.* Slow-growing biofilm communities are inherently resistant to the action of antibiotics, due in no small part to ECM production (10). The ECM can act as a barrier that inhibits antibiotics from reaching the cells in the biofilm (63, 64). Δ*cysE* resistance to curli inhibition by sub-inhibitory concentrations of antibiotics may be a reason why cysteine auxotrophs are commonly selected for and isolated from chronic infections.

Data presented in this manuscript provide a number of clues for the production of curli *in vivo.* Numerous data point to curli being produced not only at 37°C but also in human hosts. Sepsis patients have been observed to have anti-bodies against curli. Additionally UPEC strains that cause sepsis produce curli at 37°C at a higher rate than non-sepsis strains (45). Additionally, *Salmonella,* that produce curli cause an increase in gut epithelial cell junctions and *in vivo* have lower titers in the cecum and mesenteric tissue (46). Interestingly, lots of the cysteine auxotrophs isolated from Gillespie, Borderon, and McIver are from chronic infections (30, 31, 61). Perhaps cysteine auxotrophs grow to large numbers in certain conditions, such as during mecillinam treatment, and produce curli and form biofilms that are resistant to the host and drug treatment. Cystinuria leads to high amounts of cysteine in the host and renal impairment leads to increases in homocysteine and sulfur based amino acids in the urine, which could also lead strains to acquire mutations in cysteine biosynthesis genes (65, 66).

Materials and Methods

Strains and growth conditions All strains were grown up in broth shaking overnight at 37°C. UTI89 strains (67) are all all referred to their genotypes and can be referenced in the supplemental material along with primers used for strain construction. Mutations were performed as previous described via lamda red recombination (21, 68).

Rugose biofilms are 4µL dots of 1-OD_{600} cells washed 2x in YESCA broth then plated and incubated on YESCA (10g casamino acids and 1 g yeast extract/L) CR (50µg/mL) media for 48 hours at 26°C as previously described (6). 37°C biofilms were incubated for 24 hours. For exogenous addition to biofilms, biofilms were plated 1cm from sterile filter disks containing the compound of interest. For overexpression studies 10 to 100µM of Isopropyl β-D-1-thiogalactopyranoside (IPTG) was added to the plates.

Spread plates for antibiotics assays were performed as follows. 0.1-OD_{600} cells were spread on plates with sterile cotton swab then the plate was rotated 60° swabbed and rotated 60° swabbed. Sterile filter disks contained 20µL of compound of interest. ETEST strips (Biomerieux) contain increasing concentrations of compounds of interest.

Western Blot analysis CsgA western blots were performed as previously described (21). Rugose biofilms were collected in 1mL 50mM potassium phosphate buffer (KPI) (pH 7.2) and tissue homogenized (Fischer Tissuemizer) for 10 seconds. 150µL of 1-OD_{600} cells were spun down and resuspended in hexafluoroisopopanol (HFIP) then incubated in a Savant SPD SpeedVac at 45°C for 45 minutes before resuspension in 2x SDS-running buffer. Samples were heated at 95°C for 10 minutes then 8µL are loaded onto a 15% SDS-PAGE gel and run at 25mA for 45 min. Gel was semi-dry transferred at 25V for 10minutes at room temperature onto PVDF membrane. Non-CsgA blots were performed in the same manner with a few modifications. HFIP

was excluded and gels were wet transferred at 4°C at 12V for 12 hours. All blots were blocked in 5% skim milk Tris buffered saline-Tween 20 (TBST) overnight at 4°C. Primary antibody treatment was 1 h at RT (1:8000 CsgA, 1:5000 CsgD, 1:2000 His (ABGENT monoclonal San Diego, CA)) followed by 3x5min washes in TBST. Secondary antibody treatment was 1 h at RT (1:15000 Licor IR dye anti-mouse and anti-rabbit) followed by 3x5min washes in TBST. Blots were visualized on Licor Odyssey CLX imager.

B-galactosidase assays- B-galactosidase assays were performed on rugose biofilms suspended in 1mL KPI and diluted 1:10 as previously described (21, 34). 90µL of reaction buffer, 7µL cells, were incubated for 20min at 30°C before 4mg/mL ortho-nitrophenyl-β-galactoside (ONPG) was added. 50µL 1M NA_2CO_3 addition was added once a yellow color developed in the reaction. 420nm and 550nm absorbance on a Tecan Infinite 200 plate reader were measured in addition to OD_{600} of 1:10 diluted cells. Biological triplicate average of each strain with pRJ800 (promoterless) was subtracted from each reaction, and each reaction was normalized with biological triplicate average of pRJ800-16s (16s promoter upstream of *lacZ*). All genes of interest were assayed in biological triplicate and significance was determined by a student's two-tailed T-test.

Transposon Screen The screens were in UTI89 streptomycin resistant *ΔcysE* background and were plated on YESCA CR plates at 37 or 26°C as previously described (21, 69). *ΔcysE* was conjugated with BW25113 pFD1 containing the IPTG inducible transposase (NDH587) via mixing, pelleting, and incubation on YESCA media plates at 37°C for 2.5 hours on a cellulose filter. Cells were collected in 1mM IPTG YESCA, incubated for 3 hours at 37°C, then pelleted and resuspended in 10mL streptomycin and kanamycin YESCA to select for *ΔcysE* transposon mutants. Cells were diluted 1:10,000 prior to plating. Mutants were identified via random primer

sequencing. Mariner 1 and marine 2 primer colony PCR yielded DNA outside of the transposon and nested PCR with mariner 3 and 4 amplified this region. Sanger sequencing at University of Michigan Sequencing Core using mariner 4 revealed the location of transposon insertions.

S4B staining

Colonies were collected in 800µL of 50mM potassium phosphate buffer (pH7.2) (KPI) and tissue homogenized on setting 3 for 15 seconds (Fisher Tussiuemizer). Cells were stained with.05mg/mL S4B (70), incubated for 10min at RT in a shaker at 200RPM. Cells were spun down for 1 min at 13000 RPM and washed 2x in KPI and resuspended in 100µL of KPI. Stained cells were diluted 1:10 and imaged on a Tecan Infinite 200 plate reader at excitation 535nm and emission 595nm. Unstained cells treated similarly to stained cells were read and subtracted from the stained cell suspensions. Cell suspensions were normalized by OD_{600}. Error bars represent biological triplicate reactions standard deviation.

Figures

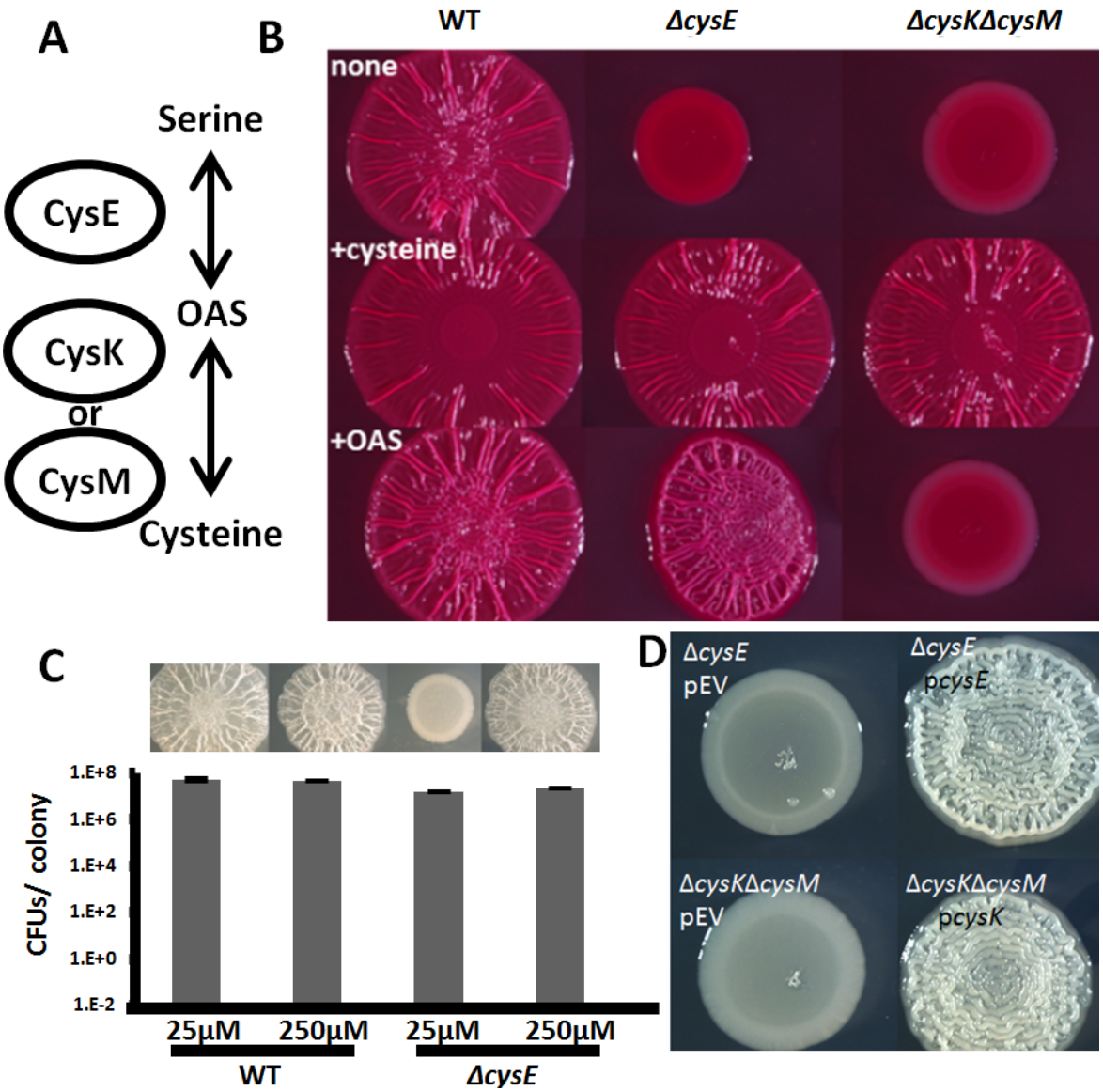

Figure 3.1- Cysteine is required for rugose biofilm formation. A) Cysteine biosynthesis. CysE converts Serine into OAS and OAS is converted into cysteine by either CysK or CysM. B) 4μL dots of 1-OD_{600} cells were spotted onto YESCA CR media and incubated at 26°C for 48 hours. 20μL of 10% (w/v) OAS or cysteine were added to sterile paper disks 1cm from the colonies. Cysteine auxotrophs formed smooth red colonies that wrinkled in the presence of cysteine. Δ*cysE* colonies wrinkled in the presence of OAS whereas Δ*cysK*Δ*cysM* mutants were still smooth, showing the lack of cysteine and not OAS caused the smooth colony biofilm. C) Colonies were resuspended in 1mL KPI and serial diluted and plated to determine CFUs. All measurements were done in biological triplicate. D) Δ*cysE* and Δ*cysK*Δ*cysM* were complemented with p*cysE* and p*cysK*. Induction of the plasmid resulted in wrinkled colonies.

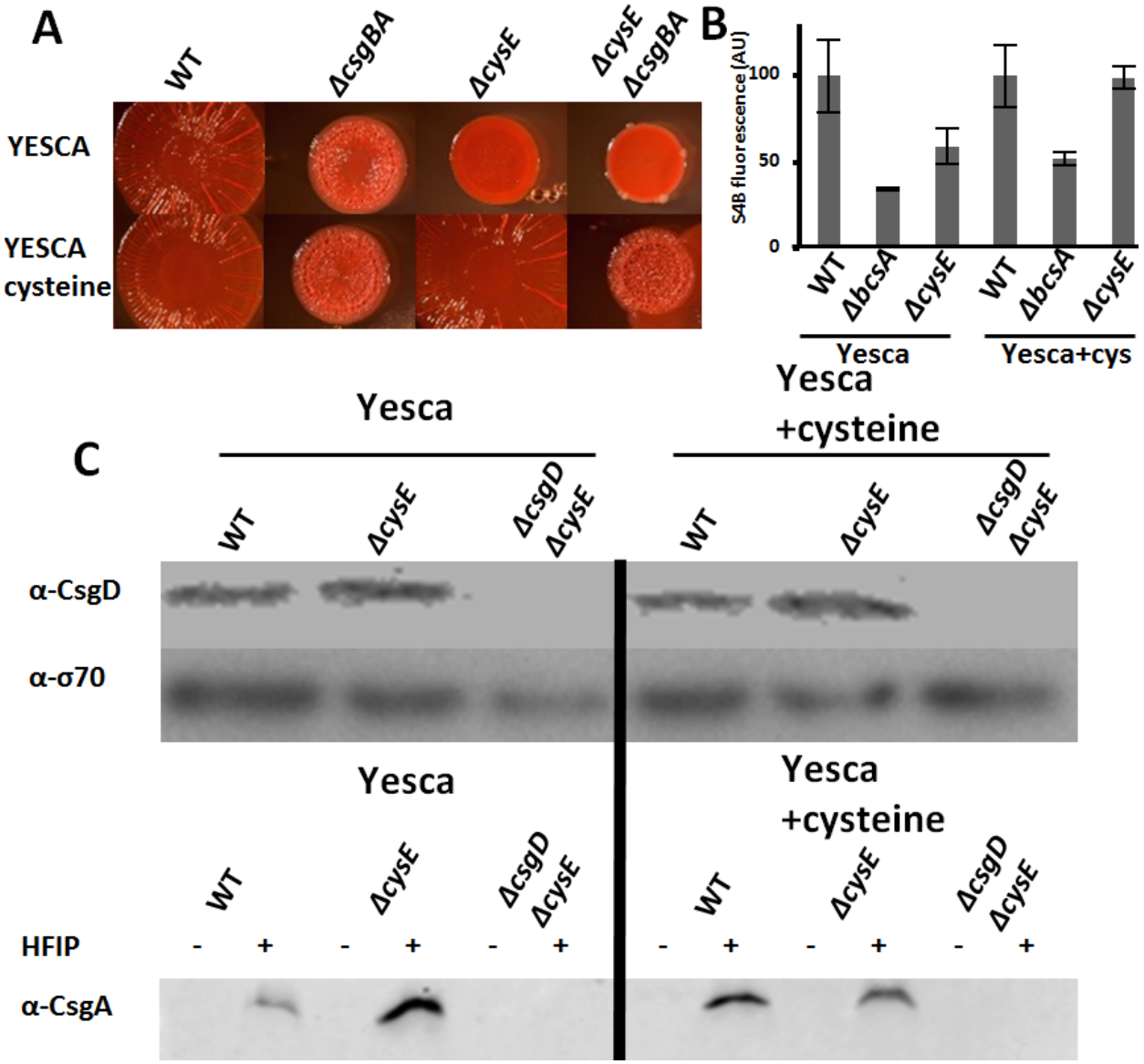

Figure 3.2- Cysteine auxotrophy uncouples curli and cellulose production. A) rugose colonies were grown at 26°C for 48 hours on YESCA CR plates or YESCA CR plates with 250μM cysteine added to the plates. Δ*csgBA* mutants cannot spread and Δ*cysE*Δ*csgBA* colonies still bound CR. B) Pontamine Fast Scarlet 4B (S4B) was used to stain cells. Stained cells were washed prior to fluorescence readings being taken. Higher fluorescence correlates with binding of more dye and cellulose production. C) Western blot analysis revealed Δ*cysE* produces similar levels of CsgD to WT, but has increased CsgA production. 250μM cysteine addition to the media decreases the increased CsgA production in Δ*cysE*.

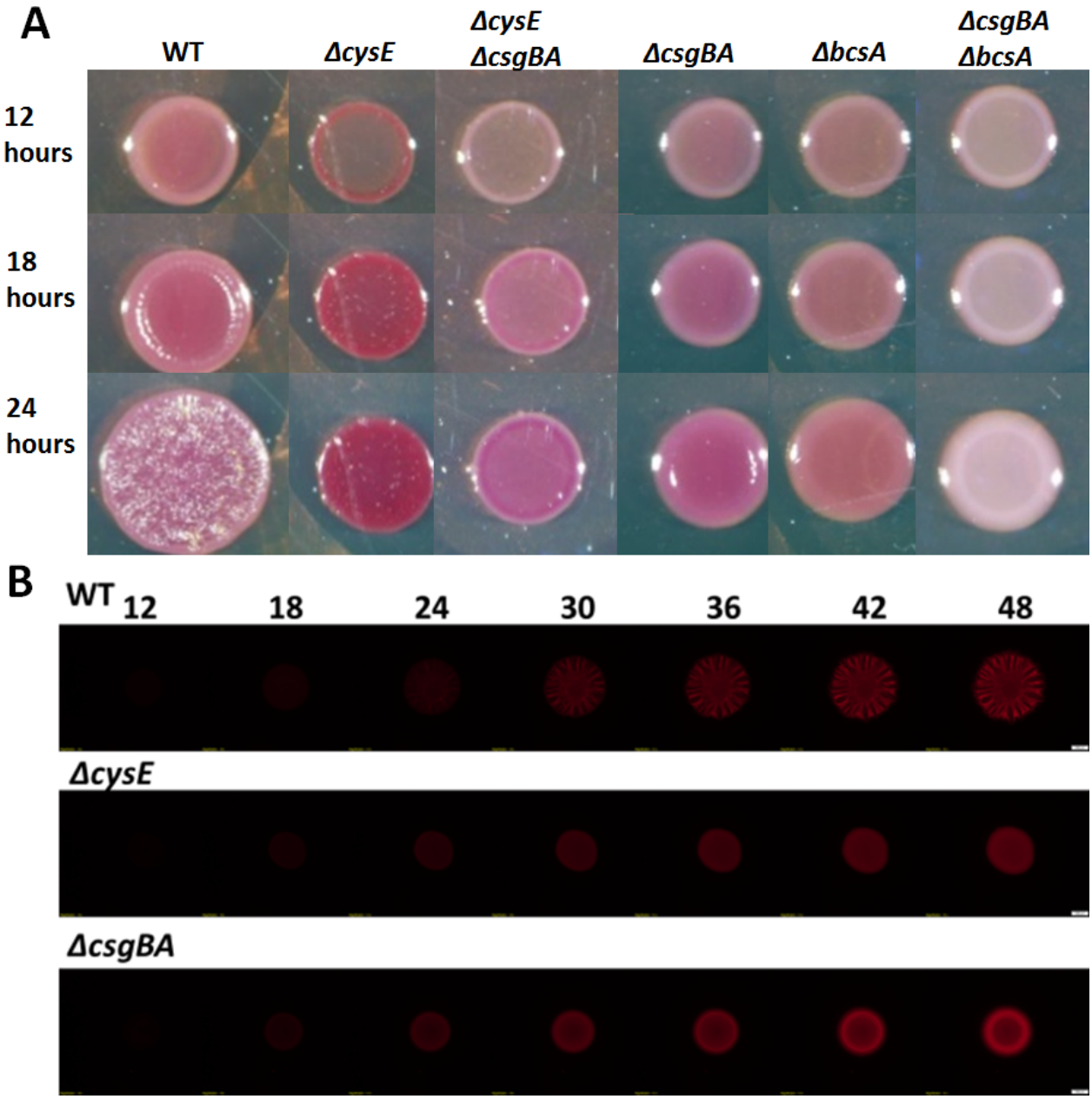

Figure 3.3- Spatiotemporal CR binding and curli transcription of rugose colonies. A) Time lapse photography captured 2µL dots of rugose colonies on YESCA CR plates incubated in a stage incubator at 26°C. Images were taken at 12, 18, and 24 hours. WT, *ΔcysE, ΔcsgBA* and Δ*bcsA* all bound CR at 12 hours, but *ΔcysEΔcsgBA* and *ΔcsgBAΔbcsA* did not bind CR. Δ*cysE*Δ*csgBA* bound CR at 18 hours showing delayed cellulose production. B) 2µL dots of WT, *ΔcysE*, and *ΔcsgBA* harboring *csgBA-mCherry* chromosomal insertions were grown in a stage incubator and imaged at 12, 18, 24, 30,36, 42, and 48 hours. mCherry fluorescence was not significantly increased at any time point measured.

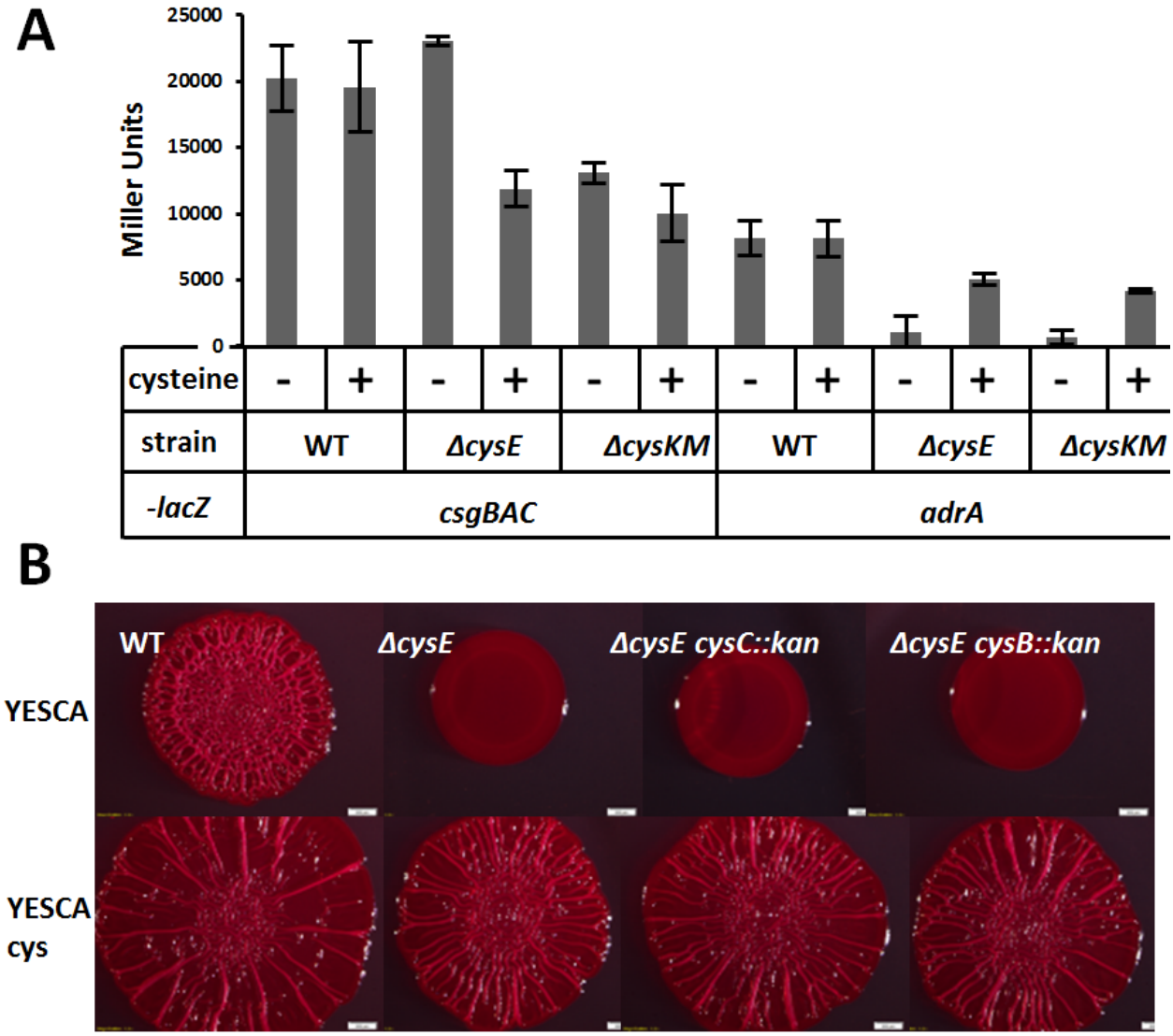

Figure 3.4- Cysteine auxotrophs ECM transcription and the role of *cysC.* A) *csgBAC* and *adrA* transcription in rugose colonies. WT, *ΔcysE,* and *ΔcysKΔcysM* harboring prj800, prj800-*16s,* prj800-*csgBAC,* and prj800-*adrA* were grown as 4µL dots at 26°C for 48 hours on YESCA(-cysteine) or YESCA +250µM cysteine (+cysteine) media. β-galactosidase assays were done following previous studies (Hufnagel *et al.* 2014). Base readings of prj800 were subtracted from each strain and Miller units were normalized by prj800-16s readings. *ΔcysE* and *ΔcysKΔcysM* prj800-*csgBAC (csgBAC-lacZ)* showed similar or decreased *csgBAC* transcription in comparison to WT. *ΔcysE* and *ΔcysKΔcysM* prj800-*adrA* showed decreased *adrA* transcription in comparison to WT, but *adrA* transcription was increased in colonies grown on YESCA cys media. All readings were performed in biological triplicate error bars represent standard deviation. B) PAPs doesn't induce the *ΔcysE* smooth colony morphotype. 4µL dots of WT, *ΔcysE, ΔcysE cysC::kan,* and *ΔcysE cysB::kan* were plated on YESCA CR and YESCA 250µM cysteine CR plates and incubated at 26°C for 48 hours. *ΔcysE, ΔcysE cysC::kan,* and *ΔcysE cysB::kan* all displayed a smooth colony morphotype on YESCA, and a spreading and wrinkling colony on YESCA cysteine plates.

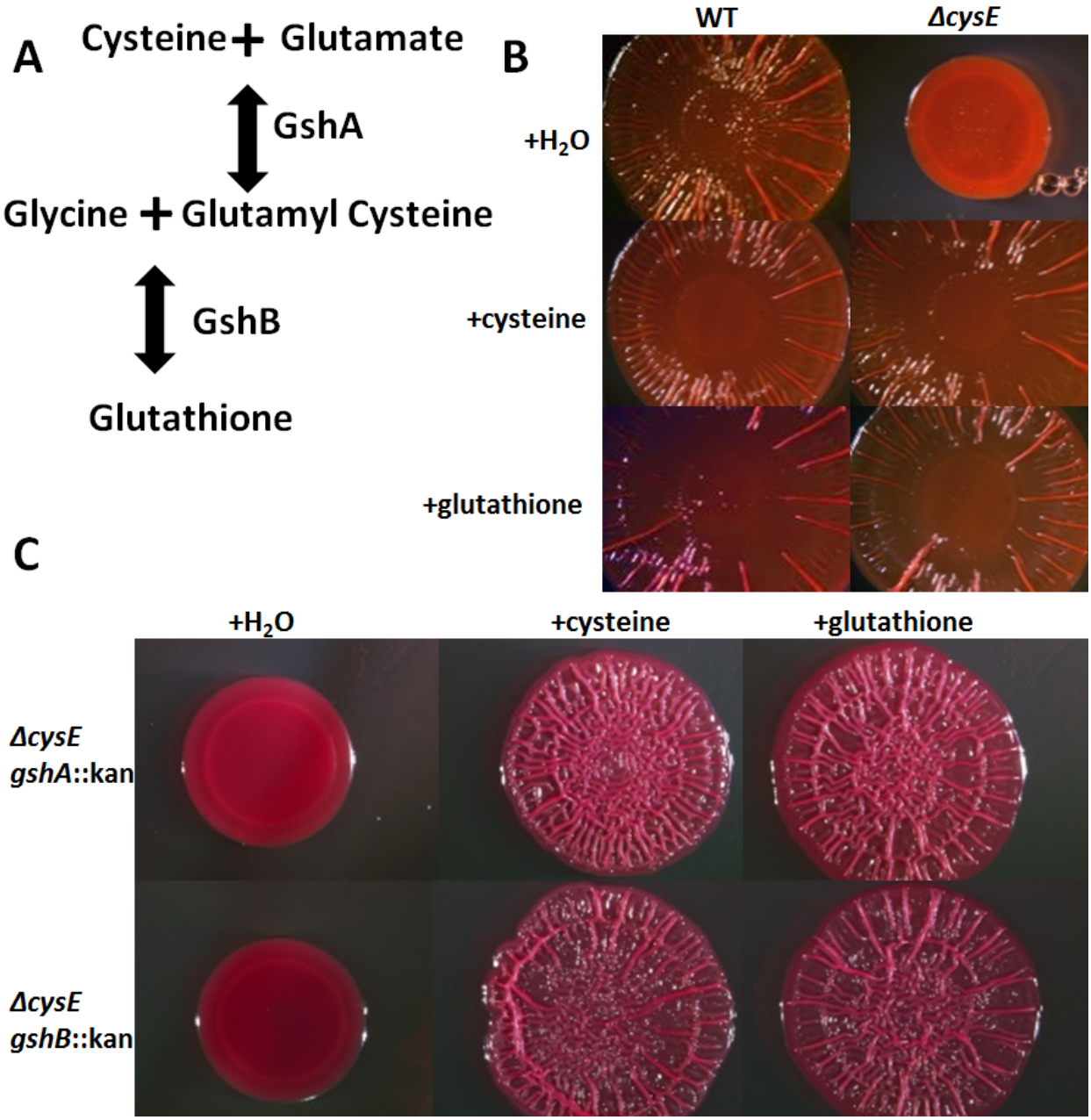

Figure 3.5- Glutathione and cysteine restore colony wrinkling to cysteine auxotrophs. A) Glutathione biosynthesis pathway. GshA converts cysteine and glutamate to glutamyl cysteine, and GshB converts glycine and glutamyl cysteine to glutathione. B) 4µL dots were plated 1cm from 10% (w/v) of cysteine and glutathione added to sterile filter disks and grown on YESCA CR plates at 26°C for 48 hours. Cysteine and glutathione restore wrinkling to WT and *ΔcysE* colonies. C) *ΔcysE gshA::kan* and *ΔcysE gshB::kan* 26°C colonies wrinkle in the presence of both cysteine and glutathione.

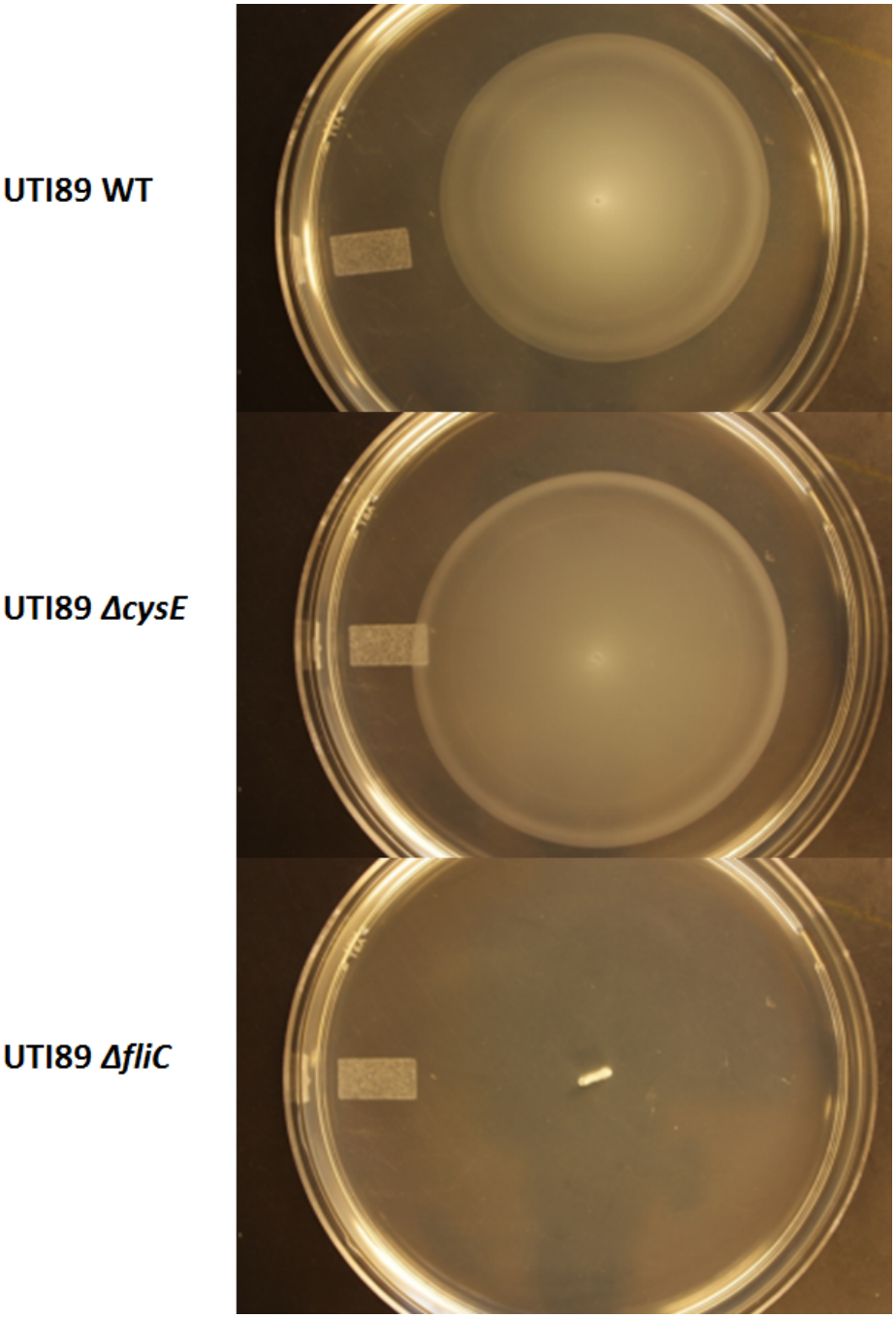

Figure 3.6- UTI89 *ΔcysE* is motile. UTI89 WT, *ΔcysE,* and *ΔfliC* were inoculated into YESCA .25% agar motility plates and incubated at 26°C for 16 hours prior to imaging.

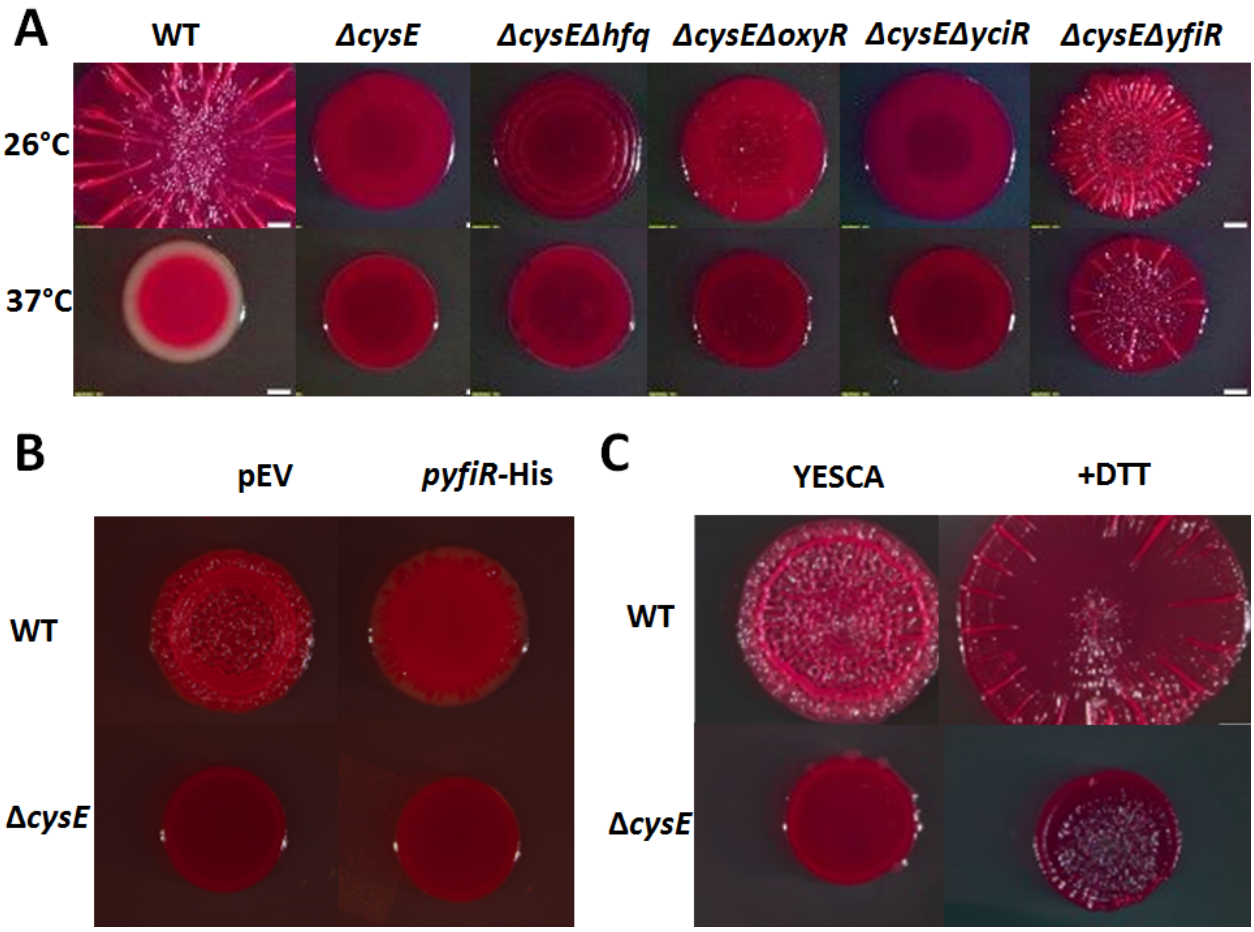

Figure 3.7- *yfiR* controls the smooth colony morphotype of *ΔcysE.* A) Secondary mutations found in 26°C transposon screen. 4µL dots of WT, *ΔcysE, ΔcysEΔhfq, ΔcysEΔoxyR, ΔcysEΔyciR,* and *ΔcysEΔyfiR* grown at 26°C for 48 hours and 37°C for 24 hours. Transposon mutations in *ΔcysE* that restore colony wrinkling were deleted via lambda red mutagenesis. *ΔcysEΔhfq* partially restored colony wrinkling and *ΔcysEΔyfiR* drastically increased colony wrinkling in comparison to *ΔcysE* at 48 hours. B) *yfiR* overexpression decreases WT colony wrinkling. WT and *ΔcysE* harboring p*yfiR-HIS* were grown at 26°C for 48 hours on YESCA CR 100µM IPTG plates. *yfiR* overexpression caused WT to phenocopy *ΔcysE*. C) 500mM DTT addition to a sterile paper disk induced *ΔcysE* colony wrinkling and caused an increase in WT colony spreading.

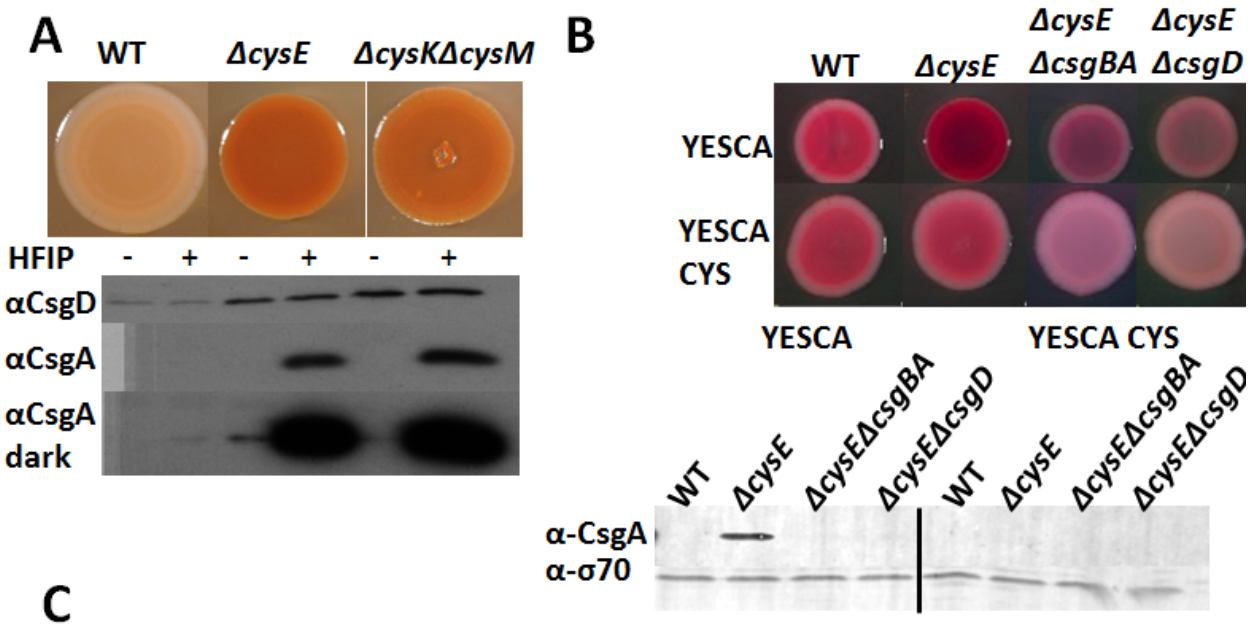

C

	# isolates	# cysteine auxotrophs	CR binding 26°C	CR binding 37°C
Group1 isolates	53	0	27 (50.94%)	1 (1.89%)
Group2 isolates	12	12	8 (66.67%)	7 (58.33%)

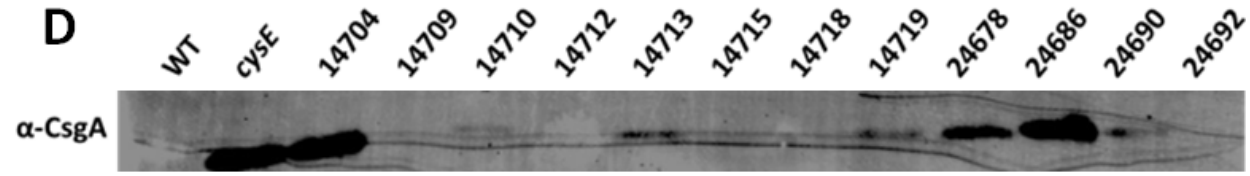

Figure 3.8- Cysteine auxotrophs produce curli at 37°C. A) WT, *ΔcysE* and *ΔcysKΔcysM* were grown on YESCA CR plates at 37°C for 24 hours. *ΔcysE* and *ΔcysKΔcysM* have increased CR binding. Western blot analysis revealed that *ΔcysE* and *ΔcysKΔcysM* have increased CsgD and CsgA levels than WT. B) Cysteine auxotrophs require *csgD* and *csgBA* to bind CR at 37°C. *ΔcysEΔcsgD* and *ΔcysEΔcsgBA* were unable to bind CR when grown 37°C for 24 hours on YESCA CR plates. C) Graph showing cysteine auxotrophs isolated from patients have an increased propensity to bind CR at 37°C. Two different sets of clinical isolates were grown on YESCA CR plates at 26°C for 48 hours or 37°C for 24 hours. Group 1 contained no cysteine auxotrophs and had 1 isolate that bound CR at 37°C. Group 2 contained all cysteine auxotrophs and 7/12 strains bound CR at 37°C. D) Clinical cysteine auxotrophs produce curli at 37°C. Isolates from Group 2 (Figure 3.8C) grown at 37°C were subjected to western blot analysis against CsgA. CsgA was found to be present in 14704, 14710, 14713, 14719, 24678, 24686, and 24690.

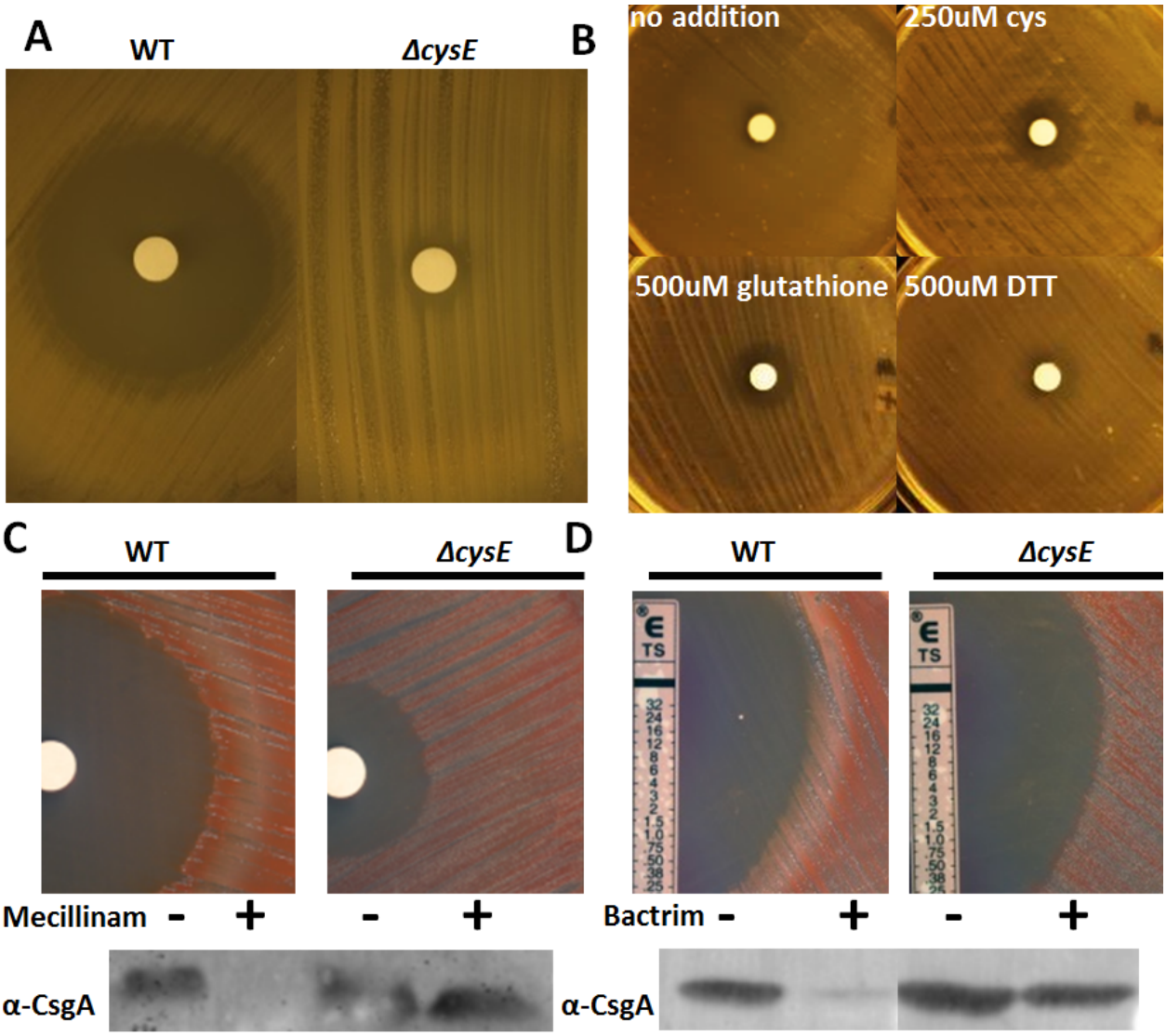

Figure 3.9- The effect of mecillinam on UTI89 biofilms. A) *ΔcysE* showed increased resistance to mecillinam. WT and *ΔcysE* were spread on LB plates with a sterile filter disk containing 20µL of 10mg/mL mecillinam. *ΔcysE* had a decreased zone of inhibition. B) *ΔcysE* colonies spread on YESCA plates supplemented with cysteine, glutathione, or DTT had a sterile filter disk containing 20µL of 10mg/ml mecillinam and were incubated at 37°C for 24 hours. The zone of inhibition of *ΔcysE* increased with the addition of cysteine, glutathione, and DTT. C) WT and *ΔcysE* were spread onto YESCA CR plates with a sterile filter disk containing 20µL 10mg/mL of mecillinam and grown at 26°C for 48 hours. Pictures were taken prior to collecting cells at the edge of the plate (-mecillinam) and next to the zone of inhition (+mecillinam) that were then subjected to western blot analysis against CsgA. Mecillinam inhibited WT CR binding and curli production, but *ΔcysE* was resistant to the curli inhibition. D) Bactrim ETEST strips were laid onto WT and *ΔcysE* YESCA CR spread plates that were incubated at 26°C for 48 hours. Cells were collected at the edge of the plate (-mecillinam) and next to the zone of inhibition (+mecillinam) prior to testing for CsgA protein levels via western blot analysis. *ΔcysE* was resistant to Bactrim-mediated inhibition of CR binding and CsgA production.

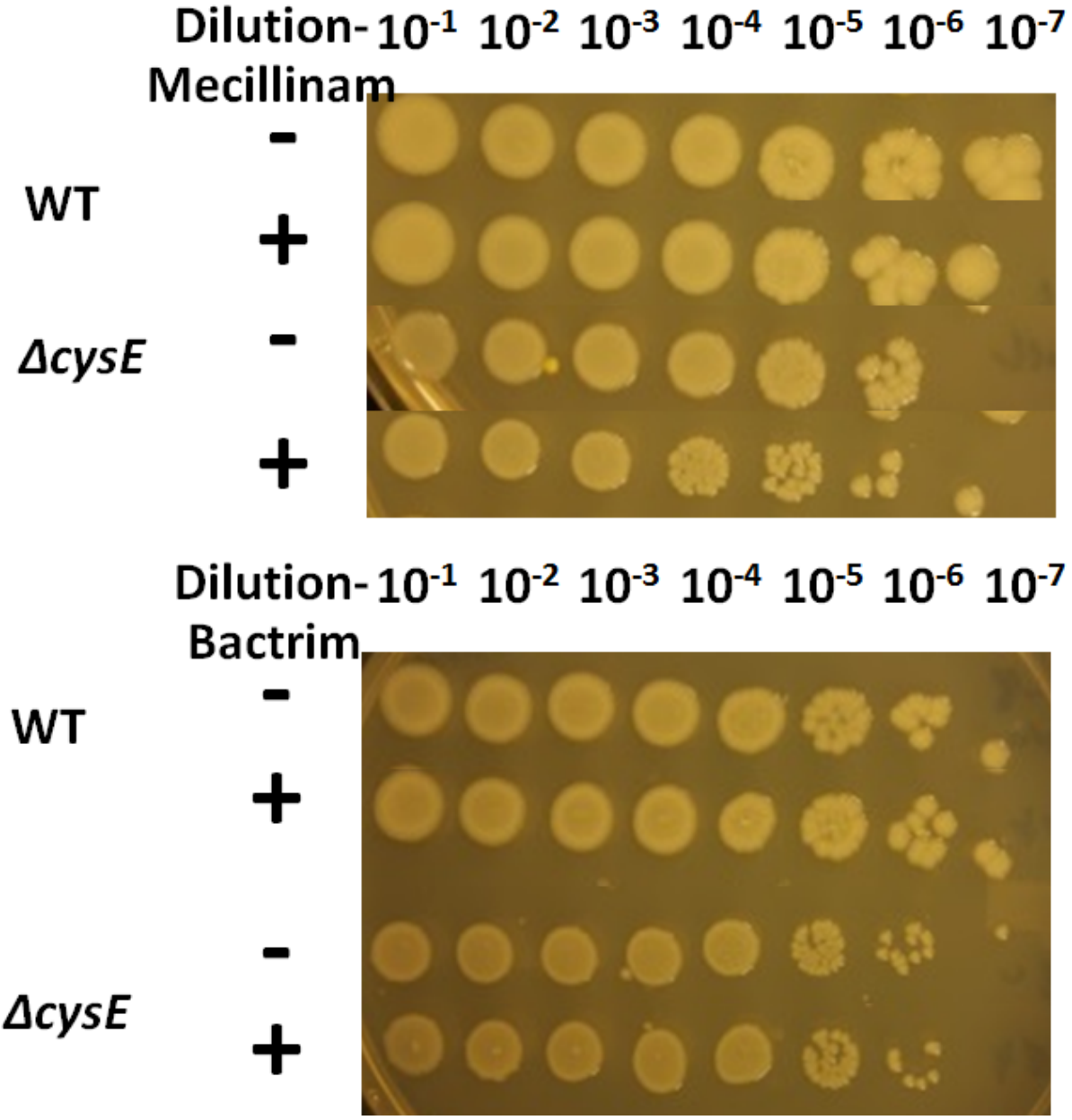

Supplemental Figure 3.10- Cells harvested next to the zone of inhibition of mecillinam and bactrim are viable. Cells harvested in Figure 3.9C and Figure 3.9D for Western blot analysis were normalized by OD_{600} followed by serial dilution in KPI prior to plating 4µL dots onto LB plates for CFU determination. Plates were incubated at 37°C for 18 hours. Cells grown near and further from the zone of inhibition of both WT and *ΔcysE* had the same cell viability by CFU count.

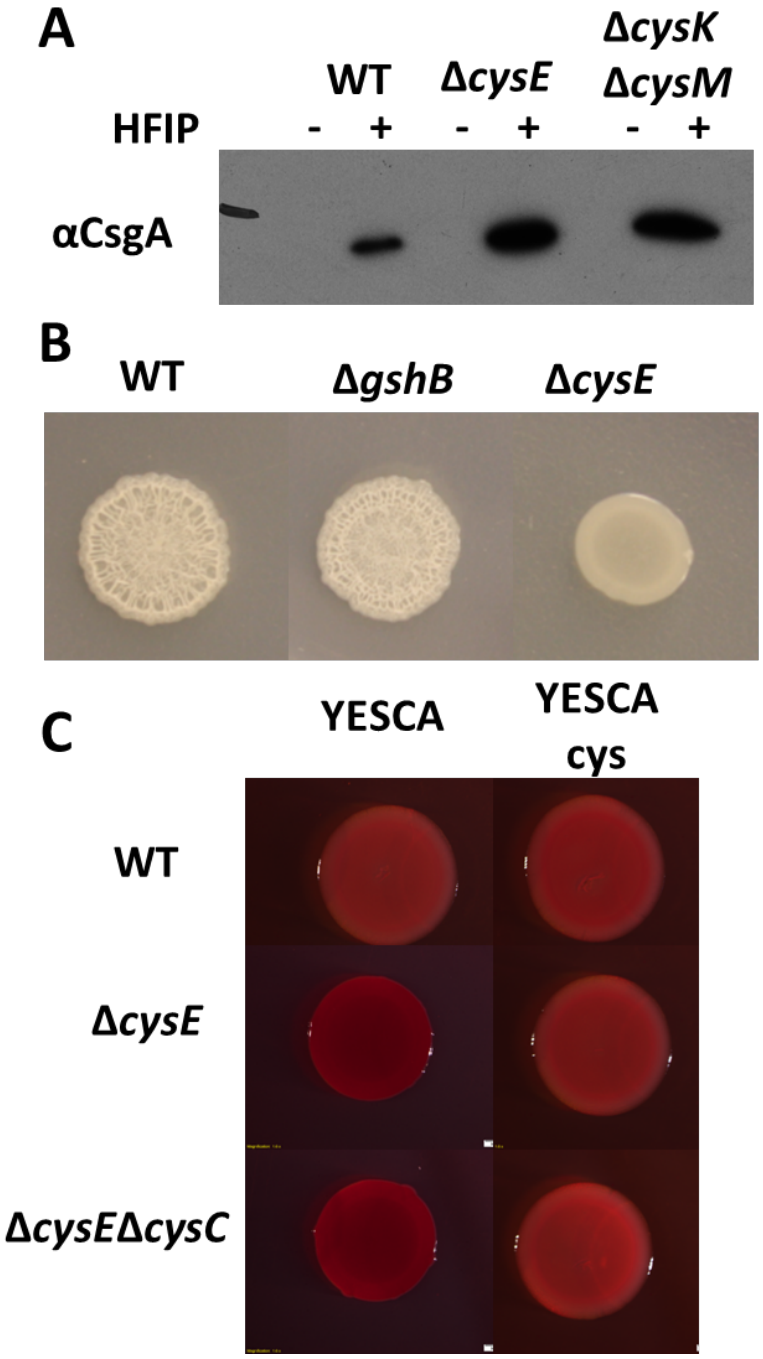

Figure 3.11- Cysteine auxotrophy not PAPS leads to the uncoupling of ECM. A) Western blot analysis of cells grown at 26°C for 48 hours on YESCA showing *ΔcysE* and *ΔcysKΔcysM* have increased CsgA in comparison to WT. B) WT, *ΔgshB,* and *ΔcysE* 4µL dots grown at 26°C for 48 hours on YESCA plates. *ΔgshB* mutation alone does not induce the smooth colony morphotype of cysteine auxotrophs. C) Colonies grown at 37°C for 24 hours on YESCA CR plates. *ΔcysEΔcysC* still binds CR at 37°C similar to the *ΔcysE* strain.

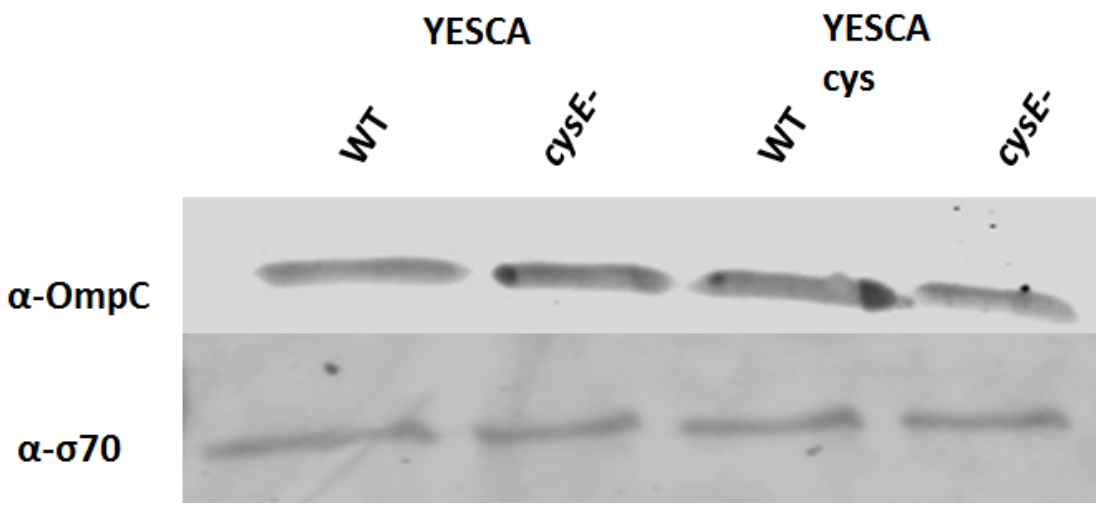

Figure 3.12- OmpC levels are similar in WT and *ΔcysE*. WT and *ΔcysE* colonies grown at 37°C for 24 hours on YESCA and YESCA cysteine plates were probed for OmpC and σ-70 levels via western blot analysis. OmpC levels were unchanged in *ΔcysE* in comparison to WT colonies.

Table 3.1- Gene mutations that induce Δ*cysE* wrinkling

#isolated	insertion gene	function
1	***amyA***	cytoplasmic α-amylase
1	***degS***	cleaves misfolded outermembrane proteins and the anti sigma factor rseA
1	***dsbA***	periplasmic oxidoreductase
2	***dsbB***	periplasmic oxidoreductase
1	***hflX***	GTPase (lots of RXXXR motifs) associated with ribosome located next to hfq
1	***hfq***	Protein that has been said to both increase and decrease stability of csgD transcript. Acts to stabilize other small RNAs
9	***mtlA* (8 siblings)**	mannitol permease
2	***opgG***	osmoregulated periplasmic glucan branching
5	***opgH***	osmoregulated periplasmic glucan glycosyl transferase
1	***serC***	in biosynthesis of serine and pyridoxine
1	***ssb* on plasmid**	Not found in lab strains additional SSB
1	***sufI***	stabilizes divisomal assembly during stress
1	***ugpC***	glycerol-3-phosphate import
1	***xylR***	transcriptional regulator
1	***ychA***	predicted transcriptional regulator
1	***yciR***	phosphodiesterase(gmr) paired with ydaM which increases mlrA and csgD
1	***yfiR***	periplasmic inhibitor of YfiN
1	***yhbE***	Unknown-has domain for cysteine/cystine export

Table 3.2- Gene mutations that inhibit Δ*cysE* CR binding at 37°C

#isolated	insertion gene	function
1	***aceF***	Pyruvate dehydrogenase produces acetyl coA from pyruvate
1	***apaG***	
1	***aroB***	Chorismate pathway DHQ synthase
3	***aroE***	Shikimate dehydrogenase involved in chorismate pathway that leads to indole and tryptophan
4	***aspA***	Aspartate to fumarate and ammonia
1	***csgG***	Curli outermembrane secrection pore
3	***cyaA***	Adenylate cyclase
1	***damX***	Cell division, next to aroB
1	***dcuA***	Uptakes C4 dicarboxylates like fumarate
13	***envZ***	Osmotic responsive regulator of OmpR
1	***Gmk***	GMP kinase
3	***Lon***	protease
1	***mdH***	Oxidation of malate to OAA
1	***nhaA***	Sodium antiporter
1	***nudH***	mRNA degradation
5	***ompR***	Transcriptional regulator required for *csgD* production
1	***Psd***	Phosphatidyl serine decarboxylase
1	***ptsP***	Nitrogen PTS system PEP to PtsO
1	***qseC***	Sensor kinase that will decrease curli expression
5	***relA***	Stringent response activates ppgpp
1	***rnE***	Ribonuclease E mRNA degradation
1	***rpoS***	Sigma factor
3	***sdhA***	Succinate dehydrogenase from succinate to fumarate and ubiquinone
3	***sdhB***	Succinate dehydrogenase
1	***sdhC***	SD
1	***sdhD***	SD
2	***sucA***	2 oxoglutarate dehydrogenase which gets converted to succinyl coA CO2
1	***sucC***	Succinyl CoA synthetase necessary for peptidoglycan biosynthesase
1	***sucD***	SD
1	***Tig***	Trigger factor cytosolic chaperone
1	***trpA***	Tryptophan synthase produces indole from glycerol-3-phosphate
3	***truA***	Catalyzes pseudouridine in tRNAS, stabilizes mRNA

1	***ubiE***	Ubiquinone and menaquinone biosynthesis
1	***Upp***	Pyrimidine biosynthesis
1	***ygdT***	KO leads to an increase in tyrosine
1	***yhjJ***	Predicted zinc dependent peptidase with sec signal
1	***yhjQ***	SD
1	***yleB***	Ubiquinone biosynthesis from chorismate
1	***yrdA***	Induced by spermine, potential carbonic anhydrase
1	***yrfF***	Part of RCS system

Table 3.3- Plasmid list Chapter 3

Plasmids	Reference
p*yfiR-his*	Hufnagel *et al.* 2014
p*csgBAC*	DePas *et al.* 2013
p*adrA*	DePas *et al.* 2013
p*16s*	Hufnagel *et al.* 2014
prj800	Barnhart *et al.* 2006
p*cysE*	Yizhou Zhou thesis
p*cysK*	Yizhou Zhou thesis

Table 3.4- Primer list Chapter 3

Primers	Description	sequence
DH1	*cysE* RS F	GCCCGCGCAGAACGGGCCGGTCATTATCTCATCGTGTGGAGT AAGCAATGGTGTAGGCTGGAGCTGCTTC
DH2	*cysE* RS *R*	TACATCGCATCCGGCACGATCACAGGACATTAGATCCCATCC CCATACTCCATATGAATATCCTCCTTAG
DH16	*cysK* RS F	GGT ATG CTA CCT GTT GTA TCC CAA TTT CAT ACA GTT AAG GAC AGG CCA TGG TGT AGG CTG GAG CTG CTT C
DH17	*cysK RS R*	CTT TTT TAC GCA TTT TTT ACA AGC TGG CAT TAC TGT TGC AGT TCT TTC TCC ATA TGA ATA TCC TCC TTA G
DH18	*cysM RS F*	AGA CGC GTA AGC GTC GCA TCA GGC AAC ACC ACG TAT GGA CAG AGA TCG TGG TGT AGG CTG GAG CTG CTT C
DH19	*cysM RS R*	ACG GAT AAA ACG GTG CCT GCG CAA TAA TCT TAA ATC CCC GCC CCC TGG CTC ATA TGA ATA TCC TCC TTA G
WD449	*hfq RS F*	GAA TCG AAA GGT TCA AAG TAC AAA TAA GCA TAT AAG

		GAA AAG AGA GAA TGG TGT AGG CTG GAG CTG CTT C
WD450	*hfq RS R*	CTC CCC GTG TAA AAA AAT AGC CCG AAA CCT TAT TCG GTT TCT TCG CTG TCC ATA TGA ATA TCC TCC TTA G
WD216	*oxyR RS F*	CTA TGC TAC CTA TCG CCG CGA ACT ATC GTG GCA ATG GAG GAT GGA TAA TGG TGT AGG CTG GAG CTG CTT C
WD217	*oxyR RS R*	AAG CCT ATC GGG TAG CTG CGC TAA ATG GCT TAA ACC GCC TGT TTT AAA ACC ATA TGA ATA TCC TCC TTA G
DH188	*cysC RS F*	CGC CAT TTC CCG CAT TGG GGT GCG CGC GAT TTA CTG GGA GAT AAA TAA TGG TGT AGG CTG GAG CTG CTT C
DH189	*cysC RS R*	CGA ACC GGG CAT GAA AAC CCG GTG GTG TCT CAG GAT CTG ATA ATA TCG TTC ATA TGA ATA TCC TCC TTA G
DH192	*cysB RS F*	GTG ACG AAA AAA CGA TGT TCT GAT GGC GTC TAA GTG GAT GGT TTA ACA TGG TGT AGG CTG GAG CTG CTT C
DH193	*cysB RS R*	ATA AAA GGT GCC GAA AAT AAC GCA AGA AAT TAT TTT TCC GGC AGT TTT ATC ATA TGA ATA TCC TCC TTA G
DH85	*Salmonella cysE RS F*	ACC CGC ACA GAA CGG GTT GGT CGT TTT CTG CCC GTC TGG AGT AAG CCA TGC ATA TGA ATA TCC TCC TTA G
DH86	*Salmonella cyseE RS R*	ACA GCG TTT TTT AGT TGT ACC GCG CAA TTC AGA TGC CGT CGC CAT ACT CAG TGT AGG CTG GAG CTG CTT C
WD439	*fliC RS F*	GTC AGT CTC AGT TAA TCA GGT TAC GGC GAT TAA CCC TGC AGC AGA GAC AGC ATA TGA ATA TCC TCC TTA G
WD440	*fliC RS R*	GGA AAC CCA AAA CGT AAT CAA CGA CTT GCA ATA TAG GAT AAC GAA TCA TGG TGT AGG CTG GAG CTG CTT C
DH232	*opgG RS F*	GCA CAC AAA GGG GGA AGT GCT TAC TAA TTA TGA AAC ATA AAC TAC AAA TGG TGT AGG CTG GAG CTG CTT C
DH233	*opgG RS R*	TGG GCA TTG CGT CAA TGT ACT CAG TTG TCT TAT TCA TTG GCA GGT AAC TGC ATA TGA ATA TCC TCC TTA G
DH236	*yciR RS F*	TAT AGC GCT AAG TAT ATA TAT TCA TCT ACT TAT GTG CGC TTC AGG TAG CGC ATA TGA ATA TCC TCC TTA G
DH237	*yciR RS R*	CCT TTT ATT TAA CTG CGG ACT CCG CTG TTA ACC GGA GGA TAT GCA TCA TGG TGT AGG CTG GAG CTG CTT C

Table 3.5- Strain list Chapter 3

Strain name	Strain Genotype	Reference	Notes
CL1166	UTI89 *ΔcysE*	This Thesis Chapter	kan casette RS into *cysE* with DH1 and DH2 amplifying Kan casette. PCP20 used to remove Kan casette
CL1236	UTI89 ΔcysKΔcysM	This Thesis Chapter	kan casette RS into *cysK* with DH16 and DH17 amplifying Kan casette, followed by kan casette RS into cysM with DH18 and DH19 amplifying Kan casette. PCP20 used to remove Kan casettes

CL1483	UTI89 ΔcysEΔcsgBA	This Thesis Chapter	kan casette RS into *cysE in a* csgBA- strain with DH1 and DH2 amplifying Kan casette. PCP20 used to remove Kan casette
CL1564	UTI89 ΔcsgD cysE::kan	This Thesis Chapter	kan casette RS into *cysE* with DH1 and DH2 in a *csgD*- strain amplifying Kan casette. PCP20 used to remove Kan casette
CL1977	UTI89 ΔgshA cysE::kan	This Thesis Chapter	kan casette RS into *cysE* with DH1 and DH2 in a *gshA-strain* amplifying Kan casette.
CL1980	UTI89 ΔcysE ΔgshB	This Thesis Chapter	kan casette RS into *cysE* with DH1 and DH2 in *gshB*- amplifying Kan casette. PCP20 used to remove Kan casette
CL2010	UTI89 ΔcysE hfq::kan	This Thesis Chapter	kan casette RS into *hfq* with WD449 and WD450 in a cysE- strain amplifying Kan casette.
CL2036	UTI89 ΔcysE oxyR::kan	This Thesis Chapter	kan casette RS into *oxyR* with WD 216 and WD217 in a cysE- strain amplifying Kan casette.
CL1979	UTI89 ΔcysEΔyfiR	This Thesis Chapter	kan casette RS into *cysE* with DH1 and DH2 in a yfiR strain amplifying Kan casette. PCP20 used to remove Kan casette
CL1502	UTI89 ΔcysE pckr101	This Thesis Chapter	cysE strain transformed with pCKR101.
CL1962	UTI89 ΔcysE pckr101-*yfiR-his*	This Thesis Chapter	cysE strain transformed with pCKR101-*yfiR-his*
CL1945	UTI89 ΔcysE ΔcysC	This Thesis Chapter	kan casette RS into *cysE* with DH1 and DH2 in a cysC- strain amplifying Kan casette. PCP20 used to remove Kan casette
CL1948	UTI89 ΔcysE cysB::kan	This Thesis Chapter	kan casette RS into *cysB* with DH192 and DH193 in a cysE- strain amplifying Kan casette.
CL1452	UTI89 ΔcysE prj800	This Thesis Chapter	cysE strain transformed with pRJ800
CL1512	UTI89 ΔcysE prj800-csgBAC	This Thesis Chapter	cysE strain transformed with pRJ800-csgBAC
CL1450	UTI89 ΔcysE prj800-adrA	This Thesis Chapter	cysE strain transformed with pRJ800-adrA.
CL1545	UTI89 ΔcysKΔcysM prj800	This Thesis Chapter	cysKM- strain transformed with pRJ800
CL154	UTI89	This	cysKM- strain transformed with pRJ800-csgBA

7	ΔcysKΔcysM prj800-csgBAC	Thesis Chapter	
CL1548	UTI89 ΔcysKΔcysM prj800-adrA	This Thesis Chapter	cysKM- strain transformed with pRJ800-adrA
CL1565	UTI89 ΔfliC	This Thesis Chapter	kan casette RS into *fliC* with WD439 andWD440 amplifying Kan casette. PCP20 used to remove Kan casette
CL2015	UTI89 ΔcysEΔugpQ	This Thesis Chapter	kan casette RS into *cysE* with DH1 and DH2 in a ugpQ- strain amplifying Kan casette. PCP20 used to remove Kan casette
CL2011	UTI89 ΔcysEΔopgG	This Thesis Chapter	kan casette RS into *opgG* with DH233 and DH234 in a cysE- strain amplifying Kan casette. PCP20 used to remove Kan casette
CL2064	UTI89 ΔcysE yciR::kan	This Thesis Chapter	kan casette RS into *yciR* with DH236 and DH237 amplifying Kan casette.
CL2061	UTI89 ΔcysE yfiN::kan	This Thesis Chapter	kan casette RS into *yfiN in a cysE- strain* amplifying Kan casette.

Acknowledgements-Will DePas helped with the experimental designs on this project. Janet Price helped with the S4B staining. My high school student Isabella Comai and undergraduate Jesse Kelly helped greatly with the procurement, CR staining, auxotrophy testing, and western blotting of the Swedish UPEC isolates (Figure 3.8).

References

1. **Sabir S, Ahmad Anjum A, Ijaz T, Asad Ali M, Ur Rehman Khan M, Nawaz M.** 2014. Isolation and antibiotic susceptibility of *E. coli* from urinary tract infections in a tertiary care hospital. Pak J Med Sci **30:**389-392.
2. **Manges AR, Johnson JR.** 2012. Food-borne origins of *Escherichia coli* causing extraintestinal infections. Clinical infectious diseases : an official publication of the Infectious Diseases Society of America **55:**712-719.
3. **Yamamoto S, Tsukamoto T, Terai A, Kurazono H, Takeda Y, Yoshida O.** 1997. Genetic evidence supporting the fecal-perineal-urethral hypothesis in cystitis caused by *Escherichia coli*. The Journal of urology **157:**1127-1129.
4. **Manges AR, Johnson JR, Foxman B, O'Bryan TT, Fullerton KE, Riley LW.** 2001. Widespread distribution of urinary tract infections caused by a multidrug-resistant *Escherichia coli* clonal group. N Engl J Med **345:**1007-1013.
5. **Hufnagel DA, Tukel C, Chapman MR.** 2013. Disease to dirt: the biology of microbial amyloids. PLoS Pathog **9:**e1003740.
6. **Depas WH, Hufnagel DA, Lee JS, Blanco LP, Bernstein HC, Fisher ST, James GA, Stewart PS, Chapman MR.** 2013. Iron induces bimodal population development by *Escherichia coli*. Proc Natl Acad Sci U S A **110:**2629-2634.
7. **DePas WH, Syed AK, Sifuentes M, Lee JS, Warshaw D, Saggar V, Csankovszki G, Boles BR, Chapman MR.** 2014. Biofilm formation protects *Escherichia coli* against killing by *Caenorhabditis elegans* and *Myxococcus xanthus*. Appl Environ Microbiol **80:**7079-7087.
8. **White AP, Gibson DL, Kim W, Kay WW, Surette MG.** 2006. Thin aggregative fimbriae and cellulose enhance long-term survival and persistence of *Salmonella*. J Bacteriol **188:**3219-3227.
9. **Zhou Y, Smith D, Leong BJ, Brannstrom K, Almqvist F, Chapman MR.** 2012. Promiscuous cross-seeding between bacterial amyloids promotes interspecies biofilms. The Journal of biological chemistry **287:**35092-35103.
10. **Stewart PS, Franklin MJ.** 2008. Physiological heterogeneity in biofilms. Nat Rev Microbiol **6:**199-210.
11. **Jubelin G, Vianney A, Beloin C, Ghigo JM, Lazzaroni JC, Lejeune P, Dorel C.** 2005. CpxR/OmpR interplay regulates curli gene expression in response to osmolarity in *Escherichia coli*. J Bacteriol **187:**2038-2049.

12. **Gerstel U, Romling U.** 2001. Oxygen tension and nutrient starvation are major signals that regulate *agfD* promoter activity and expression of the multicellular morphotype in *Salmonella* typhimurium. Environ Microbiol **3:**638-648.
13. **Olsen A, Arnqvist A, Hammar M, Normark S.** 1993. Environmental regulation of curli production in *Escherichia coli*. Infect Agents Dis **2:**272-274.
14. **Hammar M, Arnqvist A, Bian Z, Olsen A, Normark S.** 1995. Expression of two *csg* operons is required for production of fibronectin- and Congo red-binding curli polymers in *Escherichia coli* K-12. Mol Microbiol **18:**661-670.
15. **Zogaj X, Nimtz M, Rohde M, Bokranz W, Romling U.** 2001. The multicellular morphotypes of *Salmonella* typhimurium and *Escherichia coli* produce cellulose as the second component of the extracellular matrix. Mol Microbiol **39:**1452-1463.
16. **Chapman MR, Robinson LS, Pinkner JS, Roth R, Heuser J, Hammar M, Normark S, Hultgren SJ.** 2002. Role of *Escherichia coli* curli operons in directing amyloid fiber formation. Science **295:**851-855.
17. **Bokranz W, Wang X, Tschape H, Romling U.** 2005. Expression of cellulose and curli fimbriae by *Escherichia coli* isolated from the gastrointestinal tract. Journal of Medical Microbiology **54:**1171-1182.
18. **Romling U, Sierralta WD, Eriksson K, Normark S.** 1998. Multicellular and aggregative behaviour of *Salmonella* typhimurium strains is controlled by mutations in the *agfD* promoter. Mol Microbiol **28:**249-264.
19. **Collinson SK, Emody L, Muller KH, Trust TJ, Kay WW.** 1991. Purification and characterization of thin, aggregative fimbriae from *Salmonella* enteritidis. J Bacteriol **173:**4773-4781.
20. **Omadjela O, Narahari A, Strumillo J, Melida H, Mazur O, Bulone V, Zimmer J.** 2013. BcsA and BcsB form the catalytically active core of bacterial cellulose synthase sufficient for in vitro cellulose synthesis. Proc Natl Acad Sci U S A **110:**17856-17861.
21. **Hufnagel DA, DePas WH, Chapman MR.** 2014. The disulfide bonding system suppresses CsgD-independent cellulose production in *Escherichia coli*. J Bacteriol **196:**3690-3699.
22. **Weber H, Pesavento C, Possling A, Tischendorf G, Hengge R.** 2006. Cyclic-di-GMP-mediated signalling within the sigma network of *Escherichia coli*. Molecular microbiology **62:**1014-1034.
23. **Ryjenkov DA, Simm R, Romling U, Gomelsky M.** 2006. The PilZ domain is a receptor for the second messenger c-di-GMP: the PilZ domain protein YcgR controls motility in enterobacteria. Journal of Biological Chemistry **281:**30310-30314.
24. **Fang X, Gomelsky M.** 2010. A post-translational, c-di-GMP-dependent mechanism regulating flagellar motility. Molecular Microbiology **76:**1295-1305.
25. **Sturgill G, Toutain CM, Komperda J, O'Toole GA, Rather PN.** 2004. Role of CysE in production of an extracellular signaling molecule in Providencia stuartii and *Escherichia coli*: Loss of *cysE* enhances biofilm formation in *Escherichia coli*. Journal of Bacteriology **186:**7610-7617.
26. **Rossi E, Motta S, Mauri P, Landini P.** 2014. Sulfate assimilation pathway intermediate phosphoadenosine 5 '-phosphosulfate acts as a signal molecule affecting production of curli fibres in *Escherichia coli*. Microbiology-Sgm **160:**1832-1844.

27. **Lee J, Bansal T, Jayaraman A, Bentley WE, Wood TK.** 2007. Enterohemorrhagic *Escherichia coli* biofilms are inhibited by 7-hydroxyindole and stimulated by isatin. Applied and Environmental Microbiology **73:**4100-4109.
28. **Ren DC, Zuo RJ, Barrios AFG, Bedzyk LA, Eldridge GR, Pasmore ME, Wood TK.** 2005. Differential gene expression for investigation of *Escherichia coli* biofilm inhibition by plant extract ursolic acid. Applied and Environmental Microbiology **71:**4022-4034.
29. **Singh P, Brooks JF, 2nd, Ray VA, Mandel MJ, Visick KL.** 2015. CysK Plays a Role in Biofilm Formation and Colonization by *Vibrio fischeri*. Appl Environ Microbiol **81:**5223-5234.
30. **Gillespie WA.** 1952. Biochemical mutants of coliform bacilli in infections of the urinary tract. J Pathol Bacteriol **64:**551-557.
31. **Borderon E, Horodniceanu T.** 1978. Metabolically deficient dwarf-colony mutants of *Escherichia coli*: deficiency and resistance to antibiotics of strains isolated from urine culture. J Clin Microbiol **8:**629-634.
32. **KS. GTaG.** 2002. Cysteine-Dependent Uropathogens:Isolation, Identification and Susceptibility to Antimicrobial Agents. JamahiriyaMed J **2:**52-54.
33. **Thulin E, Sundqvist M, Andersson DI.** 2015. Amdinocillin (Mecillinam) resistance mutations in clinical isolates and laboratory-selected mutants of *Escherichia coli*. Antimicrob Agents Chemother **59:**1718-1727.
34. **Miller J.** 1972. Experiments in Molecular Genetics. Cold Spring Harbor Lab Press, Cold Spring Harbor, NY.
35. **Meyer Y, Buchanan BB, Vignols F, Reichheld JP.** 2009. Thioredoxins and glutaredoxins: unifying elements in redox biology. Annu Rev Genet **43:**335-367.
36. **Toledano MB, Kumar C, Le Moan N, Spector D, Tacnet F.** 2007. The system biology of thiol redox system in *Escherichia coli* and yeast: differential functions in oxidative stress, iron metabolism and DNA synthesis. FEBS Lett **581:**3598-3607.
37. **Apontoweil P, Berends W.** 1975. Glutathione biosynthesis in *Escherichia coli* K 12. Properties of the enzymes and regulation. Biochim Biophys Acta **399:**1-9.
38. **Finley JW. SJ, Johnston PH., and Friedman M.** 1978. Inhibition of lysinoalanine formation in food protein. Journal of Food Science **43:**619-621.
39. **Lindenberg S, Klauck G, Pesavento C, Klauck E, Hengge R.** 2013. The EAL domain protein YciR acts as a trigger enzyme in a c-di-GMP signalling cascade in E. coli biofilm control. Embo Journal **32:**2001-2014.
40. **Malone JG, Jaeger T, Manfredi P, Dotsch A, Blanka A, Bos R, Cornelis GR, Haussler S, Jenal U.** 2012. The YfiBNR Signal Transduction Mechanism Reveals Novel Targets for the Evolution of Persistent *Pseudomonas aeruginosa* in Cystic Fibrosis Airways. PLoS Pathog **8**.
41. **Wassarman KM, Repoila F, Rosenow C, Storz G, Gottesman S.** 2001. Identification of novel small RNAs using comparative genomics and microarrays. Genes & Development **15:**1637-1651.
42. **Altuvia S, WeinsteinFischer D, Zhang AX, Postow L, Storz G.** 1997. A small, stable RNA induced by oxidative stress: Role as a pleiotropic regulator and antimutator. Cell **90:**43-53.
43. **Storz G, Tartaglia LA, Ames BN.** 1990. The Oxyr Regulon. Antonie Van Leeuwenhoek International Journal of General and Molecular Microbiology **58:**157-161.

44. **Bian Z, Brauner A, Li Y, Normark S.** 2000. Expression of and cytokine activation by *Escherichia coli* curli fibers in human sepsis. J Infect Dis **181:**602-612.
45. **Hung C, Marschall J, Burnham CAD, Byun AS, Henderson JP.** 2014. The Bacterial Amyloid Curli Is Associated with Urinary Source Bloodstream Infection. PLoS One **9**.
46. **Oppong GO, Rapsinski GJ, Newman TN, Nishimori JH, Biesecker SG, Tukel C.** 2013. Epithelial cells augment barrier function via activation of the Toll-like receptor 2/phosphatidylinositol 3-kinase pathway upon recognition of *Salmonella enterica* serovar Typhimurium curli fibrils in the gut. Infect Immun **81:**478-486.
47. **Cegelski L, Pinkner JS, Hammer ND, Cusumano CK, Hung CS, Chorell E, Aberg V, Walker JN, Seed PC, Almqvist F, Chapman MR, Hultgren SJ.** 2009. Small-molecule inhibitors target *Escherichia coli* amyloid biogenesis and biofilm formation. Nat Chem Biol **5:**913-919.
48. **Potrykus K, Cashel M.** 2008. (p)ppGpp: Still Magical? Annual Review of Microbiology **62:**35-51.
49. **Clarke MB, Hughes DT, Zhu C, Boedeker EC, Sperandio V.** 2006. The QseC sensor kinase: a bacterial adrenergic receptor. Proc Natl Acad Sci U S A **103:**10420-10425.
50. **Kostakioti M, Hadjifrangiskou M, Pinkner JS, Hultgren SJ.** 2009. QseC-mediated dephosphorylation of QseB is required for expression of genes associated with virulence in uropathogenic *Escherichia coli*. Molecular Microbiology **73:**1020-1031.
51. **Dwyer DJ, Belenky PA, Yang JH, MacDonald IC, Martell JD, Takahashi N, Chan CTY, Lobritz MA, Braff D, Schwarz EG, Ye JD, Pati M, Vercruysse M, Ralifo PS, Allison KR, Khalil AS, Ting AY, Walker GC, Collins JJ.** 2014. Antibiotics induce redox-related physiological alterations as part of their lethality. Proceedings of the National Academy of Sciences of the United States of America **111:**E2100-E2109.
52. **Belenky P, Ye JD, Porter CBM, Cohen NR, Lobritz MA, Ferrante T, Jain S, Korry BJ, Schwarz EG, Walker GC, Collins JJ.** 2015. Bactericidal Antibiotics Induce Toxic Metabolic Perturbations that Lead to Cellular Damage. Cell Reports **13:**968-980.
53. **Kallen AJ, Welch HG, Sirovich BE.** 2006. Current antibiotic therapy for isolated urinary tract infections in women. Arch Intern Med **166:**635-639.
54. **Baraquet C, Harwood CS.** 2013. Cyclic diguanosine monophosphate represses bacterial flagella synthesis by interacting with the Walker A motif of the enhancer-binding protein FleQ. Proceedings of the National Academy of Sciences of the United States of America **110:**18478-18483.
55. **Diner EJ, Beck CM, Webb JS, Low DA, Hayes CS.** 2012. Identification of a target cell permissive factor required for contact-dependent growth inhibition (CDI). Genes & Development **26:**515-525.
56. **Serra DO, Richter AM, Hengge R.** 2013. Cellulose as an Architectural Element in Spatially Structured *Escherichia coli* Biofilms. J Bacteriol **195:**5540-5554.
57. **Epstein EA, Reizian MA, Chapman MR.** 2009. Spatial Clustering of the Curlin Secretion Lipoprotein Requires Curli Fiber Assembly. J Bacteriol **191:**608-615.
58. **Goyal G KP, Van Gerven N, Gubellini F, Van den Broeck I, Troupoiotis-Tsailaki A, Jonkheere W, Pejau-Arnaudet G, Pinkner JS, Chapman MR, Hultgren SJ, Howorka S, Fronzes R, and Remaut H.** 2014. Structural and mechanistic insights into the bacterial amyloid secretion channel CsgG. Nature **In Press**.
59. **Reading NC, Torres AG, Kendall MM, Hughes DT, Yamamoto K, Sperandio V.** 2007. A novel two-component signaling system that activates transcription of an

enterohemorrhagic *Escherichia coli* effector involved in remodeling of host actin. Journal of Bacteriology **189:**2468-2476.
60. **Moreira CG, Sperandio V.** 2010. The Epinephrine/Norepinephrine/Autoinducer-3 Interkingdom Signaling System in *Escherichia coli* O157:H7. Microbial Endocrinology: Interkingdom Signaling in Infectious Disease and Health doi:10.1007/978-1-4419-5576-0_12**:**213-227.
61. **Mciver CJ, Tapsall JW.** 1993. Study of Growth Requirements Other Than Cysteine of Naturally-Occurring Escherichia-Coli and Klebsiella Spp Auxotrophic for Cysteine. Journal of Clinical Microbiology **31:**2790-2793.
62. **Mciver CJ, Tapsall JW.** 1987. Cysteine Requirements of Naturally-Occurring Cysteine Auxotrophs of *Escherichia-Coli*. Pathology **19:**361-363.
63. **Doroshenko N, Tseng BS, Howlin RP, Deacon J, Wharton JA, Thurner PJ, Gilmore BF, Parsek MR, Stoodley P.** 2014. Extracellular DNA Impedes the Transport of Vancomycin in *Staphylococcus epidermidis* Biofilms Preexposed to Subinhibitory Concentrations of Vancomycin. Antimicrobial Agents and Chemotherapy **58:**7273-7282.
64. **Ganeshnarayan K, Shah SM, Libera MR, Santostefano A, Kaplan JB.** 2009. Poly-N-Acetylglucosamine Matrix Polysaccharide Impedes Fluid Convection and Transport of the Cationic Surfactant Cetylpyridinium Chloride through Bacterial Biofilms. Applied and Environmental Microbiology **75:**1308-1314.
65. **Claes DJ, Jackson E.** 2012. Cystinuria: mechanisms and management. Pediatric Nephrology **27:**2031-2038.
66. **Wilcken DEL, Gupta VJ.** 1979. Sulfur-Containing Amino-Acids in Chronic Renal-Failure with Particular Reference to Homocystine and Cysteine-Homocysteine Mixed Disulfide. European Journal of Clinical Investigation **9:**301-307.
67. **Mulvey MA, Schilling JD, Hultgren SJ.** 2001. Establishment of a persistent *Escherichia coli* reservoir during the acute phase of a bladder infection. Infect Immun **69:**4572-4579.
68. **Datsenko KA, Wanner BL.** 2000. One-step inactivation of chromosomal genes in *Escherichia coli* K-12 using PCR products. Proc Natl Acad Sci U S A **97:**6640-6645.
69. **Rubin EJ, Akerley BJ, Novik VN, Lampe DJ, Husson RN, Mekalanos JJ.** 1999. In vivo transposition of mariner-based elements in enteric bacteria and mycobacteria. Proc Natl Acad Sci U S A **96:**1645-1650.
70. **Hoch HC, Galvani CD, Szarowski DH, Turner JN.** 2005. Two new fluorescent dyes applicable for visualization of fungal cell walls. Mycologia **97:**580-588.

Chapter 4

CRP-cAMP directly regulates *csgD* and uropathogenic *Escherichia coli* biofilms.

Abstract

The extracellular matrix protects *E. coli* from immune cells, oxidative stress, predation, and other environmental stresses. Production of the *E. coli* extracellular matrix is regulated by transcription factors that are tuned to environmental conditions. The biofilm master-regulator protein CsgD upregulates curli and cellulose, the two major polymers in the extracellular matrix. Here we find that cAMP directly regulates curli, cellulose, and UPEC biofilms through *csgD*. The alarmone cAMP is produced by adenylate cyclase (CyaA) and we found that deletion of *cyaA* resulted in lower extracellular matrix production and biofilm formation. The catabolite repressor protein (CRP) transcriptionally activates and directly binds to the *csgD* promoter of the uropathogenic *E. coli,* UTI89 leading to curli and cellulose production. Glucose, which inhibits CyaA activity, was able to block extracellular matrix formation when added to the growth media. Δ*cyaA* and Δ*crp* are unable to produce rugose biofilms, pellicles, curli, cellulose, or CsgD. Using site-directed mutagenesis and electrophoretic mobility shift assays we characterized 3 putative CRP binding sites within the *csgD* promoter. Together our work shows that cAMP and CRP influence *E. coli* biofilms through direct transcriptional regulation of *csgD*.

Importance

CRP-cAMP influences transcription of over 7% of the *E. coli* genome (1). Glucose inhibits *E. coli* biofilm formation, and Δ*cyaA* and Δ*crp* mutants are impaired for biofilm formation (2). A microarray study found that CRP influences *csgD* transcription (1), but it was not known if this regulation was mediated by CRP binding to the *csgD* promoter region. We determined that cAMP and CRP regulate curli and cellulose production and the formation of rugose and pellicle biofilms through direct binding to 3 distinct sites on the *csgD* promoter. Additionally, we propose that cAMP may work as a signaling compound for UPEC to transition from the bladder to inside epithelial cells during intracellular bacterial community formation.

Introduction

Escherichia coli are a multi-faceted gram-negative bacteria with a wealth of tools, structures, and mechanisms that aid in survival in disparate environments ranging from stool to the urinary tract (3). Biofilms are a lifestyle employed in multiple environments characterized by adherence, slow growth, resistance to environmental insults, and production of an extracellular matrix (ECM) (4). CsgD is the major biofilm regulator of *E. coli* and many other enterobacteriaceae (5-7) promoting production of two *E. coli* surface appendages the amyloid fiber curli and the fibrous glycan chain, cellulose (4). CsgD acts as a planktonic brake via motility inhibition through repression of motility-associated genes, while promoting self and surface attachment (8-10).

During urinary tract infections (UTI), *E. coli* use a variety of tools to evade the host and establish a population. *E. coli* are found in ~80% of UTIs, more than any other causative agent, and they have the ability to thrive in the bladder and urinary tract environment (11). Initially,

curli and other factors play a role in establishing an initial bacterial titer (12). Once in the bladder, *E. coli* utilize type-1 pili to invade bladder epithelial cells (13). *E. coli* then form a biofilm-like structure known as an intracellular bacterial community (IBC) with the ECM component K1 capsule coating the cells and protecting them from host cell recognition (14). *E. coli* recognition of multiple environments is critical to production of these various UTI-related appendages at the various stages of UTI and IBC formation.

Catabolite Repressor Protein (CRP) is a transcriptional regulator that is activated by the alarmone cyclic AMP (cAMP) (15). cAMP is produced by the adenylate cyclase, CyaA, in low glucose environments leading to activation of CRP (15). CRP inactivation acts to equip *E. coli* for glucose acquisition. A global CRP-cAMP analysis revealed 7% of *E. coli's* genome is altered via CRP activation, including *csgD* transcription (1). The study by *Zheng et al.* used a laboratory strain of *E. coli* and hence didn't investigate UPEC specific virulence factors in their course of study, such as type-1 pili and K1 capsule (1, 13). Interestingly, further studies found that CRP is an inhibitor of Type-1 pili formation in UPEC strains (16).

Glucose inhibits *E. coli* biofilms, and Δ*cyaA* and Δ*crp* laboratory strains have a decreased propensity for biofilm formation (2, 17). Additionally, Zheng *et al.* revealed three putative CRP binding cites on the promoter of *csgD* (1). We hypothesized that CRP directly binds to the *csgD* reporter and hence regulates production of both curli and cellulose. This study investigates the effect of CRP on uropathogenic *E. coli* (UPEC) biofilms, CsgD and CsgA protein levels, cellulose production, *csgD* transcriptional analysis, and investigation of CRP binding regions on the *csgD* promoter of the *E. coli* cystitis isolate, UTI89.

Our study found glucose inhibits biofilm formation independently of pH, and that cAMP directly regulates biofilm formation, curli, cellulose, and CsgD protein levels of UPEC through three specific sites on the *csgD* promoter. Additionally we have identified 2 putative binding sites on the *kpsM,* which encodes the secretion pore for K1 capsule. All in all, this work shows that cAMP acts as a regulator of another set of UTI-associated virulence factors in combination with type-1 pili.

Results and Discussion

We tested the effect of glucose addition on curli production. We spread *E. coli* K12 BW25113 onto YESCA CR plates and added acetic acid, 20% glucose, and H_20 and incubated the colonies for 48 hours at 26°C (Figure 4.1A). We found that Congo red (CR) binding was decreased in the presence of glucose (Figure 4.1A). Since glucose metabolism can acidify the media, we added acetic acid to plates to control for curli expression under acidic conditions (Figure 4.1A). Acidic bi-products from glycolysis were previously reported in *Salmonella* to change the biofilm phenotype (18). CsgA is the major subunit of curli fibers and western blot analysis determined that CsgA levels are decreased in the presence of glucose, but not in the presence of acid (Figure 4.1B). Neither glucose nor acetic acid affected viability (Figure 4.1C).

We tested the ability of the CRP-cAMP complex to regulate *csgD* transcription and biofilms in the UPEC strain UTI89. Rugose or wrinkled colony biofilms were grown on YESCA or YESCA Congo red (CR) plates containing 0.1% galactose and buffered with MES (Figure 4.2A). CR binds to both curli and cellulose (19). Galactose was added so that the strains lacking the CRP-cAMP complex had a utilizable carbon source, since CRP-cAMP mutants do not grow efficiently on most other carbon sources (20). The exogenous addition of cAMP caused an

increased wrinkling in the rugose biofilm and increased curli production in WT strains (Figure 4.2A). Δ*cyaA* and Δ*crp* colonies appeared white on CRI plates (Fig 4.2A). Exogenous addition of cAMP restored rugose biofilm formation and curli production to the *cyaA* mutant strain (Fig 4.2A). Predictably, the Δ*crp* mutant was not rescued by cAMP addition (Figure 4.2A). The lack of CR binding in Δ*cyaA* and Δ*crp* strains indicates that neither curli nor cellulose was being produced, as both ECM components bind to CR.

Pellicles are a curli and cellulose dependent static biofilm that forms at the air-liquid interface of cultures (12, 21). Pellicle formation was inhibited by glucose addition, and Δ*cyaA* and Δ*crp* strains were unable to form pellicles (Figure 4.2B). The addition of cAMP to the media restored pellicle formation in the Δ*cyaA* strain but not in Δ*crp* (Figure 4.2B).

Since CR binding was abolished in *cyaA* and *crp* mutants (Figure 4.1A), and Δ*crp* and Δ*cyaA* were unable to form pellicle biofilms, we hypothesized that there might be defective expression of the master biofilm regulator, CsgD. β-galactosidase assays demonstrated decreased transcription of *csgD* in Δ*cyaA* and Δ*crp* colonies in comparison to UTI89 WT (Figure 4.3A). Exogenous cAMP addition increased transcription of WT and Δ*cyaA*, however the levels were similar in the presence and absence of cAMP in a Δ*crp* strain (Figure 4.3A). Western blot analysis additionally revealed increased CsgD in the presence of cAMP in WT and Δ*cyaA*, however there is a modest increase in CsgD in the presence of cAMP in Δ*crp* strains, suggesting either a change in physiology in the presence of this nucleotide or a secondary responder to cAMP being present in UTI89 (Figure 4.3B). The lack of CsgD in Δ*cyaA* and Δ*crp* mutants is the cause of the lack of curli and cellulose, since CsgD regulates both extracellular matrix components (19, 22). The positive link between *csgD* expression and CRP are consistent with previous findings in *E. coli* (1, 2, 17) but are in contrast with findings in *Salmonella enterica*

(18). *S. enterica* and *E. coli* reside in differing hosts, host niches, and extra-host environments (23, 24), which may influence the evolution of glucose-dependent or independent *csgD* phenotypes of these two species.

Next, we determined if CRP could bind directly to the *csgD* promoter. Electrophoretic mobility assays show that CRP binds the intergenic region between *csgDEFG* and *csgBAC* only in the presence of cAMP, and that cAMP alone does not influence DNA gel migration (Figure 4.4A). Zheng *et al.* 2004 identified 3 putative binding sites of various homology on the *csgD* promoter (1). We identified the putative CRP binding sites in the UTI89 *csgD* promoter, determined homologous base pairs (bp), and decided the best bp to target for site-directed mutagenesis (Figure 4.4B). Three sites were chosen based on highly conserved bp in the CRP binding consensus, and nucleotides were changed to the least conserved nucleotide found in each individual site for the CRP-binding consensus according to PRODORIC (25) (Figure 4.4B). Mutational analysis yielded 3 single mutants (sites 1,2, and 3), 3 double mutants (1/2,1/3, and 2/3), and a triple mutant (1/2/3) of 315bp of the *csgD* promoter. CRP bound to DNA of all single and double mutants for the 3 sites of interest; however CRP binding was abrogated by mutating all three predicted sites, showing that CRP only bound at these three particular locations on the *csgD* promoter (Figure 4.4B). Interestingly, mutation of these 3 sites for the entire *csgDEFG* and *csgBAC* intergenic region was still able to bind to CRP, hinting that CRP may be able to interact with the *csgBAC* promoter as well (data not shown).

Bladder infection leads to UPEC invading bladder cells in a type-1 pili dependent manner (26). Once in the interior of these cells UPEC begin a program leading to a biofilm-like community encased in K1 capsule that is resistant to host-immune system detection (13, 14). Host cells recognize *E. coli* lipopolysaccharide and upregulate cAMP production in exocytic

compartments (27, 28). In contrast, cAMP concentration is low outside of host cells, which allows for type-1 pili production, as type-1 pili are repressed by CRP (16, 29). There is only a moderate correlation between curli production and initial titers of UPEC during UTI (12), however perhaps cAMP-mediated curli production play a role intracellularly or during the biofilm-like IBC formation process, as curli are important for other *E. coli* biofilm models (4). If cAMP does act to initiate the IBC formation program, then cAMP should also upregulate other IBC extracellular matrix components, such as K1 capsule. K1 capsule mutants (*Δkps*) do not form IBCs and are penetrated by neutrophils (14). *In silico* analysis determined that the promoter of *kpsMT* contains two predicted CRP binding sites with high homology to the CRP consensus binding sites (Figure 4.4B). *kpsM* encodes the transporter for K1 capsule, whereas *kpsT* encodes the ATPase that is necessary for export of the capsule (30). cAMP could potentially act as a sensor that transitions UPEC from the kidney, to cell invasion, to the formation of IBCs through the inhibition of type-1 pili, upregulation of K1 capsule, and potentially curli through *csgD*.

Materials and Methods

Strains and growth conditions Overnight cultures were grown shaking at 37°C overnight. All UTI89 mutants were made via lamda red recombination (31). All primers and strain names can be found in supplemental material. Strains in the manuscript are referred to by their mutation.

For the glucose addition plates (Figure 4.1), .1-OD_{600} of WT *E. Coli* K12 BW25113 cells were spread with glass beads. Sterile filter paper disks were added to the cells and 15µL of .1M acetic, 1M acetic acid, 20% (w/v) (D)-glucose, and H_2O. Plate was incubated at 26°C for 48

hours. Blue inoculating loops were used to collect cells around the sterile filter paper disks and were imaged (Figure 4.1A). Cells were normalized by optical density and then serial diluted prior to plating 4μL dots on LB media that was then incubated at 37°C overnight (Figure 4.1C).

Rugose biofilms were grown as previously described (32), with a few exceptions. 4μL of 1-OD_{600} overnight cells were dotted and incubated at 26°C for 48 hours on YESCA (10g Casamino acids and 1 g yeast extract/L) Congo red (CR) (50μg CR/L) plates supplemented with 15mM 2-(N-morpholino)ethanesulfonic acid (MES) and 0.1% galactose (w/v) (pH 6.7). Images were capture on an Olympus SZX16 microscope with an Olympus DP72 camera. Pellicles were prepared by adding 2μL of overnight culture into 2mL YESCA and grown statically at 26°C for 48 hours (33). Pellicles were stained with 2mL .1% (w/v) crystal violet for 5 minutes, followed by 3 washes with 2mL H_2O, and were imaged on a Fluorchem 8900 (Alpha Innotech, San Leandro, CA).

Western blot analysis- Western blots were performed as previously described (32, 34). Rugose biofilms were collected with blue inoculating loops in 1mL 50mM potassium phosphate (KPI) buffer (pH 7.2) and briefly vortexed. 150μL of 1-OD_{600} cells were spun down, then resuspended in 2x SDS-running buffer for CsgD western blots or hexafluoisopropanol (HFIP) for CsgA western blots. HFIP treated cells were incubated in a Savant SPD SpeedVac at 45°C for 45 minutes prior to 2x SDS-running buffer addition. Samples were heated at 95°C for 10minutes prior to 8μL loading and electrophoresis in a 15% SDS-PAGE gel for 45 min at 25mA. CsgA Western blots were transferred onto a PVDF membrane from semi-dry transfer apparatus at 25V for 10minutes at room temperature, whereas CsgD Western blots were wet transferred onto a nitrocellululose membrane in 25mM CAPS (N-cylclohexyl-3-aminopropanesulfonic acid)

transfer buffer in 10% mtahanol at 12V overnight at 4°C. All blots were blocked overnight in 5% skim milk with Tris buffered saline-Tween 20 (TBST) buffer at 4°C. Primary antibody treatment was 1 h (1:8000 dilution for α-CsgA (α-rabbit), 1:5000 dilution for α-CsgD (α-rabbit), 1:10000 dilution for α-σ70 (anti-mouse) followed by 3x5minutes washes in TBST. Secondary antibody treatment was 1 h (1:15000 Licor secondary antibodies α-rabbit and α-mouse IR dyes (Santa Cruz)). Blots were imaged on Licor Odyssey CLX imager.

β-galactosidase assays- Miller assays were performed as previously described (32, 35). Rugose biofilms were resuspended in KPI and diluted 1:10. Reaction buffer (90μL), 7μL of diluted cells were incubated at 30°C for 20min prior to 20μLof 4mg/mL ortho-nitrophenyl-β-galactoside (ONPG) addition. 50μL 1M Na_2CO_3 addition stopped reactions after a yellow color developed in the reaction. The absorbance of reactions at 420nm and 550nm on a Tecan Infinite 200 plate reader were measured along with OD_{600} of the cell dilutions. All strains were assayed in biological triplicate with pRJ800 (no promoter upstream of *lacZ* (EV*)*, pRJ800-*csgD* (*csgD* promoter upstream of *lacZ),* and pRJ800-16s (16s promoter upstream of *lacZ).*The average of the EV readings were subtracted from each biological triplicate of the pRJ800-*csgD &* 16s readings in all strains. Averages and standard deviations were taken from the biological triplicates with the EV values subtracted.

Electrophoretic mobility shift assays- Electrophoretic mobility shift assay (EMSA) reactions contained 1μL 10x EMSA buffer (Licor), 1μL DTT/tween, .5uL 1μg/uL Poly (deoxyinosinic deoxycytidylic) acid (PolydIdC), 3μL DNA (300-500ng/uL), 2μL of .4mg/mL CRP, and 1μL 2mM cAMP and were incubated at room temperature for 1 hour. 6x DNA load dye (Fermentas) was added to samples prior to running on an agarose gel at 120V. Gels were run for 50 minutes,

followed by 10-20min incubation in an ethidium bromide (EtBr) bath, followed by an additional electrophoresis for 50minutes. 2% agarose gel was used for the *csgD_csgBAC* intergenic region, and a 4% agarose (Amresco 3:1 High Resolution Blend) gel was used to electrophorese the *csgD* promoter and mutant promoters.

Figures:

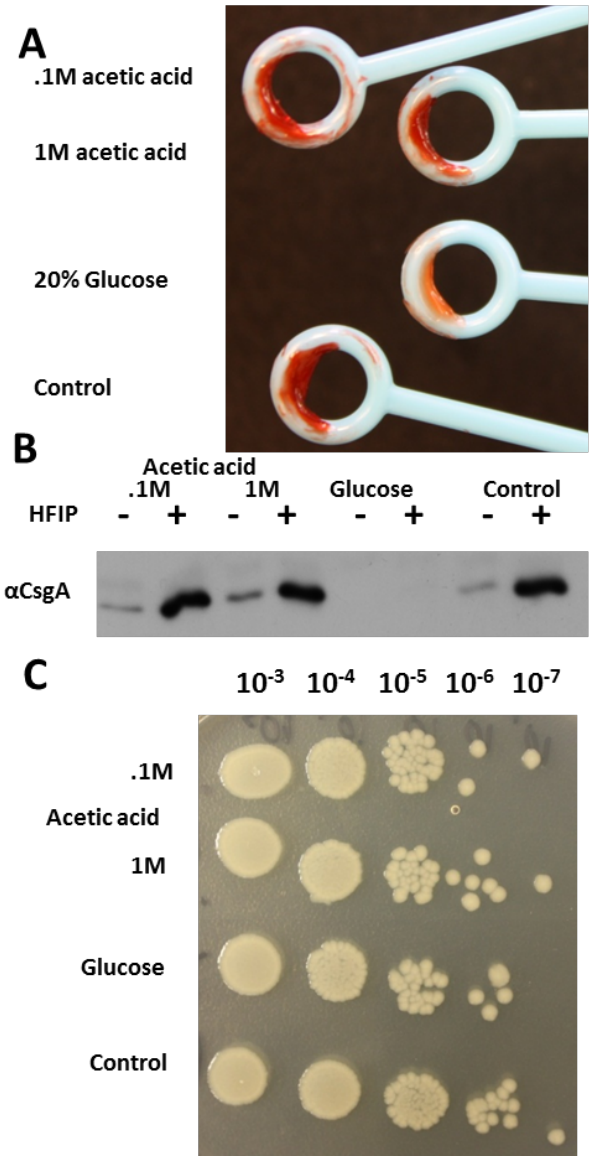

Figure 4.1- Glucose inhibits CR binding and CsgA. (A) *E. coli* K12 BW25113 was evenly spread on YESCA CR plates and incubated at 26°C for 48 hours. Addition of a sterile filter paper disk allowed for addition of 15µL of.1M acetic acid, 1M acetic acid, 20% glucose, and H_2O. Sterile blue inoculating loops isolated the bacteria for imaging of CR binding. (B) Western blot analysis of cells isolated from the YESCA CR plates revealed that CsgA levels are decreased in the presence of glucose. HFIP addition allows for monomerization of the CsgA subunit of the curli fiber. (C) Cells isolated from YESCA CR plates were normalized by OD_{600} , followed by serial dilutions and plating of 4µL dots onto LB plates that were then incubated prior to imaging. Serial dilutions revealed that acetic acid and glucose treatment did not affect viability of the cells.

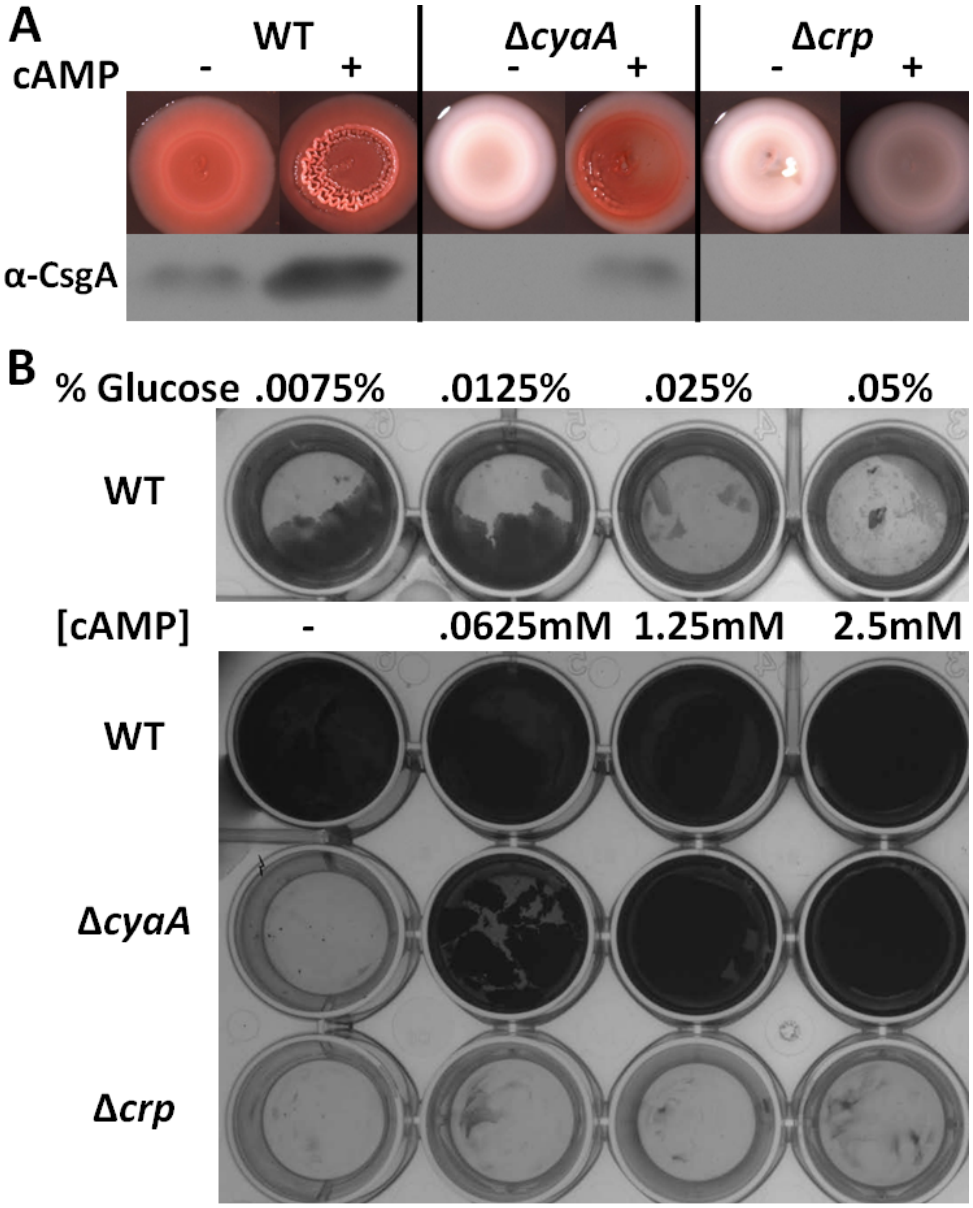

Figure 4.2- CRP-cAMP regulates UTI89 biofilm formation and CsgD. (A) cAMP induced biofilm formation and CsgA production in UTI89 WT and Δ*cyaA*. UTI89 colonies were grown on YESCA CR medium supplemented with 15mM MES (pH 6.7) and .1% (w/v) galactose for 48 hours at 26°C. Colonies were spotted 6mm from a sterile paper disk containing 15µL of 100mM cAMP or in the absence of cAMP. Anti-CsgA Western blots showed an upregulation of CsgA in the presence of cAMP in WT and Δ*cyaA*. Δ*cyaA* did not produce CsgA in the absence of cAMP, and Δ*crp* did not produce CsgA in the presence or absence of cAMP. (B) Pellicles were inhibited by glucose and required active CRP-cAMP. Pellicles were grown statically in YESCA at 26°C for 48 hours. Biofilms were stained with crystal violet and washed with H_2O prior to imaging. The top row shows glucose addition to YESCA media inhibited WT UTI89 pellicle formation. The bottom rows show that cAMP addition to the media can restored pellicle formation to the normally non-pellicle forming Δ*cyaA,* however Δ*crp* did not form a pellicle in the presence or absence of cAMP.

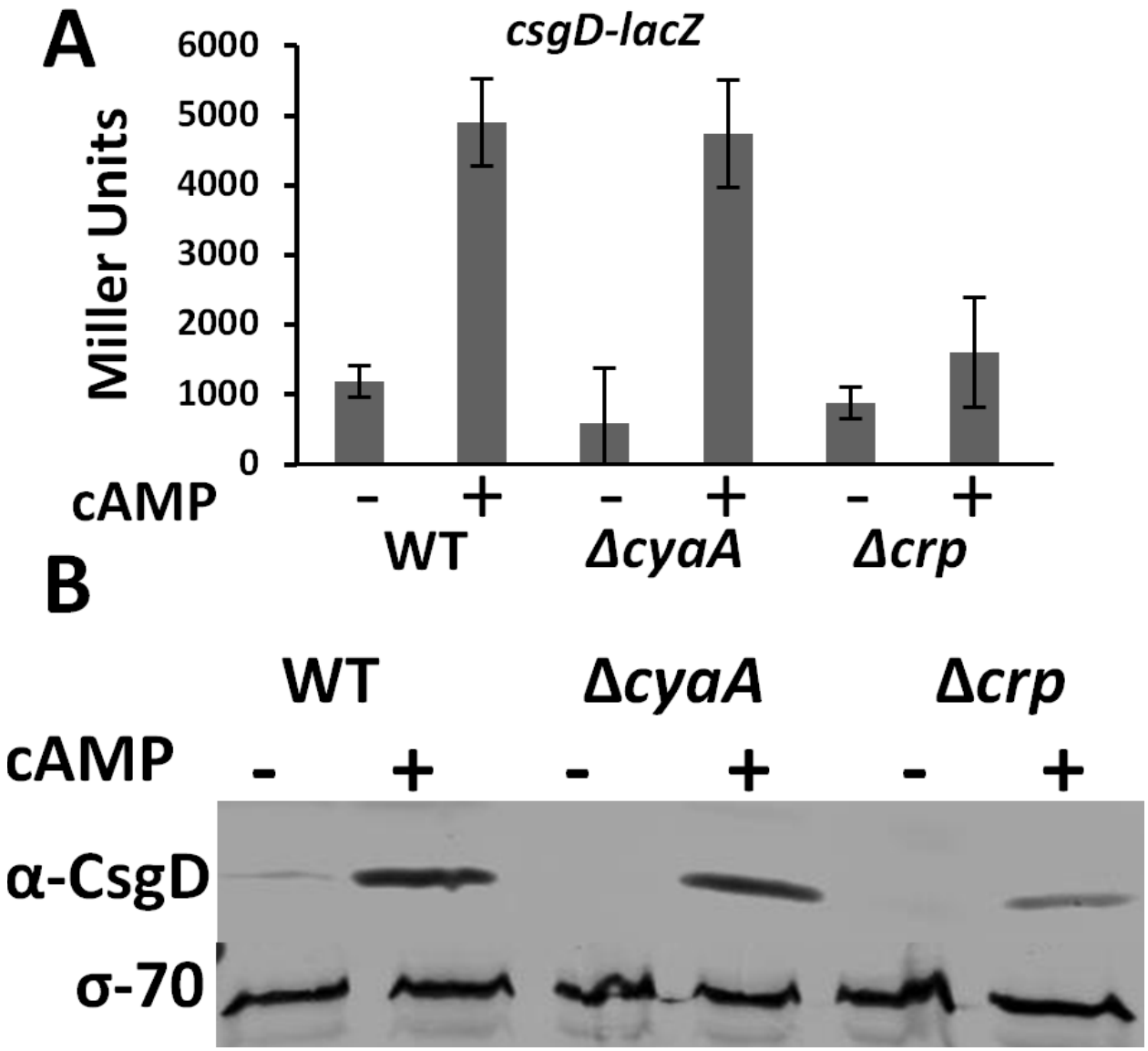

Figure 4.3- CRP-cAMP controls *csgD* transcription and CsgD levels. (A) β-galactosidase assays were performed on UTI89 WT, Δ*cyaA,* and Δ*crp* transformed with pRJ800, pRJ800-*csgD,* and pRJ800-16s (*rrsA*). pRJ800 readings were subtracted from prj800-*csgD* and pRJ800-16s, and pRJ800-*csgD* readings were normalized by pRJ800-16s readings. *csgD* transcription was upregulated in the presence of cAMP for both UTI89 WT and Δ*cyaA,* whereas Δ*crp* transcription wasn't significantly increased. Error bars represent standard deviation. (B) Anti-CsgD Western blots showed WT has higher basal levels of CsgD, and that WT and Δ*cyaA* had a large upregulation of CsgD in the presence of cAMP. Interestingly, Δ*crp* had a slight increase in CsgD levels. Anti-σ-70 was used as a loading control.

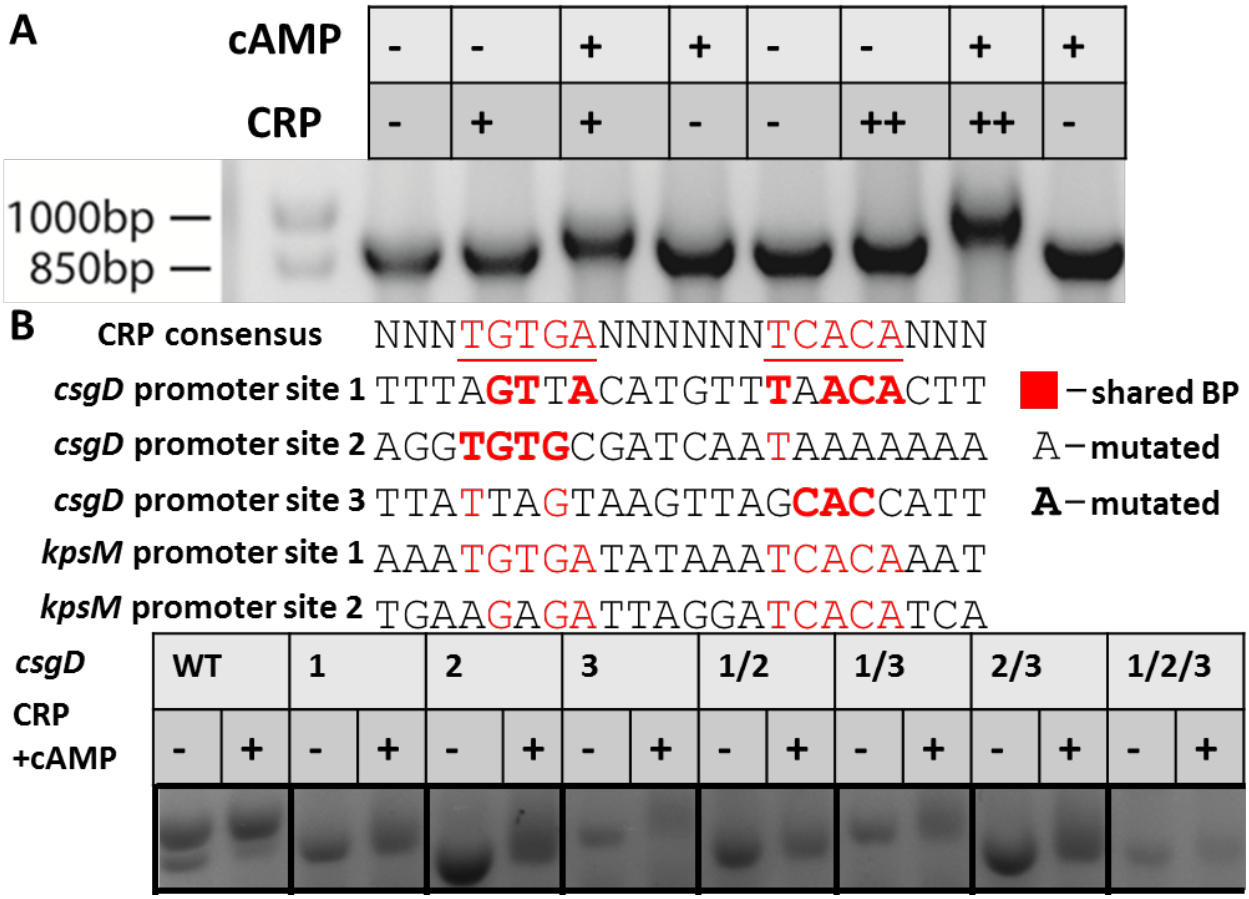

Figure 4.4- CRP-cAMP binds to the *csgD* promoter at sites 1, 2, and 3. (A) CRP and cAMP caused a gel shift of UTI89 *csgD* intergenic region. *csgD-csgBAC* intergenic region was incubated in various reactions with and without CRP and/or cAMP, and then was loaded and run at 120mV in 2% (w/v) agarose gels. Bands were visualized via ethidium bromide staining. CRP without cAMP and cAMP without CRP did not influence the migration of the *csgD* promoter. 2µL of CRP in the EMSA reaction caused a more significant gel shift. (B) Sites 1,2, and 3 are all the sites on the *csgD* promoter that bind to CRP. CRP consensus binding pattern is shown at top. *csgD* sites 1, 2, and 3 all showed homology to the CRP consensus (highlighted in red), and the bp that were mutated for the following gel shift were bolded. The *kpsM* promoter also showed significant homology to the CRP consensus. On the bottom the WT *csgD* promoter and various *csgD* site mutants were incubated with or without CRP and cAMP. CRP-cAMP induced a gel-shift in WT and all mutants except for the *csgD* promoter that was mutated for sites 1, 2, and 3 altogether.

Table 4.1- EMSA segment sequences

EMSA segments	Sequence	Description of creation
csgD full length promoter	GATCGGATCCTTAAGAAATTAAATCATTTCAACTTGGTTGTTA ACGCAACCTGTATTTTGTTAACGCTGCGTTACGATGGAAAGT ATGTCTGCGGAAATATTTTTAATAACTCACCCGCACGTTGTAT TTTTCTTTTTTTGTTCATACCAAAGTATTAAAACCCACGTAAA TACGCTGTTATCTACGCAAAAATATTTTGTTTTCTTTTAAATCT CCGTTTTCCGCTATCAAAAATCACCAGACAGTCATTCTTCTTG CCCGTCGCTGATTGCTGCGATATGTCTTGCGCACAAGTCGTGA CAAACCTCGTCTTTTTGCAGTAAAAAATTGTCCACGGTGGTAT GGAGAAAAAACAAGAACGTTTTTCATGACGAAAGGACTACA GCGAAATATTTTTTATATGCATTATTAGTAAGTTAGCACCATT TGTATGATTTTTTAAAATTGTGCAATAAAAACCAAATGTACA ACTTTTCTATCATTTATAAACTTAATAAAACCTTAAGGTTAAC ATTTTAATATAATGAGTTACATTTAGTTACATGTTTAACACTT GATTTAAGATTTGTAATGGCTAGATTGAAATCAGATGTAATC CATTAGTTTTATATTTTACCCATTTAGGGCTGATTTATTACTAC ACACAGCAGTGCAACATCTGTCAGTACTTCTGGTGCTTCTATT TTAGAGGCAGCTGTCAGGTGTGCGATCAATAAAAAAAGCGG GGTTTCATCTCTAGAGATC	Primers DH113 and DH114 amplified from UTI89 WT gDNA
csgD WT	TTATTAGTAAGTTAGCACCATTTGTATGATTTTTTAAAATTGT GCAATAAAAACCAAATGTACAACTTTTCTATCATTTATAAACT TAATAAAACCTTAAGGTTAACATTTTAATATAATGAGTTACAT TTAGTTACATGTTTAACACTTGATTTAAGATTTGTAATGGCTA GATTGAAATCAGATGTAATCCATTAGTTTTATATTTTACCCAT TTAGGGCTGATTTATTACTACACACAGCAGTGCAACATCTGTC AGTACTTCTGGTGCTTCTATTTTAGAGGCAGCTGTCAGGTGTG CGATCAATAAAAAA	Primers DH291 and DH293 amplified from UTI89 WT gDNA
csgD 1	TTATTAGTAAGTTAGCACCATTTGTATGATTTTTTAAAATTGT GCAATAAAAACCAAATGTACAACTTTTCTATCATTTATAAACT TAATAAAACCTTAAGGTTAACATTTTAATATAATGAGTTACAT TTAGTTACATGTTTACCACTCGATTTAAGATTTGTAATGGCTA GATTGAAATCAGATGTAATCCATTAGTTTTATATTTTACCCAT TTAGGGCTGATTTATTACTACACACAGCAGTGCAACATCTGTC AGTACTTCTGGTGCTTCTATTTTAGAGGCAGCTGTCAGGTGTG CGATCAATAAAAAA	Primers DH 291 + DH116 and Primers DH293 +DH 115 amplified the two segments of this promoter. The two segments were then amplified

		via SOEing reaction by primers DH 291 +DH293
csgD 2	TTATTAGTAAGTTAGCACCATTTGTATGATTTTTTAAAATTGT GCAATAAAAACCAAATGTACAACTTTTCTATCATTTATAAACT TAATAAAACCTTAAGGTTAACATTTTAATATAATGAGTTACAT TTAGTTACATGTTTAACACTTGATTTAAGATTTGTAATGGCTA GATTGAAATCAGATGTAATCCATTAGTTTTATATTTTACCCAT TTAGGGCTGATTTATTACTACACACAGCAGTGCAACATCTGTC AGTACTTCTGGTGCTTCTATTTTAGAGGCAGCTGTCAGGGCGC CGATCAATAAAAAA	Primers DH 291 and DH294
csgD 3	TTATTAGTAAGTTAGACGCATTTGTATGATTTTTTAAAATTGT GCAATAAAAACCAAATGTACAACTTTTCTATCATTTATAAACT TAATAAAACCTTAAGGTTAACATTTTAATATAATGAGTTACAT TTAGTTACATGTTTAACACTTGATTTAAGATTTGTAATGGCTA GATTGAAATCAGATGTAATCCATTAGTTTTATATTTTACCCAT TTAGGGCTGATTTATTACTACACACAGCAGTGCAACATCTGTC AGTACTTCTGGTGCTTCTATTTTAGAGGCAGCTGTCAGGTGTG CGATCAATAAAAAA	Primers DH292 and DH 293
csgD 1/2	TTATTAGTAAGTTAGCACCATTTGTATGATTTTTTAAAATTGT GCAATAAAAACCAAATGTACAACTTTTCTATCATTTATAAACT TAATAAAACCTTAAGGTTAACATTTTAATATAATGAGTTACAT TTAGTTACATGTTTACCACTCGATTTAAGATTTGTAATGGCTA GATTGAAATCAGATGTAATCCATTAGTTTTATATTTTACCCAT TTAGGGCTGATTTATTACTACACACAGCAGTGCAACATCTGTC AGTACTTCTGGTGCTTCTATTTTAGAGGCAGCTGTCAGGGCGC CGATCAATAAAAAA	DH 291+DH116 and DH294+DH 115 amplified, followed by SOEing reaction with DH291+294
csgD1/ 3	TTATTAGTAAGTTAGACGCATTTGTATGATTTTTTAAAATTGT GCAATAAAAACCAAATGTACAACTTTTCTATCATTTATAAACT TAATAAAACCTTAAGGTTAACATTTTAATATAATGAGTTACAT TTAGTTACATGTTTACCACTCGATTTAAGATTTGTAATGGCTA GATTGAAATCAGATGTAATCCATTAGTTTTATATTTTACCCAT TTAGGGCTGATTTATTACTACACACAGCAGTGCAACATCTGTC AGTACTTCTGGTGCTTCTATTTTAGAGGCAGCTGTCAGGTGTG CGATCAATAAAAAA	DH292+DH 116 and DH293+DH 115 amplified, followed by SOEing reaction DH292+293

csgD2/3	TTATTAGTAAGTTAGACGCATTTGTATGATTTTTTAAAATTGT GCAATAAAAACCAAATGTACAACTTTTCTATCATTTATAAACT TAATAAAACCTTAAGGTTAACATTTTAATATAATGAGTTACAT TTAGTTACATGTTTAACACTTGATTTAAGATTTGTAATGGCTA GATTGAAATCAGATGTAATCCATTAGTTTTATATTTTACCCAT TTAGGGCTGATTTATTACTACACACAGCAGTGCAACATCTGTC AGTACTTCTGGTGCTTCTATTTTAGAGGCAGCTGTCAGGGCGC CGATCAATAAAAAA	DH292+DH294
csgD1/2/3	TTATTAGTAAGTTAGACGCATTTGTATGATTTTTTAAAATTGT GCAATAAAAACCAAATGTACAACTTTTCTATCATTTATAAACT TAATAAAACCTTAAGGTTAACATTTTAATATAATGAGTTACAT TTAGTTACATGTTTACCACTCGATTTAAGATTTGTAATGGCTA GATTGAAATCAGATGTAATCCATTAGTTTTATATTTTACCCAT TTAGGGCTGATTTATTACTACACACAGCAGTGCAACATCTGTC AGTACTTCTGGTGCTTCTATTTTAGAGGCAGCTGTCAGGGCGC CGATCAATAAAAAA	DH292+DH116 and DH294+DH115 amplified, followed by SOEing reaction DH292+294

Table 4.2- Primer list Chapter 4

Primers	Description	sequence
DH9	*crp* RS F	GGC GTT ATC TGG CTC TGG AGA AAG CTT ATA ACA GAG GAT AAC CGC GCA TGG TGT AGG CTG GAG CTG CTT C
DH10	*crp RS R*	CTA CCA GGT AAC GCG CCA CTC TGA CGG GAT TAA CGA GTG CCG TAA ACG ACC ATA TGA ATA TCC TCC TTA G
DH11	cyaA RS F	GTT GGC GGA ATC ACA GTC ATG ACG GGT AGC AAA TCA GGC GAT ACG TCT TGG TGT AGG CTG GAG CTG CTT C
DH12	cyaA RS R	CGG ATA AGC CTC GCT TTC CGG CAC TTT CAT CAC GAA AAA TAC TGC TGC AAC ATA TGA ATA TCC TCC TTA G
DH113	*prj800 csgD F*	GAT CGG ATC CTT AAG AAA TTA AAT C
DH114	*prj800 csgD R*	GAT CTC TAG AGA TGA AAC CCC GCT T
DH291	*prj800 csgD FC site 3 WT buried*	TTA TTA GTA AGT TAG CAC CAT TTG TAT GAT T
DH292	*prj800 csgD FC site 3 mutant buried*	TTA TTA GTA AGT TAG ACG CAT TTG TAT GAT T
DH115	*prj800 csgD F mutant 1*	ACA TGT TTA CCA CTC GAT TTA AGA T
DH116	*prj800 csgD R mutant 1*	ATC TTA AAT CGA GTG GTA AAC ATG T
DH293	*prj800 csgD RB*	TTT TTT ATT GAT CGC ACA CCT GAC AGC TGC C

	WT 2 buried	
DH294	*prj800 csgD RB mutant 2 buried*	TTT TTT ATT GAT CGG CGC CCT GAC AGC TGC C

Table 4.3- Strain list Chapter 4

Strain name	Strain Genotype	Reference	Notes
CL1204	UTI89 Δcrp	This chapter	UTI89 RS kan casette into crp. PCP20 used to remove Kan casette
CL1205	UTI89 ΔcyaA	This chapter	UTI89 RS kan casette into cyaA. PCP20 used to remove Kan casette
CL1955	UTI89 Δcrp prj800	This chapter	UTI89 Δcrp transformed with prj800
CL1953	UTI89 ΔcyaA prj800	This chapter	UTI89 ΔcyaA transformed with prj800
CL1633	UTI89 Δcrp prj800-csgD	This chapter	UTI89 Δcrp transformed with prj800-csgD
CL1631	UTI89 ΔcyaA prj800-csgD	This chapter	UTI89 ΔcyaA transformed with prj800-csgD
CL1954	UTI89 Δcrp prj800-rrsA	This chapter	UTI89 Δcrp transformed with prj800-rrsA
CL1952	UTI89 ΔcyaA prj800-rrsA	This chapter	UTI89 ΔcyaA transformed with prj800-rrsA

Acknowledgments

We thank Blaise Boles, Robert Bender, William Depas, and Margery Evans for in depth discussions on this project. We thank Ute Romling for supplying the anti-CsgD antibody. Sarah Greene ran the first EMSA (Figure 4.4A) (Washington University St. Louis) and Jerry Pinkner purified CRP for the project (Figure 4.4) both are members of Scott Hultgren's lab (Washington University St. Louis).

1. **Zheng D, Constantinidou C, Hobman JL, Minchin SD.** 2004. Identification of the CRP regulon using in vitro and in vivo transcriptional profiling. Nucleic Acids Res **32:**5874-5893.
2. **Jackson DW, Simecka JW, Romeo T.** 2002. Catabolite repression of *Escherichia coli* biofilm formation. Journal of Bacteriology **184:**3406-3410.
3. **Hufnagel DA, Tukel C, Chapman MR.** 2013. Disease to dirt: the biology of microbial amyloids. PLoS Pathog **9:**e1003740.
4. **Hufnagel DA, Depas WH, Chapman MR.** 2015. The Biology of the *Escherichia coli* Extracellular Matrix. Microbiol Spectr **3**.
5. **Hammar M, Arnqvist A, Bian Z, Olsen A, Normark S.** 1995. Expression of two csg operons is required for production of fibronectin- and Congo red-binding curli polymers in *Escherichia coli* K-12. Mol Microbiol **18:**661-670.
6. **Evans ML, Chapman MR.** 2013. Curli biogenesis: Order out of disorder. Biochim Biophys Acta doi:10.1016/j.bbamcr.2013.09.010.
7. **Romling U, Bian Z, Hammar M, Sierralta WD, Normark S.** 1998. Curli fibers are highly conserved between *Salmonella* typhimurium and *Escherichia coli* with respect to operon structure and regulation. J Bacteriol **180:**722-731.
8. **Ogasawara H, Yamamoto K, Ishihama A.** 2011. Role of the biofilm master regulator CsgD in cross-regulation between biofilm formation and flagellar synthesis. J Bacteriol **193:**2587-2597.

9. **Austin JW, Sanders G, Kay WW, Collinson SK.** 1998. Thin aggregative fimbriae enhance *Salmonella* enteritidis biofilm formation. Fems Microbiology Letters **162:**295-301.
10. **Zhou Y, Smith D, Leong BJ, Brannstrom K, Almqvist F, Chapman MR.** 2012. Promiscuous cross-seeding between bacterial amyloids promotes interspecies biofilms. The Journal of biological chemistry **287:**35092-35103.
11. **Sabir S, Ahmad Anjum A, Ijaz T, Asad Ali M, Ur Rehman Khan M, Nawaz M.** 2014. Isolation and antibiotic susceptibility of E. coli from urinary tract infections in a tertiary care hospital. Pak J Med Sci **30:**389-392.
12. **Cegelski L, Pinkner JS, Hammer ND, Cusumano CK, Hung CS, Chorell E, Aberg V, Walker JN, Seed PC, Almqvist F, Chapman MR, Hultgren SJ.** 2009. Small-molecule inhibitors target *Escherichia coli* amyloid biogenesis and biofilm formation. Nat Chem Biol **5:**913-919.
13. **Mulvey MA, Schilling JD, Hultgren SJ.** 2001. Establishment of a persistent *Escherichia coli* reservoir during the acute phase of a bladder infection. Infect Immun **69:**4572-4579.
14. **Anderson GG, Goller CC, Justice S, Hultgren SJ, Seed PC.** 2010. Polysaccharide capsule and sialic acid-mediated regulation promote biofilm-like intracellular bacterial communities during cystitis. Infect Immun **78:**963-975.
15. **Fic E, Bonarek P, Gorecki A, Kedracka-Krok S, Mikolajczak J, Polit A, Tworzydlo M, Dziedzicka-Wasylewska M, Wasylewski Z.** 2009. cAMP Receptor Protein from *Escherichia coli* as a Model of Signal Transduction in Proteins - A Review. Journal of Molecular Microbiology and Biotechnology **17:**1-11.
16. **Muller CM, Aberg A, Straseviciene J, Emody L, Uhlin BE, Balsalobre C.** 2009. Type 1 Fimbriae, a Colonization Factor of Uropathogenic *Escherichia coli*, Are Controlled by the Metabolic Sensor CRP-cAMP. Plos Pathogens **5**.
17. **Sutrina SL, Daniel K, Lewis M, Charles NT, Anselm CKE, Thomas N, Holder N.** 2015. Biofilm Growth of *Escherichia coli* Is Subject to cAMP-Dependent and cAMP-Independent Inhibition. Journal of Molecular Microbiology and Biotechnology **25:**209-225.
18. **Gerstel U, Romling U.** 2001. Oxygen tension and nutrient starvation are major signals that regulate agfD promoter activity and expression of the multicellular morphotype in *Salmonella* typhimurium. Environ Microbiol **3:**638-648.
19. **Zogaj X, Nimtz M, Rohde M, Bokranz W, Romling U.** 2001. The multicellular morphotypes of *Salmonella* typhimurium and *Escherichia coli* produce cellulose as the second component of the extracellular matrix. Mol Microbiol **39:**1452-1463.
20. **Lengeler J.** 2009. The Biology of the Prokaryotes. Wiley-Blackwell.
21. **Hung C, Zhou YZ, Pinkner JS, Dodson KW, Crowley JR, Heuser J, Chapman MR, Hadjifrangiskou M, Henderson JP, Hultgren SJ.** 2013. *Escherichia coli* Biofilms Have an Organized and Complex Extracellular Matrix Structure. Mbio **4**.
22. **Depas WH, Hufnagel DA, Lee JS, Blanco LP, Bernstein HC, Fisher ST, James GA, Stewart PS, Chapman MR.** 2013. Iron induces bimodal population development by *Escherichia coli*. Proc Natl Acad Sci U S A **110:**2629-2634.
23. **van Elsas JD, Semenov AV, Costa R, Trevors JT.** 2011. Survival of *Escherichia coli* in the environment: fundamental and public health aspects. ISME J **5:**173-183.

24. **Winfield MD, Groisman EA.** 2003. Role of nonhost environments in the lifestyles of *Salmonella* and *Escherichia coli*. Appl Environ Microbiol **69:**3687-3694.
25. **Munch R, Hiller K, Barg H, Heldt D, Linz S, Wingender E, Jahn D.** 2003. PRODORIC: prokaryotic database of gene regulation. Nucleic Acids Res **31:**266-269.
26. **Martinez JJ, Mulvey MA, Schilling JD, Pinkner JS, Hultgren SJ.** 2000. Type 1 pilus-mediated bacterial invasion of bladder epithelial cells. EMBO J **19:**2803-2812.
27. **Flores-Mireles AL, Walker JN, Caparon M, Hultgren SJ.** 2015. Urinary tract infections: epidemiology, mechanisms of infection and treatment options. Nature Reviews Microbiology **13:**269-284.
28. **Song JM, Bishop BL, Li GJ, Grady R, Stapleton A, Abraham SN.** 2009. TLR4-mediated expulsion of bacteria from infected bladder epithelial cells. Proceedings of the National Academy of Sciences of the United States of America **106:**14966-14971.
29. **Greene SE, Pinkner JS, Chorell E, Dodson KW, Shaffer CL, Conover MS, Livny J, Hadjifrangiskou M, Almqvist F, Hultgren SJ.** 2014. Pilicide ec240 Disrupts Virulence Circuits in Uropathogenic *Escherichia coli*. Mbio **5**.
30. **Whitfield C, Roberts IS.** 1999. Structure, assembly and regulation of expression of capsules in *Escherichia coli*. Molecular Microbiology **31:**1307-1319.
31. **Datsenko KA, Wanner BL.** 2000. One-step inactivation of chromosomal genes in *Escherichia coli* K-12 using PCR products. Proc Natl Acad Sci U S A **97:**6640-6645.
32. **Hufnagel DA, DePas WH, Chapman MR.** 2014. The disulfide bonding system suppresses CsgD-independent cellulose production in *Escherichia coli*. J Bacteriol **196:**3690-3699.
33. **Andersson EK, Bengtsson C, Evans ML, Chorell E, Sellstedt M, Lindgren AE, Hufnagel DA, Bhattacharya M, Tessier PM, Wittung-Stafshede P, Almqvist F, Chapman MR.** 2013. Modulation of curli assembly and pellicle biofilm formation by chemical and protein chaperones. Chemistry & Biology **20:**1245-1254.
34. **Zhou Y, Smith DR, Hufnagel DA, Chapman MR.** 2013. Experimental manipulation of the microbial functional amyloid called curli. Methods Mol Biol **966:**53-75.
35. **Miller J.** 1972. Experiments in Molecular Genetics. Cold Spring Harbor Lab Press, Cold Spring Harbor, NY.

Chapter 5

Discussion, Thoughts, and Future Projects

Biofilm formation is a prevalent and complex microbial lifestyle. The age old question of, "should I stay or should I go" is constantly asked by bacteria. A wealth of nutrients will cause bacteria to tailor their cellular machinery to acquire nutrients and to divide as quickly as possible. A concentration gradient of various amino acids will lead to chemotaxis towards the desired compound, whereas droughts and desiccation will cause bacteria to adhere, conserve available nutrients, and to create a protective ECM. Understanding the molecular pathways that guide bacterial lifestyles will provide insights into physiology, stress resistance, motility, and adherence. The data presented in my thesis reveal novel ECM activation pathways, the response of the ECM to novel oxidative conditions, and the influence of catabolite repression on *E. coli* biofilms.

Unfinished Projects

What Causes Colony Spreading?

Colony spreading requires expression of both curli and cellulose in *E. coli* and *Salmonella* (Figure 5.1) (1). Δ*cysE* colonies produce both curli and cellulose but do not spread (Figure 3.1 and 3.2). I hypothesize that the lack of spreading is due to delayed cellulose

production, as upregulating cellulose production via mutation of *yfiR* helps rescue the spreading phenotype of *cysE* mutants though not to WT levels (Figure 3.7A). Δ*cysE* colonies may produce a tertiary extracellular component that inhibits colony spreading, which would inhibit *ΔcysEΔyfiR* from spreading like a WT colony. Why does spreading require both curli and cellulose? I hypothesize that cellulose modulates CsgA amyloid polymerization, causing an amphipathic intermediate co-polymer that induces spreading of bacteria across the agar surface.

Scanning electron microscopy (SEM) analysis in multiple studies reveals the ECM of biofilms expressing both curli and cellulose look completely different from biofilms expressing curli *or* cellulose alone (2, 3). The co-expression of curli and cellulose creates a uniquely-functioning polymer matrix in the *E. coli* biofilm. For example, Zogaj *et al. 2001* looked at the hydrophobicity of colonies producing curli alone, cellulose alone, and both ECM components together (4). Water contact angle analysis revealed that cellulose alone is hydrophilic, curli alone is mildly hydrophobic, and the two components together are very hydrophobic (4), lending credence to the possibility that curli and cellulose together may have unique biophysical properties.

I hypothesize a transient soluble state of CsgA is required in conjunction with cellulose in order for bacteria in a rugose colony to move across the surface of the agar and to form a spreading phenotype similar to how the phenol soluble modulins (PSMs) function. Many amyloidogenic proteins have soluble states that have different biochemical properties compared to their amyloid state (5). The PSMs in staphylococci species have the ability to disperse biofilms with surfactant like qualities in their soluble state, while in their polymerized state they can confer protease, DNAse, and antibiotic resistance to the biofilm (6, 7). Additionally, *S.*

aureus can form spreading communities on low agar plates that are dependent on PSM production (Syed AK and Boles BR Thesis 2015).

To test the role of curli in colony spreading mutational analysis was performed in the *csg* operon. Laboratory Δ*csgB* strains secrete soluble CsgA (8), so this was the first strain of interest. Intriguingly, UTI89 Δ*csgB* colonies did not spread as much as WT, but spread slightly more than Δ*csgBA* (Figure 5.2). Interestingly, UTI89 Δ*csgA* strains had a colony morphotype similar to that of Δ*csgBA* yet did not spread at the edges in contrast to Δ*csgB* (Figure 5.2). Δ*csgF* mutants bound CR, but did not wrinkle, save for a single line around the colony (Figure 5.2). Δ*csgBF* restored some colony wrinkling but no spreading. For future directions, the Δ*csgF* strain should be complemented *in trans* with *csgF* to see if CsgF is actually required for the production of the ECM. If CsgF is required for wrinkling, this is a very interesting development. In our current model of curli biogenesis CsgF is cell surface associated and is necessary for CsgB and curli surface attachment (9, 10). Δ*csgF* binds CR, so it appears to be producing either curli or cellulose but not wrinkling. Δ*csgF* in laboratory strains secrete curli subunits in a soluble fashion and have decreased polymerized and mis-localized curli (9). Since Δ*csgBA* can wrinkle without curli, perhaps Δ*csgF* also interfaces with cellulose production/function, which is why this strain is unable to wrinkle (Figure 5.2). To test if CsgF is involved in the production of cellulose, a *ΔcsgFΔyfiR* colony should be tested for colony wrinkling. *yfiR* mutation leads to constitutive cellulose production through activation of YfiN (Chapter 3). If this strain doesn't wrinkle, then CsgF is required for cellulose production. Altogether, it appears that cell-surface tethering with CsgB and CsgF is required for colony spreading, but soluble vs. polymerized CsgA should still be investigated as a possible surfactant. Perhaps properly localized CsgB on the cell surface allows cells to be moved along with a surfactant like copolymer between cellulose and curli.

To test if soluble vs. polymerized CsgA influences colony spreading, colony spreading in UTI89 Δ*csgA* expressing CsgA^{slowgo} (mutant CsgA that polymerizes into an amyloid in a slow fashion (11)) *in trans* should be monitored. Δ*csgA* still expresses CsgB and CsgF, so perhaps these cells will be able to interface with curli and cellulose. Increased spreading of Δ*csgA* expressing CsgA^{slowgo} vs. WT CsgA would show that soluble CsgA induces rugose colony spreading. Additionally, freshly purified CsgA^{slowgo} and CsgA should be added exogenously to a Δ*csgA* colony and see if this is able to restore colony spreading. To test if soluble CsgA is required for colony spreading, rugose colonies should be assayed for spreading with *in trans* expression of CsgA* (a rapidly polymerizing CsgA mutant). CsgA* is only in its soluble state for a small window of time, so if Δ*csgA* expressing CsgA* doesn't spread, then we would conclude that soluble CsgA is required for the rugose colony to spread. There is toxicity associated with CsgA*, so exogenous polymerized and soluble CsgA will be added to a Δ*csgA* mutant colony. If soluble CsgA induces spreading, while polymerized CsgA does not, then soluble CsgA is required for the colony spreading.

Checking for the surfactant qualities of CsgA could be performed with freshly purified vs. polymerized CsgA. A simple assay for detection of surfactant is the methylene blue surfactant assay (MBAS) (12). MBAS tests for surfactants with acidic water and chloroform with methylene blue. Increased surfactant will cause association of methylene blue with the chloroform at the top of the biphasic solution (12). If longer time is needed for surfactant testing, CsgA^{slowgo} (a CsgA mutant that polymerizes into an amyloid in a delayed fashion) should be assayed and compared to CsgA^{slowgo} that has been incubated for a long enough period to allow for amyloid polymerization. Our hypothesis may still be correct, even if soluble CsgA does not function as a surfactant. CsgA in the presence of cellulose may make a surfactant like co-

polymer between CsgA and cellulose that the bacteria can utilize in order to slide across the surface of the agar. Since Δ*csgB* mutants produce lots of soluble CsgA and are unable to spread without cellulose (Hammer 2009), perhaps soluble or polymerized CsgA doesn't display surfactant properties without cellulose present. We can repeat these assays in the presence of carboxymethyl cellulose (CMC) to see if both ECM components must be present for this surfactant-like property. The Cegelski lab has shown that a ethanolamine modification is present on UTI89 cellulose (13). Perhaps this moiety is also important for colony spreading and for surfactant properties with CsgA. The Chapman Lab has an active collaboration with the Cegelski lab and could obtain purified UTI89 cellulose to perform these experiments.

I hypothesize that the presence of cellulose is able to delay polymerization of CsgA. To test if cellulose can modulate CsgA, we will observe CsgA polymerization in the presence of CMC via thioflavin T assays (ThT). ThT assays monitor the fluorescence of an amyloid-specific die as a proxy for polymerization of amyloids. As a control, soluble glucose will be added to ThT reactions, since CMC is β-1,4 linked glycan chain. Since CMC will not go into solution, the amount of CMC or glucose added will be in a weight/volume ratio.

BcsZ Involvement in UPEC Biofilms

Δ*csgB* colonies having increased spreading points to soluble CsgA being involved in the spreading process, however there is a possibility that colony spreading is induced from curli modulation of cellulose. Cellulose production in enterobactericiae is a relatively new study (4). Recent work has shown that the cellulose synthase (BcsA) and a second inner membrane protein, BcsB, are the only protein components necessary for production of cellulose, however there is

also an outermembrane pore, BcsC, and an endogluconase, BcsZ. There is very little work on BcsZ apart from: 1) a crystal structure (14) 2) strains overexpressing *bcsZ* and purified BcsZ having endoglucanase activity on CMC *in vitro* (14) and 3) work that initially cloned this ORF and found extracellular endoglucanase activity in *E. coli* K12 (15). In *Acetobacter xylinus,* BcsZ is periplasmic and assists in the production of cellulose, however we found UTI89 *E. coli* BcsZ only had 30% amino acid identity with *A. xylinus* (Figure 5.3A).

Rugose colony formation requires *bcsZ*. Δ*bcsZ* colonies produced non-spreading, non-wrinkling colonies that deeply bound CR at 26°C (Figure 5.3B). At 37°C, Δ*bcsZ* strains had slightly decreased CR binding in comparison to WT. This may be due to a slight decrease in cellulose production. Using the vector pCA24N-*bcsZ* from the ASKA collection (16) this gene was overexpressed in a WT strain and found that there was decreased colony spreading, however wrinkling on the interior of the colony was increased at 26°C (Figure 5.3C). Additionally, CR binding was decreased at 37°C, which could be due to over-activity of the enzyme leading to decreased cellulose production (Figure 5.3C).

There are many things to follow up on in this project. The first experiment is to complement the *bcsZ* mutant *in trans,* to ensure that the mutation in *bcsZ* is not causing polar effects on other genes in the *bcs* operon leading to a decrease in cellulose production. The operon is structured *bcsQABZC* (2). Secondly, there are many potential functions of BcsZ in biofilms. *bcsZ* influencing rugose biofilms hints that BcsZ may function in the production of cellulose. Whether BcsZ is functioning in the periplasm, during the formation and secretion of cellulose, or extracellularly, restructuring cellulose to help keep the cellulose synthase pore free is unknown, but it is required for maximal cellulose production. In *G. xylinus* BcsZ is in the periplasm and helps with the production of cellulose, but the low amount of homology means that it could

function in a different manner in *E. coli* (Figure 5.3A). To test for extracellular BcsZ, lysed and un-lysed dot blot analysis will be performed on rugose colonies expressing a tagged version of *bcsZ*. An antibody against the tag will be used to probe for BcsZ. If BcsZ is present in both samples, it is extracellular, however if BcsZ is only present in the lysed cells sample, this means BcsZ is intracellular. The presence of BcsZ outside of the cell, doesn't guarantee that it has an extracellular function. Extracellular BcsZ activity will be tested via interbacterial complementation assays. If a mixed Δ*adrA* (doesn't produce cellulose, but produces all the Bcs proteins) and Δ*bcsZ* culture develops a fully wrinkled colony, this will mean that BcsZ from Δ*adrA* has the ability to extracellularly restructure cellulose production from Δ*bcsZ*. If no change in colony morphotype is observed, then BcsZ does not function in the extracellular space or only functions on cellulose produced from the cell from which it was secreted.

BcsZ could function to free cells from the ECM when the biofilm disperses. Dispersal is a key step in the biofilm process (17). Cells being able to leave the initial biofilm and either begin growth or colonize a second disparate surface is paramount to the biofilm lifestyle (17). The mechanisms for *E. coli* cells leaving the biofilm are still unknown, and an endoglucanase that can enzymatically cleave an ECM component is a good potential target. The extracellular vs. intracellular BcsZ assays will play a big role in answering this question as well, since extracellular BcsZ could be used to enzymatically cleave holes through the encasing ECM. I hypothesize that BcsZ functions in the dispersal of UPEC biofilms. After 4-5 days of static growth, pellicles begin to break apart and cells are re-released into the lower portions of the liquid medium. WT and Δ*bcsZ* pellicles will be monitored for pellicle formation and dispersal for 7-10 days. If our hypothesis is correct, then Δ*bcsZ* pellicles will have delayed dispersal back into the media. Additionally, we can monitor pellicle dispersal for WT pellicles transformed with

pEV and p*bcsZ.* If the presence or absence of BcsZ modulates pellicle dispersal times, then BcsZ is a viable candidate for *E. coli* dispersal from the biofilm ECM.

A secondary experiment would monitor if *bcsZ* can function to release cells from the rugose colony ECM. Since Δ*bcsZ* does not produce the same rugose biofilm as WT, a cell-free ECM of WT UTI89 will be isolated via the washout assay and antibiotic treatment (18). To obtain a cell-free ECM, the ECM will be obtained via the washout assay followed by ECM treatment with kanamycin (Km) to kill all cells present. Lastly the ECM will be treated with a series of washes in sterile buffer to remove Km. The ECM will then be placed on top of Km motility agar, and WT cells and Δ*bcsZ* cells with pCA24N (Km^R) will then be placed on the top of the ECM. If the ECM is intact, then only cells that are able to traverse the ECM will be able to reach the motility plates and begin to swim. If my hypothesis is correct, Δ*bcsZ* cells will remain on top of the ECM unable to reach the agar surface, whereas WT cells will be able to utilize BcsZ to restructure the ECM and make it to the motility agar surface and begin swimming. To ensure that all cells were killed by Km, a control with the matrix alone will be added to the motility agar, to ensure that no cells survived treatment. Perhaps specific conditions upregulate *bcsZ* and spotting onto the matrix will not lead to high enough BcsZ protein levels. *bcsZ* overexpression strains will also be used in this experiment to see if high levels of this enzyme can indeed cut a hole through the ECM for the passage of bacteria to the motility agar underneath. Additionally, the motility of Δ*bcsZ* pCA24N will be assayed to ensure that it is able to swim.

Future Thoughts

The projects presented here leave many novel unanswered questions about UPEC biofilms. Glucose inhibiting biofilm at the same time makes complete sense and appears nonsensical. On one hand, cellulose is composed of β-1,4 linked glucose, so why would the presence of glucose inhibit biofilm formation? On the other hand, it makes sense because glucose is a highly desirable carbon source that cells can utilize to generate lots of ATP and rapidly divide. So cells do not want to adhere to each other, adhere to surfaces, create a physical barrier, and slow down growth in the presence of this polysaccharide.

Another interesting facet of my thesis is production of ECM components at 37°C. Curli and cellulose are optimally expressed at temperatures below 30°C (19). Other papers have looked at isolates that have the ability to produce curli at 37°C (20-22). Additionally, work in *Salmonella* has revealed that curli are important for tightening epithelial cell barriers in the guts of mice, and that the lack of curli can lead to *Salmonella* traversing the gut and causing infection in the cecal and mesenteric tissues (23). Additionally, antibodies against CsgA are present in sepsis patients (24).

Even with all of these studies, nobody has directly shown the presence of curli or cellulose production within mice or humans. Two of my projects have found environmental conditions that induce curli (lack of thiol reducing agents) (Chapter 3) and cellulose (reducing conditions) (Chapter 2) at 37°C. Additionally, I have found that cysteine auxotrophs isolated from patients have a greatly increased propensity to produce curli at 37°C (Figure 3.8).

The presence of curli should be tested within mice first. Sterile mice will be inoculated with UTI89 WT, Δ*cysE,* Δ*csgBA,* Δ*cysE*Δ*csgBA* and fresh feces will be isolated and

immediately probed for CsgA. Uropathogenic strains are able to survive in the intestinal environment similar to normal strains of *E. coli* (25). This experiment would test for: 1) whether WT UTI89 experiences any environments in the gut that induce CsgA production at 37°C. 2) Whether the 37°C CsgA production by cysteine auxotrophs is still physiologically relevant in the host and 3) whether curli are produced towards the latter stages of the intestinal tract. If CsgA is undetectable in fresh feces, isolations of the intestinal tract could be probed for CsgA. Mouse CsgA-probing experiments need to be performed quickly after fecal or intestinal isolation, to ensure that the room temperature of the laboratory is not inducing *E. coli* CsgA expression. In human patients, freshly isolated feces, catheters, and urine from patients with UTI and blood from *E. coli* sepsis patients can also be probed for CsgA production.

Two of my projects, Chapters 2 and 3 both investigate redox modulation of the ECM. These chapters also coincide with another project on which I worked, detailing the necessity of iron-mediated oxidative stress for rugose colony development (18). It is fascinating that UPEC biofilms appear so finely tuned to various levels of reductants, oxidants, and thiol buffering agents like glutathione and cysteine. Reducing conditions in non-curli producing environments leads to cellulose production alone, through the degradation of YfiR (Figure 2.5), whereas the lack of thiol reducing agents like cysteine and glutathione leads to curli production alone (Chapter 3).

Further investigation should be taken into whether cellulose can protect cells from harsh reducing environments and what role curli play in resistance to high amounts of oxidative stress (whether from iron or the lack of thiol reducing agents). Since curli are not produced under reducing conditions, are curli detrimental to the cells in reduced environments? What about potential deleterious effects of cellulose in an oxidative environment? It's curious these

components are normally so intimately coordinated via CsgD at the 12 hour mark in a rugose colony (Figure 3.2), yet these conditions induce expression of only a single ECM component. Another possible reason could be metabolic expense. Production of a glycan chain or many subunits of curli could lead to a drain on cellular energy. Oxidative and reducing conditions have evolutionarily led to production of a single advantageous or non-deleterious component for the particular environment.

My thesis is a sum of my efforts to unearth new environments and pathways that modulate the UPEC biofilm. The work presented here ranges from CRP-cAMP activation of *csgD* at three sites on the promoter to how redox modulates the ECM. I found that YfiR has a disulfide that acts as a periplasmic redox sensor that can induce CsgD protein production through YfiN activation. Δ*yfiR,* Δ*dsbB,* and Δ*dsbA* colonies induce cellulose production independent of CsgD through YfiN. I found that cysteine auxotrophs have a lack of thiol reducing agents that uncouples cellulose and curli production, through a hyper-oxidized environment presumably leading to YfiR accumulation. I found cysteine auxotrophs produce curli at 37°C and that cysteine auxotrophs isolated from patients display this same temperature-independent curli production. Finally, I found that sub-inhibitory concentrations of multiple antibiotics are inhibitory to curli production, and cysteine auxotrophs are resistant to antibiotic-mediated curli-inhibition. Further work on cysteine auxotrophs in the host, and detailing the roles of curli and cellulose in reduced and oxidizing environments could reveal many answers about the role of curli for protection of the bacteria, response to various environments, and how and why curli could be produced in the host.

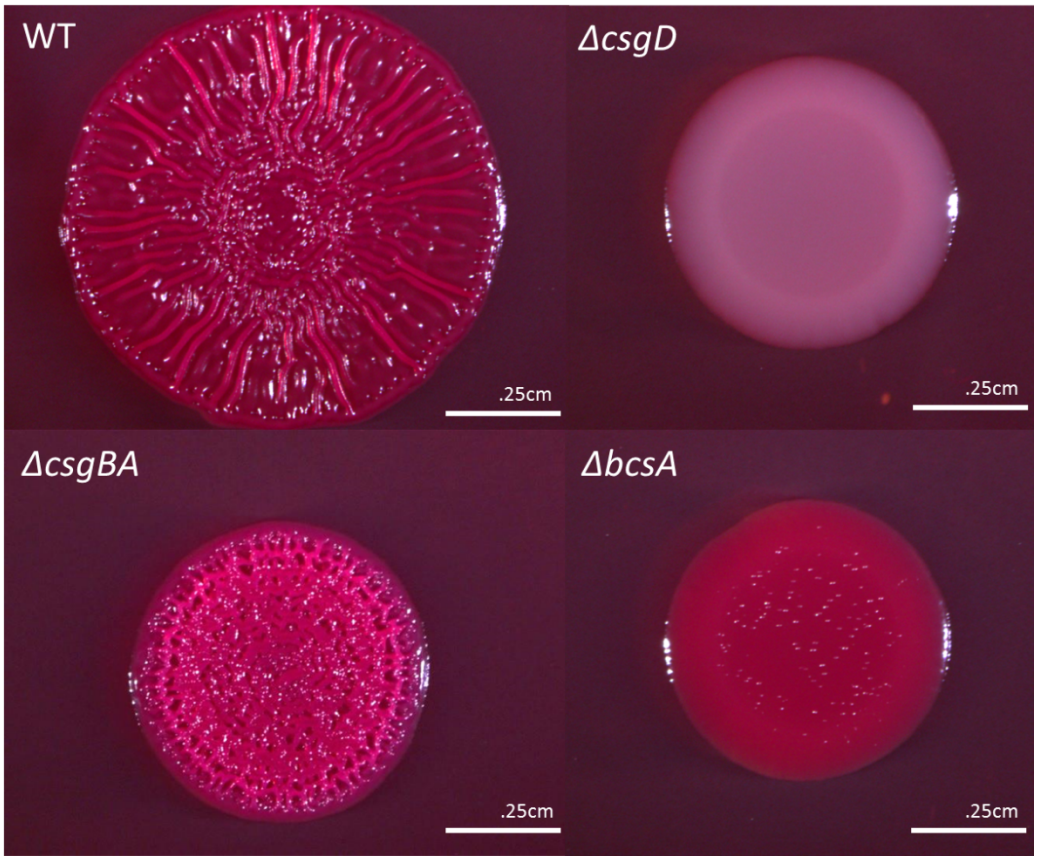

Figure 5.1- Curli and cellulose are both required for colony spreading. 4µL dots of WT, Δ*csgD,* Δ*csgBA,* and Δ*bcsA* were plated onto YESCA CR plates at 26° for 48 hours. Δ*csgD* (curli$^-$cellulose$^-$) was unable to wrinkle, spread, or bind CR. Δ*csgBA* (curli$^-$) wrinkled, did not spread, and lightly bound CR. Δ*bcsA* (cellulose$^-$) produced a smooth and red non-spreading colony.

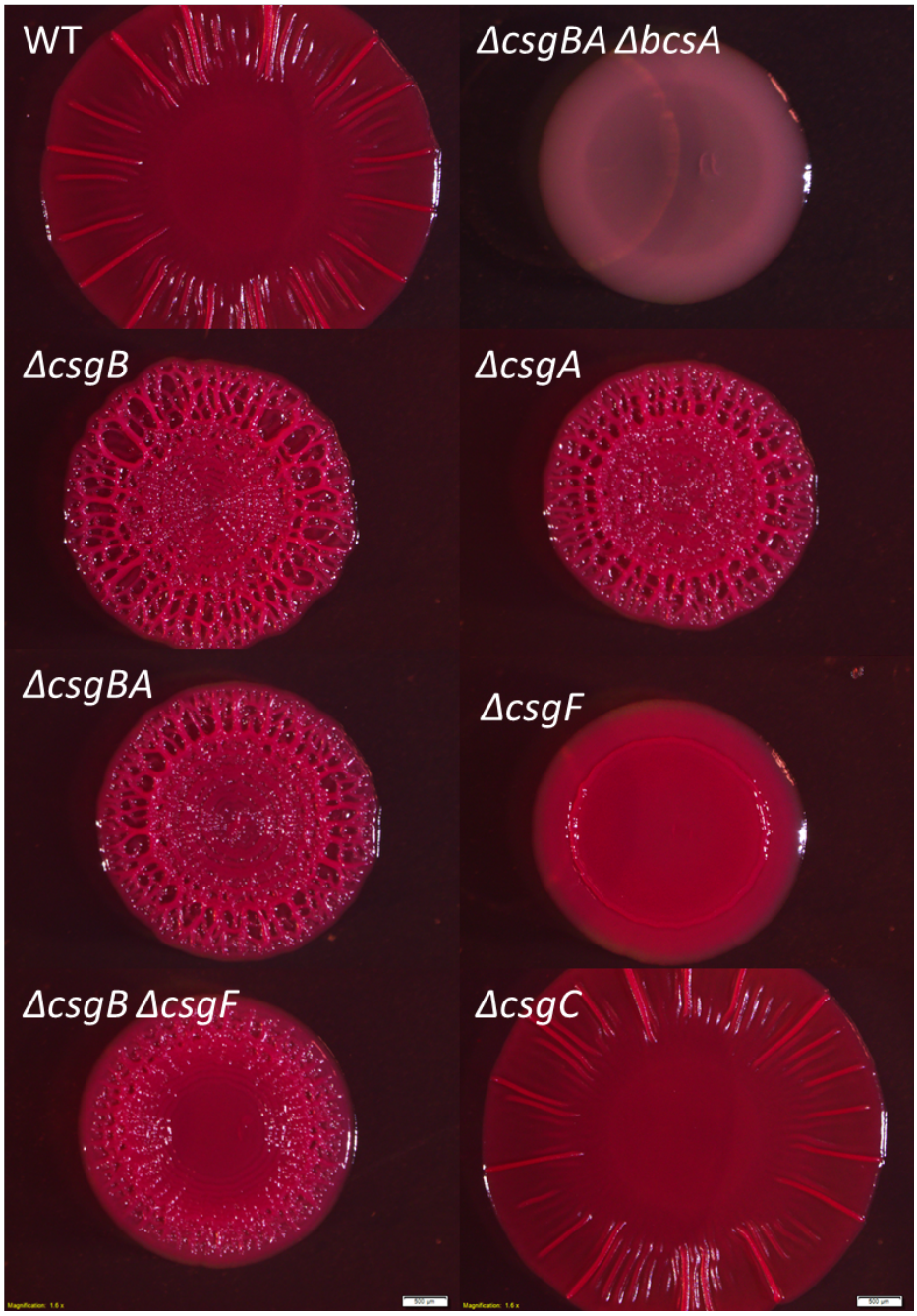

Figure 5.2- The role of *csg* genes in rugose colony development. WT, Δ*csgBA*Δ*bcsA,* Δ*csgB, ΔcsgA, ΔcsgBA, ΔcsgF, ΔcsgBF,* and *ΔcsgC* were plated on YESCA CR plates at 26°C for 48 hours. Δ*csgBA*Δ*bcsA* (curli$^-$ cellulose$^-$) was white, non-spreading and smooth. Δ*csgB* wrinkled but spread less than WT, while Δ*csgA* wrinkled but spread slightly less than Δ*csgB,* phenocopying Δ*csgBA.* Δ*csgF* was smooth, non-wrinkled and red, while Δ*csgBF* induced intermediate wrinkling. Δ*csgC* phenocopied a WT colony.

A

Score	Expect	Method	Identities	Positives	Gaps
107 bits(266)	9e-27	Compositional matrix adjust.	98/327(30%)	144/327(44%)	41/327(12%)

```
Query  30   WEQFKKDYISQEGRVIDPSDARKITTSEGQSYGMFFALAANDRAAFDNLLDWTQNNLAQG  89
            W  F+  Y   +GR+ID  ++ + + SEGQ YGM FA AA D+ AF+ +  W +NNL
Sbjct  34   WAIFRSKYFHPDGRIIDTGNSGE-SHSEGQGYGMLFAAAAGDQTAFEAIWVWARNNLQHK  92

Query  90   SLKEHLPAWLWGKKENSKWEVLDSNSASDGDVWMAWSLLEAGRLWKEQRYTDIGSALLKR  149
            +  + L +W + +  N    V D N+A+DGD+ +A  L  AG+LWK   Y      +
Sbjct  93   T--DALFSWRYLEGHNPP--VADKNNATDGDLLIALGLARAGKLWKRADYIQDAINIYAD  148

Query  150  IAREEVVTVPGLGSMLLPGKVGFAEDNSWRFNPS-YLPPTLAQYFTRFG-APWTTLRETN  207
            + +   + V G  ++LLPG VGF   ++   N S Y+ P+L Q F   G + W T+ E
Sbjct  149  VLKHMTMKV-GPYTVLLPGAVGFVTKDAVTLNLSYYVMPSLLQAFELSGESQWQTVIENG  207

Query  208  QRLL--LETAPKGFSPDWVRYEKD-------KGWQLKAEKTLISSYDAIRVYM---WVGM  255
             R++   +       PDW+   +         KGW  +       SYDAIRV +   W  M
Sbjct  208  LRIIGKAQFGEWKLPPDWLSINRQTGNFSIAKGWPPR------FSYDAIRVPLYLYWAHM  261

Query  256  M-PDSDPQKARMLNRFKPMATFTEKNGYPPEKVDVATGKAQGKGPVGFSAAMLPFLQNRD  314
            + P+      R  N F   A         P  VD+  G    + P       L
Sbjct  262  LSPELLADYTRFWNHFGASAL--------PGWVDLTNGS---RSPYNAPPGYLAVASCSG  310

Query  315  AQAVQRQRVADNFPGSDAYYNYVLTLF  341
               +       DN P    YY+  LTL
Sbjct  311  LASAGELPTLDNAPD---YYSAALTLL  334
```

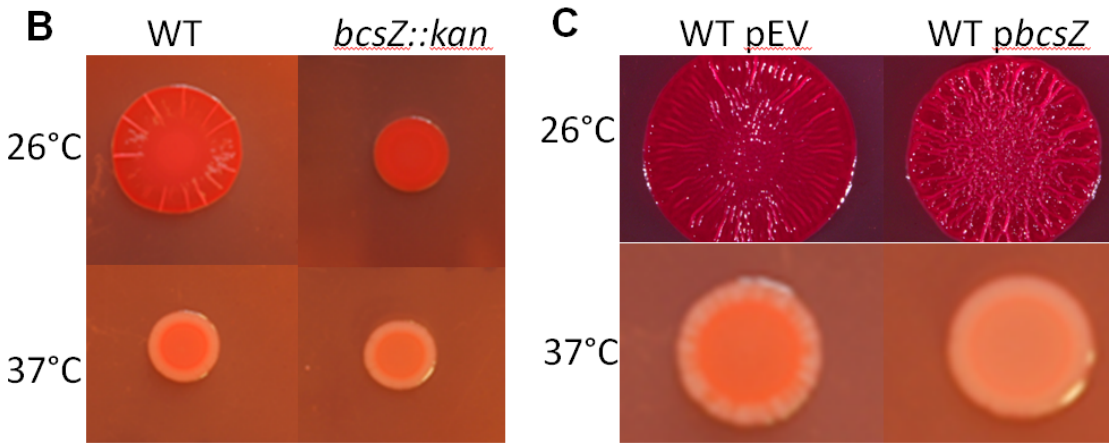

Figure 5.3- UPEC *bcsZ* involvement in biofilms. A) Amino acid comparison of *Gluconacetobacter xylinus* and UTI89 BcsZ revealed only a 30% identity between these two proteins. B) *bcsZ::kan* rugose colonies didn't spread at 26°C and had decreased CR binding at 37°C. C) *bcsZ* overexpression led to an increase to wrinkling in the center of a WT colony at 26°C and decreased CR binding at 37°C.

Acknowledgements- The BcsZ project was greatly aided by my undergraduate Jesse Kelly. He performed the mutational analysis and the transformation of p*bcsZ.* Will DePas created a handful of the *csg* mutants used to study curli-specific genes influences on rugose colony development.

1. **White AP, Gibson DL, Kim W, Kay WW, Surette MG.** 2006. Thin aggregative fimbriae and cellulose enhance long-term survival and persistence of *Salmonella*. J Bacteriol **188:**3219-3227.
2. **Serra DO, Richter AM, Hengge R.** 2013. Cellulose as an Architectural Element in Spatially Structured *Escherichia coli* Biofilms. J Bacteriol **195:**5540-5554.
3. **Hung C, Zhou YZ, Pinkner JS, Dodson KW, Crowley JR, Heuser J, Chapman MR, Hadjifrangiskou M, Henderson JP, Hultgren SJ.** 2013. *Escherichia coli* Biofilms Have an Organized and Complex Extracellular Matrix Structure. Mbio **4**.
4. **Zogaj X, Nimtz M, Rohde M, Bokranz W, Romling U.** 2001. The multicellular morphotypes of *Salmonella* typhimurium and *Escherichia coli* produce cellulose as the second component of the extracellular matrix. Mol Microbiol **39:**1452-1463.
5. **Syed AK, Boles BR.** 2014. Fold modulating function: bacterial toxins to functional amyloids. Front Microbiol **5:**401.
6. **Schwartz K, Syed AK, Stephenson RE, Rickard AH, Boles BR.** 2012. Functional amyloids composed of phenol soluble modulins stabilize *Staphylococcus aureus* biofilms. PLoS Pathog **8:**e1002744.
7. **Le KY, Dastgheyb S, Ho TV, Otto M.** 2014. Molecular determinants of staphylococcal biofilm dispersal and structuring. Front Cell Infect Microbiol **4:**167.
8. **Hammer ND, Schmidt JC, Chapman MR.** 2007. The curli nucleator protein, CsgB, contains an amyloidogenic domain that directs CsgA polymerization. Proc Natl Acad Sci U S A **104:**12494-12499.
9. **Nenninger AA, Robinson LS, Hultgren SJ.** 2009. Localized and efficient curli nucleation requires the chaperone-like amyloid assembly protein CsgF. Proc Natl Acad Sci U S A **106:**900-905.
10. **Evans ML, Chapman MR.** 2013. Curli biogenesis: Order out of disorder. Biochim Biophys Acta doi:10.1016/j.bbamcr.2013.09.010.
11. **Wang X, Chapman MR.** 2008. Sequence determinants of bacterial amyloid formation. J Mol Biol **380:**570-580.
12. **George AL, White GF.** 1999. Optimization of the methylene blue assay for anionic surfactants added to estuarine and marine water. Environmental Toxicology and Chemistry **18:**2232-2236.
13. **McCrate OA, Zhou X, Reichhardt C, Cegelski L.** 2013. Sum of the parts: composition and architecture of the bacterial extracellular matrix. Journal of molecular biology **425:**4286-4294.

14. **Mazur O, Zimmer J.** 2011. Apo- and cellopentaose-bound structures of the bacterial cellulose synthase subunit BcsZ. J Biol Chem **286:**17601-17606.
15. **Park YW, Yun HD.** 1999. Cloning of the *Escherichia coli* endo-1,4-D-glucanase gene and identification of its product. Mol Gen Genet **261:**236-241.
16. **Kitagawa M, Ara T, Arifuzzaman M, Ioka-Nakamichi T, Inamoto E, Toyonaga H, Mori H.** 2005. Complete set of ORF clones of *Escherichia coli* ASKA library (a complete set of E. coli K-12 ORF archive): unique resources for biological research. DNA Res **12:**291-299.
17. **Stewart PS, Franklin MJ.** 2008. Physiological heterogeneity in biofilms. Nat Rev Microbiol **6:**199-210.
18. **Depas WH, Hufnagel DA, Lee JS, Blanco LP, Bernstein HC, Fisher ST, James GA, Stewart PS, Chapman MR.** 2013. Iron induces bimodal population development by *Escherichia coli*. Proc Natl Acad Sci U S A **110:**2629-2634.
19. **Arnqvist A, Olsen A, Pfeifer J, Russell DG, Normark S.** 1992. The Crl protein activates cryptic genes for curli formation and fibronectin binding in *Escherichia coli* HB101. Mol Microbiol **6:**2443-2452.
20. **Romling U, Sierralta WD, Eriksson K, Normark S.** 1998. Multicellular and aggregative behaviour of *Salmonella* typhimurium strains is controlled by mutations in the *agfD* promoter. Mol Microbiol **28:**249-264.
21. **Bokranz W, Wang X, Tschape H, Romling U.** 2005. Expression of cellulose and curli fimbriae by *Escherichia coli* isolated from the gastrointestinal tract. Journal of Medical Microbiology **54:**1171-1182.
22. **Hufnagel DA, Tukel C, Chapman MR.** 2013. Disease to dirt: the biology of microbial amyloids. PLoS Pathog **9:**e1003740.
23. **Oppong GO, Rapsinski GJ, Newman TN, Nishimori JH, Biesecker SG, Tukel C.** 2013. Epithelial cells augment barrier function via activation of the Toll-like receptor 2/phosphatidylinositol 3-kinase pathway upon recognition of *Salmonella enterica* serovar Typhimurium curli fibrils in the gut. Infect Immun **81:**478-486.
24. **Bian Z, Brauner A, Li Y, Normark S.** 2000. Expression of and cytokine activation by *Escherichia coli* curli fibers in human sepsis. J Infect Dis **181:**602-612.
25. **Yamamoto S, Tsukamoto T, Terai A, Kurazono H, Takeda Y, Yoshida O.** 1997. Genetic evidence supporting the fecal-perineal-urethral hypothesis in cystitis caused by *Escherichia coli*. The Journal of urology **157:**1127-1129.